

**RPSEA**

***Final Report***

***07122-27-Final***

***Enhancing Appalachian Coalbed  
Methane Extraction by Microwave-  
Induced Fractures***

***07122-27-Pennsylvania\_StateU-  
Mathews***

***August 5th, 2010***

Jonathan P. Mathews  
Assistant Professor Energy & Mineral Engineering  
The Pennsylvania State University  
126 Holser Building  
University Park  
PA 16801

## LEGAL NOTICE

This report was prepared by **(CONTRACTOR NAME)** as an account of work sponsored by the Research Partnership to Secure Energy for America, RPSEA. Neither RPSEA members of RPSEA, the National Energy Technology Laboratory, the U.S. Department of Energy, nor any person acting on behalf of any of the entities:

- a. **MAKES ANY WARRANTY OR REPRESENTATION, EXPRESS OR IMPLIED WITH RESPECT TO ACCURACY, COMPLETENESS, OR USEFULNESS OF THE INFORMATION CONTAINED IN THIS DOCUMENT, OR THAT THE USE OF ANY INFORMATION, APPARATUS, METHOD, OR PROCESS DISCLOSED IN THIS DOCUMENT MAY NOT INFRINGE PRIVATELY OWNED RIGHTS, OR**
- b. **ASSUMES ANY LIABILITY WITH RESPECT TO THE USE OF, OR FOR ANY AND ALL DAMAGES RESULTING FROM THE USE OF, ANY INFORMATION, APPARATUS, METHOD, OR PROCESS DISCLOSED IN THIS DOCUMENT.**

In addition, one of the following statements should be included.

For interim reports:

**THIS IS AN INTERIM REPORT. THEREFORE, ANY DATA, CALCULATIONS, OR CONCLUSIONS REPORTED HEREIN SHOULD BE TREATED AS PRELIMINARY.**

For Final Reports:

**THIS IS A FINAL REPORT. THE DATA, CALCULATIONS, INFORMATION, CONCLUSIONS, AND/OR RECOMMENDATIONS REPORTED HEREIN ARE THE PROPERTY OF THE U.S. DEPARTMENT OF ENERGY.**

If appropriate, the following statement may be added to the disclaimer:

**REFERENCE TO TRADE NAMES OR SPECIFIC COMMERCIAL PRODUCTS, COMMODITIES, OR SERVICES IN THIS REPORT DOES NOT REPRESENT OR CONSTITUTE AND ENDORSEMENT, RECOMMENDATION, OR FAVORING BY RPSEA OR ITS CONTRACTORS OF THE SPECIFIC COMMERCIAL PRODUCT, COMMODITY, OR SERVICE.**

# **Enhancing Appalachian Coalbed Methane Extraction by Microwave-Induced Fractures**

Dr. Jonathan P. Mathews, Hemant Kumar, and Dr. Philip Halleck,

EMS Energy Institute and the Energy & Mineral Engineering Department

The Pennsylvania State University

Final Report RPSEA Unconventional Onshore Program

## **Abstract**

For the degassing of coal seams, either prior to mining or in unminable seams to obtain coalbed methane, it is the cleat frequency, aperture, connectivity, and mineral occlusions that influence coals permeability to gases. Unfortunately many potential coalbeds have limited permeability, thus they are often marginal for economic methane extraction. They also present a challenge in the case of enhanced coalbed methane production, with concurrent CO<sub>2</sub> sequestration, due to limited CO<sub>2</sub> injectivity. Microwave energy can, in the absence of confining stress, induce fractures in coal. Here, creation of new fractures and increasing existing cleat apertures via short burst, high-energy microwave energy was evaluated for both hydrostatically stressed and unstressed North American bituminous coal cores. A microwave-transparent argon gas pressurized (1000 psi) polycarbonate vessel, simulating hydrostatic stress of 1,875 foot depth, was utilized. Cleat frequency and distribution was examined for two cores via micro-focused X-ray computed tomography. Evaluations occurred before and after microwave exposure with and without the application of hydrostatic stress during exposure. Optical microscopy was performed for tomography cleat aperture calibration and also to examine any lithotypes influences on

fracture: initiation, propagation, frequency, and orientation. It was confirmed that new fractures are induced via high-energy microwave exposure in an unconfined bituminous core and that the aperture increased in existing cleats. Cleat/fracture volume, following microwave exposure increased from 1.8% to 16.1% of the unconfined core volume. For the first time, similar observations of fracture generation and aperture enhancement in coal were also determined for exposure under hydrostatic stress conditions. An existing cleat aperture increased from 0.17 mm to 0.32 mm, after short microwave-bursts occurring under a simulated hydrostatic stress. The cleat/fracture volume increased from 0.5% to 5.5%. Optical microscopy indicated that fracture initiated likely occurred in at least some cases at fusain microlithotypes. Presumably this was due to the open pore volumes and potential for bulk water presence or steam pressure buildup in these locations. For the major induced fractures, they were mostly horizontal (parallel to the bedding plane) and often contained within lithotype bands. Thus it appears likely that microwaves have the potential to enhance the communication between horizontal wellbore and existing cleat network, in coal seams at depth, for improved gas recovery or CO<sub>2</sub> injection.

## Introduction

Coalbed and coalmine methane is both a plague and a benefit. Its presence in mines constitutes a danger of rock bursts and explosion (particularly with CO<sub>2</sub> presence), and increases the energy use for mine ventilation. Methane is also a greenhouse gas, having a more severe potential impact on the atmosphere than an equal molar amount of CO<sub>2</sub>. Yet, coalbed methane is also a highly valuable fuel that contributes 9% (2005) of the domestic methane production. It is becoming common practice to drain methane from gassy coal seams in advance of mining operations and to seek valuable coalbed methane from other seams. However, the release of methane from coal is often a slow process. In canister tests utilizing coal cores inches in diameter, it can take months for the methane gas to be released with a significant portion being retained in the coal. Residual gas has been reported as high as 32% for high-volatile bituminous coals[1]. A method is thus needed for increasing the gas release rate from coal seams. *“Increasing field permeability in coal seams requires new ideas and greater research effort”* IEA Coal Research[2]. Inducing fractures in coal with microwave energy along in-seam boreholes has the potential to increase the extraction rate and thus the economics and production of coalbed methane.

The microwave heating of pyrite has been investigated as a coal cleaning approach[3]. The differential heating of minerals and resultant different expansion rates may generate structural brittleness that may aid in crack propagation. Experiments on pulverized size cuts of coal, where the breakage planes are expected to be the cleat system, demonstrated enhanced particle comminution after microwave treatment[4]. The selective heating of a component, within a larger matrix of components, depends upon its dielectric permittivity and loss factor. Coal is relatively transparent to microwaves[5] thus water in the coal can be rapidly heated. The high-energy water molecules and steam are likely to cause fractures in the coal and perhaps widen existing cleats. However, at in-seam conditions the coal is under stress. It is not known whether the application of microwave energy in situ where the coal has confining stress will permit the induced fractures to form.

Specifically the objectives are the conduction of preliminary studies of novel concepts for unconventional gas development in coalbed methane resources, specifically microwave exposure to coal at simulated hydrostatic stress to determine if new fractures are formed, existing cleat apertures are enhanced, and the role of lithotypes on fracture formation.

To determine the pre- and post-microwave fracture network, a non-destructive approach is necessary. X-ray computed tomography is a non-destructive technique that utilizes the difference in X-ray attenuation (density and atomic number influenced) to differentiate in 3D the structure of objects. For example, in coal research Xe gas was flowed into a lump of coal under 700 torr gas pressure and images before and after exposure compared [6]. The Xe gas, with a high atomic number, attenuates the X-rays allowing it to act as a tracer for gas flow. The gas preferentially enter the coal in the regions of higher electron density [6], presumably the mineral filled more highly fractured region with preferential flow being parallel with the bedding plane for work performed on an Illinois coal at higher gas pressure [7, 8]. Subtracted image showed the preferential location of the Xe gas in the fine cracks (cleat system). Other studies have also used this approach [9-11]. Alternatively, contrast enhancement has been achieved with Wood's metal [12, 13], but this is destructive approach or by observing epigenetic minerals [14]. More recently, with advances in resolution, the cleat structure had been directly determined [15-22].

## **Methods**

### **Samples**

A bituminous coal core of 50 mm diameter from the Pittsburgh-seam was obtained. Total moisture in the coal was determined as per the ASTM standards D3302 [23]. The coal core was divided in to two cores of approximately equal length (54 mm) and were kept under argon in a foil multi-laminated bags to limit any moisture loss or coal "weathering" [24]. One sample was used for microwave exposure in the absence of simulated hydrostatic stress, the other was exposed to simulated hydrostatic stress during microwave exposure.

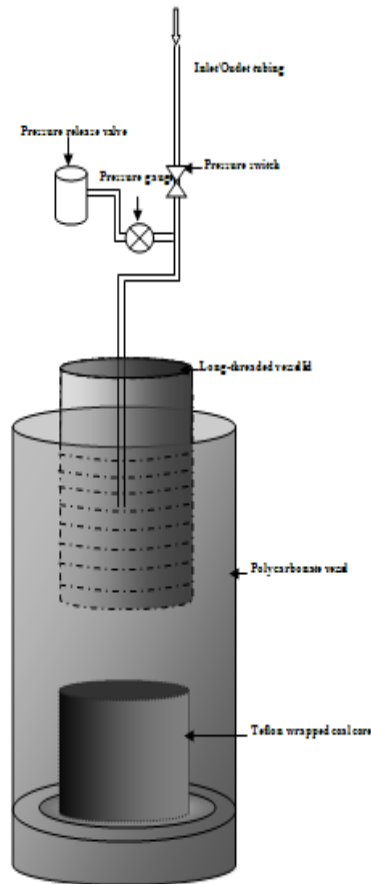
### **X-ray Computed Tomography**

An industrial X-ray CT (Universal HD-600, OMNI-X) scanner was used to obtain high-resolution coal volumetric reconstructions at 160 kV energy level with 120 or 150 mA current. Temperature was maintained via a specialized air handling system at  $76^{\circ}\text{F} \pm 1^{\circ}\text{F}$ . Volumetric scans, containing multiple stacked slices, were taken in 0.06 mm thick cross-sectional layers. Images were stored in a three dimensional matrix of  $1024 \times 1024 \times 1024$  voxels. Each voxel represents a volumetric element of  $0.056 \times 0.056 \times 0.056$  mm and

consists of a CT number (an X-ray attenuation number) that is proportional to the material density and atomic number.

### X-ray and Microwave Transparent Core Holder

No commercial X-ray and microwave-transparent core holder exist and one was



constructed specifically for this research. A high-strength glass-filled (20% silicate glass) of grade V polycarbonate microwave-transparent vessel was fabricated to contain the core (Figure 1). The core holder consisted of two parts, a long-threaded portion which contained a pressure relief valve (1000 psi) and a gas charging port. The square-cut buttress thread was half the length of the holder to ensure high-pressure gas containment. The core sat on the bottom on the holder with argon gas pressurized the surrounding space at 1000 psi. of argon gas. This gas pressure gas pressurized simulated the hydrostatic stress of 1,875 foot depth coal seam. Determination of the loss constant (Figure 2) confirmed the microwave transparent nature of the vessel.

Figure 1. Schematic of microwave- and X-ray-transparent

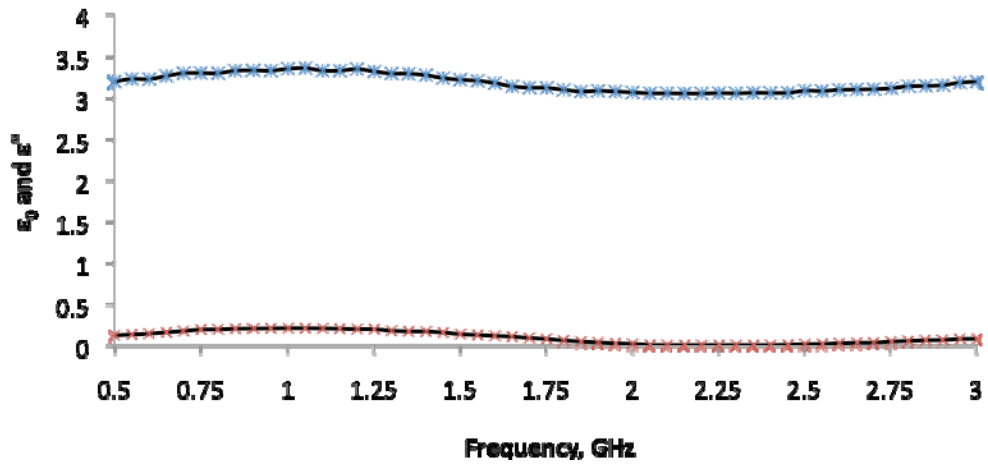


Figure 2. Variation of permittivity coefficient and loss constant with frequency

### **Microwave Exposure**

Coal cores were exposed to short-bursts of microwave energy for total of 3 seconds at 15 kW at the National Centre for Industrial Microwave Processing, The University of Nottingham, UK. X-ray CT volumetric image reconstructions were obtained for the sample prior to and after the microwave exposure. In the case of the simulated hydrostatic exposure the coal core was contained within the microwave-transparent vessel at 1000 psi argon gas pressure during exposure. Following exposure the vessel was allowed to cool prior to the slow release of the argon gas.

### **Optical Microscopy**

Following exposure, cores were impregnated with an epoxy resin in a room temperature vacuum oven until bubbling stopped. The resin was allowed to set overnight. In the case of the pressure vessel, resin impregnation occurred within the vessel to avoid handling damage. Selective surfaces, from the X-ray CT volumetric reconstruction, of the coal were cut and polished. Surface mosaics were obtained using optical microscopy under oil to aid in maceral contrast [25]. A Zeiss microscope S100 (Carl Zeiss, Jena, Germany) equipped with Zeiss Axicam HRC color camera (Carl Zeiss, Jena, Germany) was used to acquire the images of cut coal sections. Oil immersion objective lens of 32X and eyepiece of 10X were used for magnification. The stage of the microscope was programmed for movement in horizontal plane with automated control. Cleat aperture, lengths, and orientation were obtained from digital image analysis.

### **Image Processing and Image Analysis**

Image analysis was performed on the polished coal surfaces and on the volumetric reconstructions of the cores from X-ray CT data pre- and post microwave exposure. Cleat aperture, lengths, and orientation were obtained from digital image analysis of the surface using Adobe Photoshop with the ForeaPro4 plugin. The same software was used in image processing of the raw X-ray CT slice data. The X-ray CT data consists of multiple slices (approximately 600 slices) of X-ray attenuation numbers. As we were interested in volumetric data, the non-coal exterior data from the slice was removed using image masking. Slice rotations were also performed to better match pre-and post-exposure orientations. AVIZO software was used for 3-D visualization and quantification of cleat/fracture volumes and aperture sizes from CT data. For determining the threshold value to distinguish between cleat/fracture and coal, apertures obtained from AVIZO were calibrated with optical microscopy observations. Optical microscopy had a much higher resolution (about 1 micron with the optics used) than the X-ray CT had a resolution of <56 microns. For a larger single cleat, aperture calibrations were in agreement at a CT threshold of 1750. This value was used for volumetric fracture/cleat determinations. Cleat and fracture apertures were measured perpendicular the plane of the cleat.

### **Results and Discussions**

Figure 3 shows a virtual vertical slice region of a volumetric reconstruction for the core (microwave exposed without stress) pre- and post-exposure. From this and other volumetric reconstructions, the induced fractures tended to be contained mostly in the horizontal (bedding) plane similar to earlier observations [26]. The fracture volume increases from 1.8% to 16.1% for this core not exposed under stress. The core under 1000 psi simulated hydrostatic pressure during microwave exposure increased from 0.5% to 5.5%. The fracture map is shown in Figures 4. There were cleats in both cores prior to microwave exposure. After exposure new fractures were present (three vertical and six horizontal) in the case of the samples exposed while under simulated hydrostatic stress. Similarly new fractures were also induced in the core without application of stress during exposure.

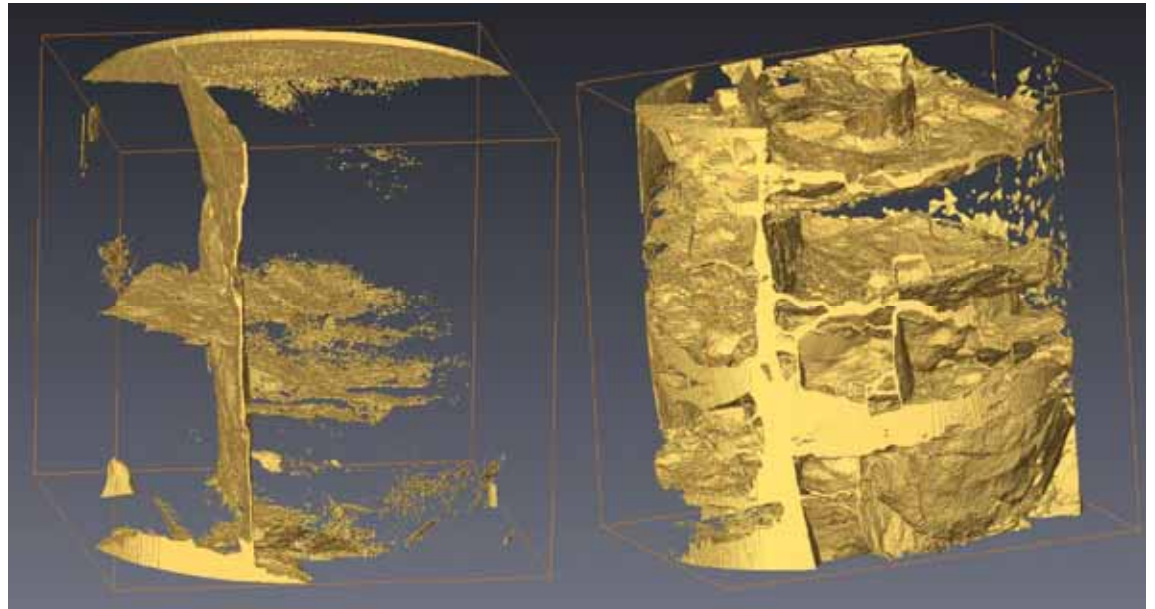


**Figure 2. Fracture map of the unconfined coal core before (left) and after (right) microwave exposure**

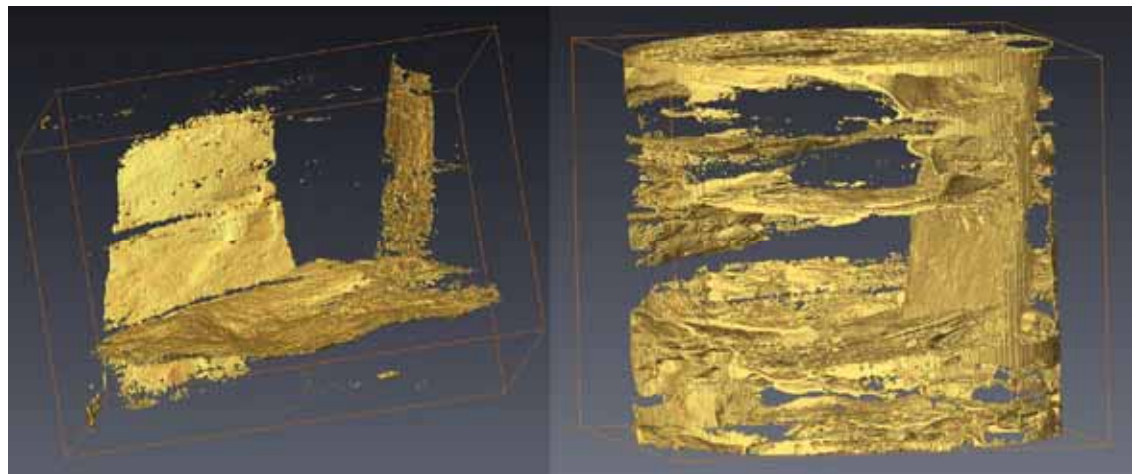


**Figure 4. Fracture map of the confined coal core before (left) and after (right) microwave exposure**

The expectation was for fractures to be generated in the vertical planes similar to the natural process; however, the new fractures generated from the microwave bursts were more frequently in the horizontal/bedding plane. This relationship is likely to be stress dependant as in the case of hydrofracking where at lower stress (shallower depth) vertical fractures may occur[27].

Apertures of the cleats, before and after exposure, and induced fracture were measured utilizing AVIZO software. The aperture increase 62% for the major cleat present while an increase of 106% was observed for the horizontal fracture (determined from the average apertures across 7-10 sections within the field of view, measured perpendicular to the fracture plane) as shown in Figure 5. Thus, existing cleats/fractures were enhanced by microwave exposure and new fractures were also created. The core also deformed during exposure with noticeable volumetric expansion, being greater at the core top. Normalized length is used for the comparison between pre and post measurement; as the fracture volume increased, the core expanded. The normalized length does assume proportional expansion rather than the spatially-specific expansion observed. However, as the aperture enhancements are spectacular the error is minimal. The aperture enhancements were not uniform between fractures or necessarily along fractures. The expansion ranged from approximately 400% to 100%. At the core edges, lost material is responsible for the larger gain observed in the post-exposure fracture 1 (Figure 5).

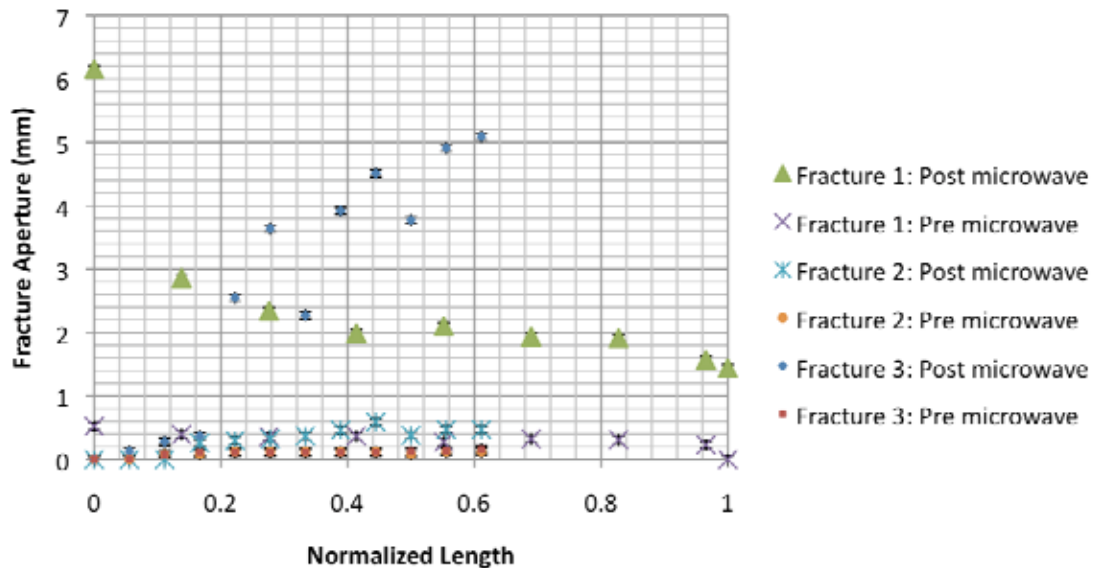


**Figure 5 Fracture apertures before and after microwave exposure without confining stress during exposure**

The gains are less extensive in the core that was stressed during exposure, where the gain may have been 250% for the single existing cleat (Figure 6). Error bars are generous, reflecting the resolution of the X-ray CT experiment at these conditions. Following microwave exposure,

the cleat aperture was remarkably uniform with regard to aperture, despite the cleat originally having a less uniform aperture.

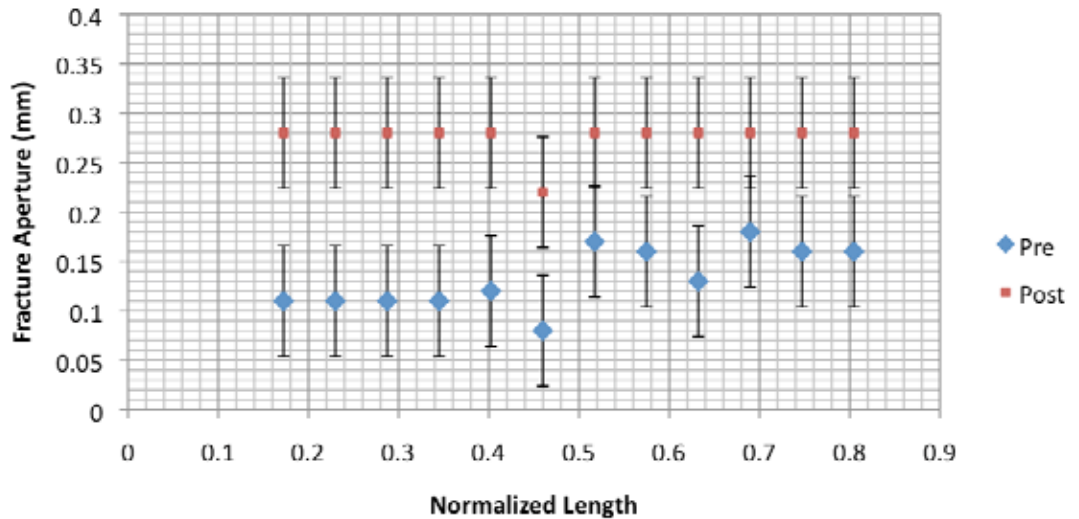


**Figure 6 Fracture apertures before and after microwave exposure under hydrostatic stressed (1000 psi) conditions.**

The fracture aperture distributions of two nascent fractures created by microwave exposure, under simulated hydrostatic stress conditions, are shown in Figure 7. The fracture had been occluded by the particles/fines generated during fracturing; occasionally the fracture apertures may be reduced due to coal slippages. The Core had expanded in the horizontal and vertical directions after the microwave exposure. However, it is unlikely that the occlusion occurs throughout the fracture (may be slice specific) and, indeed, may aid in preventing fracture closure/healing. In comparison, natural cleats tend to have uniform more aperture distributions beyond the length scales explored here. It was observed that some coal particles have dropped into the fractures. These particles may act as a proppant, if fracturing is carried out under in situ conditions. Alternatively, excessive fine generation is undesirable due to fracture plugging.

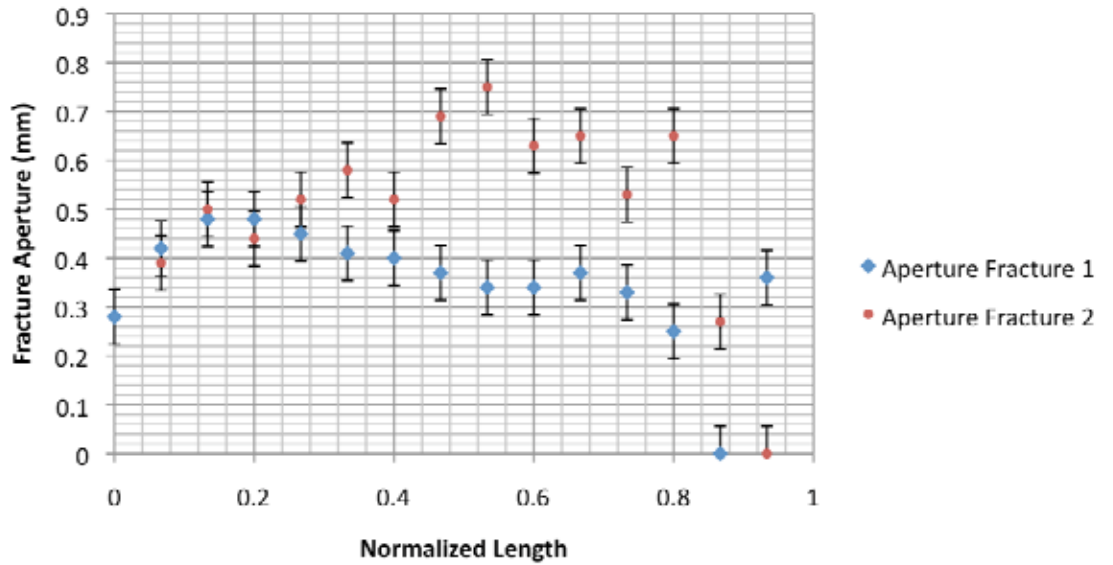


**Figure 7 Fracture apertures of new generated fractures after microwave exposure under hydrostatic stressed (1000 psi) conditions**

Fracture aperture distribution for three newly generated fractures has been shown in the Figure 8, showing that the microwave fracturing is heterogeneous. Fracture apertures show a range of values that could be the affect by fracture initiation/termination location, lithotypes, cleat propensity (length of fracture), moisture content, mineral influences, or some combination thereof. The shape of the fracture may aid in retaining open porosity while under confining stresses.

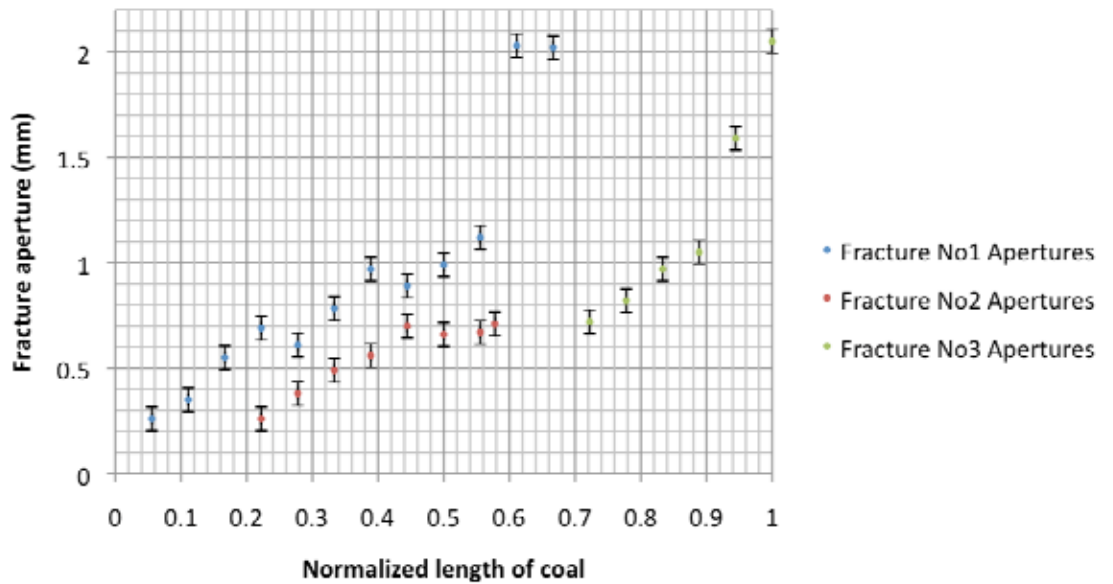


**Figure 8 Fracture apertures of new generated fractures in horizontal plane after the microwave exposure under no stress.**

The anisotropic nature of the induced fractures of the coal is likely dependent on the presence of lithotypes. Lithotypes are expected to have different fracturing strength, fracturing tendency, type and direction of failure, moisture content, porosity, and mineral content. Hence lithotypes are expected to play a role in artificial fracturing by microwave exposure. Optical microscopy was utilized in deciding the role of the microlithotype during the artificial microwave fracturing process. Optical microscopy of a polished surface of the post-microwave core produced a mosaic image of 5 assembled micrographs capturing a portion of the surface with high-resolution 600 pixels per mm in (11346 x 5848 pixels region) shown in Figure 9. The blue is false-colored to aid in identification of the resin fill. This area was selected as the likely initiation location for some major induced fractures. The fracture area was 24% of the region of view (Figure 9). New fractures were likely initiated at highly reflecting macerals at this location. These fractures appear to have propagated through vitrinite bands within the lithotype and merged into the existing cleat system. The fractures in the top right hand region appear to work along and across the fusinite or semifusinite banding. Inherently inertinite macerals are friable, and can shatter through thermal shock [28]. In Figure 9, the widest fractures

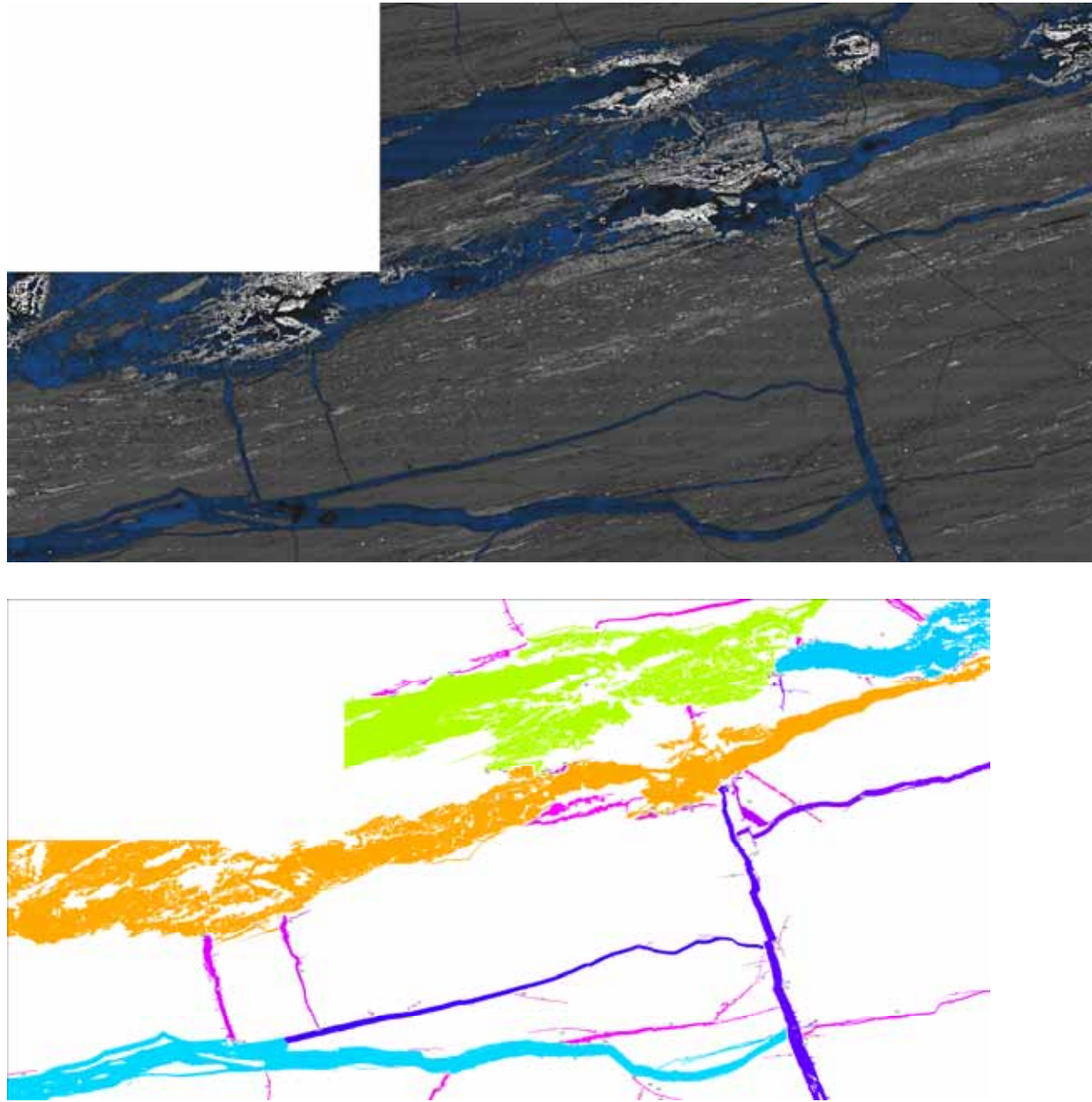


Figure 5. Mosaic of micrographs obtained from a bituminous coal surface following microwave exposure. Cleats and fractures are false-colored in blue. (upper micrograph) and false coloring by their aperture (lower).

appear between inertinite domains. However more work will be needed to support fracture initiation mechanism. In terms of microlithotype composition, the thicker vitrinite bands readily fracture along and across the bands. It is unclear if it is the bulk water in macropores or the more widely dispersed bound water in micropores that is responsible for the majority of the fracturing. However, high micropore methane pressure is thought to be one of the cleat formation mechanisms [29]. Alternatively, high macropore surfaces may yield steam condensation sites and limit the duration of the enhanced stress. In the field, the presence of methane reduces the strength of coal [30] and the fracturing may be enhanced beyond these observations.

Microscopy observation of the hydrostatically stressed core (during microwave exposure) show that the microwave-induced fractures are of type I mode opening [31]. In addition, it can be postulated that the water present in the lithotype rapidly converts into super-heated steam during microwaving at high power densities. The super-heated steam develops differential pressure inside the pore network of the coal generate potential sites for fracture generation. These fractures propagate in the weak lithotype banding until they intersect the natural fracture system, where they terminate. Elevated pore pressure is one of the proposed mechanisms for opening-mode fracture creation (in a compressive stress state) when hydrocarbon gas generation is sufficient. Alternatively, high macropore surfaces may yield steam condensation sites and limit the duration of the enhanced stress. Also in coalbeds, the presence of methane reduces the strength of coal [32]. Thus fracturing may be enhanced beyond the observations here. Microscopy observation of the hydrostatically stressed core (during microwave exposure) indicate the microwave-induced fractures are of type I mode opening (wider at one “end”). This is important for in situ conditions where a constant overburden stress may close some of the formed fractures. Mode I openings will likely remain open.

### **Potential Applications of Microwave Energy for ECBM**

Microwave induced fracturing have applicability in horizontal coal drilling where the microwave burst fractures would allow greater communication for methane degasification or to enhance CO<sub>2</sub> injectability. In Australia, for gassy seams, extensive borehole networks may be employed in advance of mining. These boreholes are potential access sites for the microwave bursts. Microwave generator and antenna can be sent to the desired location via these boreholes. High-energy microwave exposure to the coal would have higher connectivity and larger drainage area and hence a reduced “skin factor”. A low skin factor would allow higher productivity and

reduced pressure drop in the wellbore region in low-permeability coals. However, more work is required to decide the optimum moisture content of the coal seam for better production with microwave bursts. Should it be done as soon as seam is exposed or at some later stages of dewatering? Microwave-induced fracturing may also aid in mining productivity with easier extraction of a more heavily fractured coal. An alternative approach is to use a reduced diameter drill (lower cost and more rapid drilling) following with microwave-induced fracturing. However, safety issues in the employment of microwave-induced fracturing technique will need to be addressed.

### **Conclusions**

The potential use of short-bursts of microwaves for developing new fractures and enhancement of cleat apertures in bituminous coal (exposed with and without application of simulated hydrostatic stress) was evaluated. It was confirmed that the exposure of microwaves to a coal core can generate new fractures and increase the existing cleat apertures for an un-stressed core. Similar observations were found in the coal core under simulated hydrostatic stress during microwave exposure, indicating there is potential to use microwave exposure for improved connectivity between horizontal wellbore and coal seam. Cleat/fracture volume, determined from micro-focused X-ray computed tomography, following microwave exposure increased from 1.8% to 16.1% of the unconfined core volume. The cleat/fracture volume increased from 0.5% to 5.5% for the core exposed while under simulated hydrostatic stress. Induced fractures were often horizontal and terminated at the existing cleat system. Cleat aperture enhancements were also noted.

### **References**

[1] Eddy, G. E.; Rightmire, C. T.; Bryer, C. W. Relationship between methane content of coal rank and depth: Theoretical vs. observed, SPE/DOE 10800, SPE/DOE Unconventional Gas Recovery Symposium, Pittsburgh, PA, 1982; Pittsburgh, PA, 1982.

[2] Creedy, D. P.; Saghafi, A.; Lama, R., *Gas control in underground coal mining*. IEA\_Coal\_Research: London, 1997; p 1-119.

- [3] Uslu, T.; Atalay, U., Microwave heating of coal for enhanced magnetic removal of pyrite, *Fuel Processing Technology* (2004) 85, 21-29.
- [4] Lester, E.; Kingman, S., Effect of microwave heating on the physical and petrographic characteristics of a U.K. coal, *Energy & Fuels* (2004) 18, 140-147.
- [5] Lester, E.; Kingman, S.; Dodds, C., Increased coal grindability as a result of microwave pretreatment at economic energy inputs, *Fuel* (2005) 84, 423-427.
- [6] Mayolotte, D. H.; Lamby, E. J.; Kosky, P. G.; St. Peters, R. L., Computed tomography of coal during pyrolysis, *International Conference on Coal Science*, Oviedo, Spain, (1981), 612-617.
- [7] Mayolotte, D. H.; Kosky, P. G.; Lamby, E. J.; Spiro, C. L.; Davis, A.; Bensley, D. F., Applications of X-ray computed-tomography to coal studies, *Prepr. Pap. - Am. Chem. Soc., Div. Fuel Chem., St. Louis, Missouri*, (1984), 29, 44-54.
- [8] Mayolotte, D. H.; St. Peters, R. L.; Kosky, P. G.; Spiro, C. L.; Lamby, E. L.; Davis, A., Coal characterization by X-ray computed tomography, *Proceedings of the 1983 International Conference on Coal Science*, August 15-19th, Pittsburgh, U.S., (1983), 659-662.
- [9] Ertikin, T.; Radovic, L. R.; Steele, W. A.; Davis, A.; Grader, A.; Mitchell, G. D. Adsorption and transport in coalbed reservoirs, *Quarterly Report (Dec. 1990 - Feb. 1991)*; The Pennsylvania State University for the Gas Research Institute: 1991.
- [10] Karacan, C. O.; Okandan, E., Fracture cleat analysis of coals from Zonguldak Basin northwestern Turkey relative to the potential of coalbed methane production, *International Journal of Coal Geology* (2000) 44, 109-125.
- [11] Karacan, C. O.; Okandan, E., Adsorption and gas transport in coal microstructure: investigation and evaluation by quantitative X-ray CT imaging, *Fuel* (2001) 80, (4) 509-520.

- [12] Pyrak-Nolte, L. J.; Montemagno, C. D.; Nolte, D. D., Volumetric imaging of aperture distributions in connected fracture networks, *Geophysical Research Letters* (1997) 24, (18).
- [13] Montemagno, C. D.; Pyrak-Nolte, L. J., Fracture network versus single fractures: Measurement of fracture geometry with X-ray tomography, *Physics and Chemistry of the Earth Part a-Solid Earth and Geodesy* (1999) 24, (7) 575-579.
- [14] Kumar, R.; Rundwal, V. C.; Das, T. K., Identification of coal cleats/fractures using 2D and 3D imaging computed tomography, *SPE India Oil and Gas Conference and Exhibition, New Delhi, India, (1998), 6.*
- [15] Van Geet, M.; Swennen, R., Quantitative 3D-fracture analysis by means of microfocus X-ray computer tomography ( $\mu$ CT): an example from coal, *Geophysical Research Letters* (2001) 28, (17) 3333-3336.
- [16] Bossie-Codreanu, D.; Wolf, K.-H. A. A.; Ephraim, R., A new characterization method for coal bed methane, *Geologica Belgica* (2004) 7, (3-4) 137-145.
- [17] Tsotsis, T. T.; Patel, H.; Najafi, B. F.; Racherla, D.; Knackstedt, M. A.; Sahimi, M., Overview of laboratory and modeling studies of carbon dioxide sequestration in coal beds, *Ind. Chem. Res* (2004) 43, 2887-2901.
- [18] Saites, F.; Guo, R.; Mannhardt, K.; Kantzas, A., Laboratory evaluation of transport phenomena in coal for coalbed methane production, *Footiny, (2005),*
- [19] Mazumder, S.; Wolf, K.-H. A. A.; Elewaut, K.; Ephraim, R., Application of X-ray computed tomography for analyzing cleat spacing and cleat aperture in coal samples, *International Journal of Coal Geology* (2006) 68, 205-222.
- [20] Saites, F.; Guo, R.; Mannhardt, K.; Kantzas, A., Coal characterization and transport phenomena in coalbed, *CHISA, (2006),*

- [21] Saites, F.; Wang, G.; Guo, R.; Mannhardt, K.; Kantzas, A., Coalbed characterization studies with X-ray computerized tomography (CT) and micro CT techniques, Canadian International Petroleum Conferences, Calgary, Alberta, Canada, (2006), Paper 2006-027, 1-15.
- [22] Wolf, K.-H. A. A.; van Bergen, F.; Ephraim, R.; Pagnier, H., Determination of the cleat angle distribution of the RECOPOL coal seams, using CT-scans and image analysis on drilling cuttings and coal blocks, *International Journal of Coal Geology* (2008) 73, (3-4) 259-272.
- [23] ASTM, International, D3302/D3302M - 10, Standard Test Method for Total Moisture in Coal, (2010).
- [24] Glick, D. C.; Mitchell, G. D.; Davis, A., Coal sample preservation in foil multilaminate bags, *International Journal of Coal Geology* (2005) 63, (1-2) 178-189.
- [25] Lester, E.; Watts, D.; Cloke, M., A novel automated image analysis method for maceral analysis, *Fuel* (2002) 81, (17) 2209-2217.
- [26] Kingman, S.; Lester, E.; Wu, T.; Mathews, J. P.; Bradshaw, S., The potential of coal microwaving in power stations to improve grindability, *International Conference on Coal Science and Technology*, The University of Nottingham, England, (2007),
- [27] Colmenares, L. B.; Zoback, M. D., Hydraulic fracturing and wellbore completion of coalbed methane wells in the Powder River Basin, Wyoming: Implications for water and gas production, *AAPG Bulletin* (2007) 91, (1) 51-67.
- [28] Stach E.; Mackowsky M.Th.; Teichmuller M.; Taylor G.H.; Chandra D.; Teichmuller R., *Stach's Textbook of Coal Petrology*. Stuttgart, 1975.
- [29] Rogers, R. E., *Coalbed Methane: Principles and Practice*. PTR Prentice Hall: Englewood Cliffs, N.J., 1994.
- [30] Aziz, N. I.; Ming-Li, W., The effect of sorbed gas on the strength of coal – an experimental study, *Geotechnical and Geological Engineering* (1999) 17, (3) 387-402.

[31] Laubach, S. E.; Marrett, R. A.; Olson, J. E.; Scott, A. R., Characteristics and origins of coal cleat: A review, *International Journal of Coal Geology* (1998) 35, (1-4) 175-207.

[32] Aziz, N. I.; Ming-Li, W., The effect of sorbed gas on the strength of coal — an experimental study, *Geotechnical and Geological Engineering* (1999) 17, 387-402.

The Pennsylvania State University  
The Graduate School  
Department of Energy and Mineral Engineering

**INDUCING FRACTURES AND CLEAT APERTURE ENHANCEMENT IN  
BITUMINOUS COAL VIA THE APPLICATION OF MICROWAVE ENERGY APPLIED  
UNDER HYDROSTATIC STRESS CONDITIONS**

A Thesis in  
Energy and Mineral Engineering  
by  
Hemant Kumar

© 2010 Hemant Kumar

Submitted in Partial Fulfillment  
of the Requirements  
for the Degree of

Master of Science

August 2010

The thesis of Hemant Kumar was reviewed and approved\* by the following:

Jonathan P. Mathews  
Assistant Professor of Energy and Mineral Engineering  
Thesis Advisor

Zuleima T. Karpyn  
Assistant Professor of Petroleum and Natural Gas Engineering

Phillip M. Halleck  
Retired Associate Professor of Energy and Mineral Engineering

Derek Elsworth  
Professor of Energy and Mineral Engineering

Yaw D. Yeboah  
Professor of Energy and Mineral Engineering

\*Signatures are on file in the Graduate School

## ABSTRACT

For the degassing of coal seams, either prior to mining or in unminable seams as a means to obtain coalbed methane, it is the cleat frequency, aperture, connectivity, and mineral occlusions that influence coals permeability to gases. Unfortunately, many potential coalbeds have limited permeability and thus are often marginal for economic methane extraction or limited in CO<sub>2</sub> injectivity in the case of enhanced coalbed methane production or CO<sub>2</sub> sequestration. Microwave energy has been shown to induce fractures in coal in the absence of confining stress. Here, creation of new fractures and increasing existing cleat apertures via short burst, high-energy microwave energy was evaluated for both hydrostatically stressed and unstressed North American bituminous coal cores. A microwave-transparent argon gas pressurized (1,000 psi) polycarbonate vessel, simulating hydrostatic stress of 1,800 foot depth, was utilized. Cleat frequency and distribution were examined via X-ray computed tomography before and after short burst microwave exposure for two cores with and without the application of hydrostatic stress. Optical microscopy was performed for tomography cleat aperture calibration and also to examine any lithotypes influences on fracture: initiation, propagation, frequency, and orientation. It was confirmed that new fractures are induced via high-energy microwave exposure in the unconfined core and that the aperture increased in existing cleats. Cleat/fracture volume, determined from micro-focused X-ray computed tomography, following microwave exposure increased from 1.8% to 16.1% of the unconfined core volume. Similar observations of fracture generation and aperture enhancement were determined for the stressed coal, for the first time. After the short microwave-bursts cleat/fracture volume was increased from 0.5% to 5.5% under the application of hydrostatic stress of 1000 psi. Optical microscopy indicated that fracture initiated likely occurred, in at least some cases, at inertinite. Presumably this was due to the open pore volumes and potential for bulk water presence or steam pressure buildup in these locations. For the major induced fractures, they were mostly horizontal (parallel to the bedding plane) and often contained

within lithotype bands, unlike natural cleats. Cleat aperture enhancement were observed for both cores being on the order of 400% for unstressed core and lower values of around 100% for the single cleat in the cores while exposed under stress. Thus, it appears likely that microwaves have the potential to enhance the communication between bore and existing cleat networks in coal seams at depth for improved gas recovery or CO<sub>2</sub> injection.

## TABLE OF CONTENTS

Chapter 1 : INTRODUCTION.....	1
Chapter 2 : LITERATURE REVIEW.....	4
2.1 COAL AS COALBED METHANE RESERVOIR .....	4
2.1.1 Porosity .....	6
2.1.2 Permeability .....	7
2.1.3 Inseam degasification.....	10
2.1.4 Skin effect in coalbed reservoirs .....	14
2.2 METHANE FLOW IN COALBED.....	17
2.2.1 Desorption from micropores .....	19
2.2.2 Diffusion in coal matrix .....	19
2.2.3 Darcy flow in fractures.....	20
2.2.4 Effect of fracture characteristics on coalbed methane flow .....	21
2.3 COAL ANISOTROPY TO PERMEABILITY .....	21
2.3.1 Effect of stress.....	22
2.3.2 Effect of gas content on strength of coal.....	23
2.3.3 Composition .....	23
2.3.4 Effect of CO <sub>2</sub> adsorption in coal seam .....	28
2.4 ENHANCED COALBED METHANE .....	29
2.4.2 Coalbed methane stimulation.....	30
2.5 MICROWAVE APPLICATION TO COAL .....	32
2.5.1 Rapid coke making.....	35
2.5.2 Improved pyrite separation from coal .....	35
2.5.3 Improved economics of grindability (comminution) .....	36
2.6 OPTICAL MICROSCOPY AND X-RAY CT QUANTIFICATION OF CLEATS.....	37
2.7 SUMMARY .....	40
Chapter 3 : METHODS .....	42
3.1 COAL SAMPLE .....	42
3.2 MICROWAVE AND X-RAY TRANSPARENT VESSEL .....	42
3.3 X-RAY COMPUTED TOMOGRAPHY .....	46
3.4 HIGH-ENERGY MICROWAVE BURSTS .....	47
3.5 OPTICAL MICROSCOPY .....	49
Chapter 4 : RESULTS AND DISCUSSION .....	51
4.1 FRACTURE CREATION AND APERTURE ENHANCEMENT .....	51
4.1.1 Threshold number selection .....	51
4.1.2 Fractography and fracture volume determination .....	53
4.1.3 Role of lithotypes and surface porosity.....	62
4.2 POTENTIAL MECHANISMS OF MICROWAVE-INDUCED FRACTURES.....	67
4.3 POTENTIAL APPLICATION OF MICROWAVE ENERGY FOR ECBM .....	67

Chapter 5 : SUMMARY AND CONCLUSIONS.....	69
FUTURE WORK.....	71
ACKNOWLEDGEMENTS.....	72
REFERENCES.....	73
APPENDIX.....	86

## LIST OF FIGURES

<i>Figure 2-1. The mechanism of cleat formation under fluid pressure. <math>\sigma_{max}</math> is maximum stress, <math>\sigma_{min}</math> is minimum stress and <math>P_f</math> is the fluid pressure.</i> .....	9
<i>Figure 2-2. The network patterns of cleat: <math>I_1</math> (<math>\sigma_1 &gt; \sigma_2</math>) reticular sub-pattern, <math>I_2</math> (<math>\sigma_1 = \sigma_2</math>) irregular reticular sub-pattern, <math>II_1</math> (<math>\sigma_1 &gt; \sigma_2</math>) isolated straight sub-pattern, <math>II_2</math> (<math>\sigma_1 = \sigma_2</math>) isolated S pattern and <math>III</math> random pattern. Here <math>\sigma_1 =</math> Maximum stress, <math>\sigma_2 =</math> Minimum.</i> .....	10
<i>Figure 2-3. Typical layout of underground to in-seam boreholes relative to mine workings, drilled in a fan pattern from developed roadways.</i> .....	12
<i>Figure 2-4. Schematic of methane flow dynamics in coals.</i> .....	18
<i>Figure 2-5. Plan view of coal fracture system in small units of coal matrix.</i> .....	18
<i>Figure 2-6. Illustration of the extensive four major cleat classes in coal.</i> .....	29
<i>Figure 2-7. Schematic representation of hydraulic fractured coal and issues associated.</i> .....	31
<i>Figure 2-8. . Magnetic and Electric field distribution profile in a waveguide. The half wavelength of the microwave is <math>a/2</math>.</i> .....	34
<i>Figure 3-1. Pittsburgh seam bituminous coal core with inherent fracture/cleat.</i> .....	42
<i>Figure 3-2. Variation of permittivity coefficient and loss constant with frequency.</i> .....	43
<i>Figure 3-3. Schematic and photograph of microwave and X-ray transparent polycarbonate vessel containing coal core.</i> .....	45
<i>Figure 3-4. Schematic of typical industrial microwave set-up available at NCIMP, Nottingham, UK.</i> .....	48
<i>Figure 4-1. Variation of Fracture volume percentage of the coal core pre- and post- microwave bursts under no stress with X-ray CT threshold number.</i> .....	51
<i>Figure 4-2. Variation of fracture volume percentage of the coal core pre- and post- microwave bursts under hydrostatic stress with X-ray CT threshold number.</i> .....	52

<i>Figure 4-3. Photograph of hand polishing coal surface (right) and X-ray CT reconstruction at the same location (559<sup>th</sup> slice) for the microwave-exposed while stressed coal.....</i>	<i>53</i>
<i>Figure 4-4. . X-ray CT volumetric reconstructions of slices showing a horizontal fractures and a cleat before (left) and induced fracture with enhanced apertures for existing fracture/cleats after microwave exposure for adjacent core regions (right).....</i>	<i>55</i>
<i>Figure 4-5. Fracture map of the unconfined coal core before (left) and after (right) microwave exposure.....</i>	<i>56</i>
<i>Figure 4-6. Fracture map of hydrostatically confined (1000 psi) coal core before (left) and after (right) microwave exposure. Coal matrix is transparent.....</i>	<i>57</i>
<i>Figure 4-7. Fracture apertures before and after microwave exposure without confining stress during exposure. ....</i>	<i>58</i>
<i>Figure 4-8. Fracture apertures before and after microwave exposure under hydrostatic stressed (1000 psi) conditions.....</i>	<i>59</i>
<i>Figure 4-9. Fracture apertures of new generated fractures after microwave exposure under hydrostatic stressed (1000 psi) conditions.....</i>	<i>60</i>
<i>Figure 4-10. Fracture apertures of newly generated fractures in horizontal plane after microwave exposure under no stress. ....</i>	<i>61</i>
<i>Figure 4-11. Number of fractures in various aperture ranges observed by optical microscope... </i>	<i>63</i>
<i>Figure 4-12. Surface of the coal obtained from X-ray CT reconstructions at the desired location. Black color shows epoxy filled fracture surfaces. Highlighted portion is focused in the Figure 4-13. ....</i>	<i>64</i>
<i>Figure 4-13. Mosaic of micrographs obtained from the vertical bituminous coal surface following microwave exposure. Cleats and fractures are false-colored in blue (upper) and false coloring by their aperture (lower). ....</i>	<i>65</i>
<i>Figure 4-14. Fracture and mineral grain interactions for the coal stressed while exposed. ....</i>	<i>66</i>

**LIST OF TABLES**

<i>Table 2-1. Characterization of microstructures observed in coal using SEM.....</i>	<i>7</i>
<i>Table 2-2. Summary of macerals of hard coals. ....</i>	<i>25</i>
<i>Table 2-3. Types and lithotypes of bituminous coals. ....</i>	<i>27</i>
<i>Table 4-1. Relative classification of fractures identified in Figure 4-10. ....</i>	<i>62</i>

## **ACKNOWLEDGEMENTS**

I would like to express my heartfelt gratitude to my thesis advisor, Dr. Jonathan P. Mathews for his guidance and support throughout the duration of the project. I would like to acknowledge the support and knowledge transfer from Dr. Phil Halleck and Gary Mitchell. I would also like to express my gratitude to Dr. Ed Lester and Dr. S. Kingman of University of Nottingham, UK for permitting me to use their laboratory facility at National Centre for Industrial Microwave Processing, UK. This work was supported by Research Partnership to Secure Energy of America (RPSEA). Funding for this project is provided through the "Ultra-Deepwater and Unconventional Natural Gas and Other Petroleum Resources Research and Development Program" authorized by the Energy Policy Act of 2005.

I am indebted to my grandfather, Nand Lal Sharma for being the endless source of inspiration and encouragement.

## **Chapter 1 : INTRODUCTION**

Commercial-scale coalbed methane (CBM) production in the U.S. started in 1980 and is now extracted mainly from three basins: San Juan, Powder River and Black Warrior with production ranging from 115-1,000 Bcf/year initially (King and Long, 2007). Coalbed Methane has become a significant energy source, supplying 9% of U.S. domestic natural gas production in 2006 (Kendell, 2007; King and Long, 2007) . Coalbed methane annual production is increasing at the rate of 20% percent for the past 15 years (Thakur). Natural gas consumption in United States was 21.7 Tcf in 2006, the majority from domestic production (~97%) (Energy Information Administration, 2009). The Energy Information Administration (2006) determined 157.9 Tcf CBM U.S. recoverable reserves, which indicates that CBM could fulfill significant energy demand i.e. 7-8 years with current consumption rate.

It is also advantageous for coal degasification to be performed prior to underground mining to reduce risk of explosion, outbursts, and high-methane level work stoppages. Further, degasification improves coal productivity, and reduces ventilation expense as well as coal mining greenhouse gas emissions (Thakur). For example, Coalmine methane generated ~10% of U.S. anthropogenic methane emissions in 2004 with global contributions being 10% (Talkington and Schultz, 2004). Clearly, the benefits of domestic gas production impact climate change and energy security. Lower greenhouse gas emission may be achieved by using natural gas for electricity generation rather than coal. The average emissions rates in the United States from natural gas-fired generation are: 1135 lbs/MWh of carbon dioxide, 0.1 lbs/MWh of sulfur dioxide, and 1.7 lbs/MWh of nitrogen oxides (U.S.-E.P.A., 2000). The average emission rates in the United States from coal-fired generation are: 2,249 lbs/MWh of carbon dioxide, 13 lbs/MWh of sulfur dioxide, and 6 lbs/MWh of nitrogen oxides (U.S.-E.P.A., 2000). Compared to the average air emissions from coal-fired generation, natural gas produces half as much carbon

dioxide, less than a third as much nitrogen oxides, and one percent as much sulfur oxides at the power plant (U.S.-E.P.A., 2000). Mining, cleaning, and transporting coal to the power plant generate additional emissions. So natural gas burning power plants are more plausible solution to reduced greenhouse gas emissions.

Currently, San Juan basin dominates CBM reserves with 43% of the total reserves followed by Raton (14%), Powder River (12%), Black Warrior (11%) and Central Appalachian (10%) basins. In 1999, San Juan basin produced approximately 1,006 Bcf of coalbed gas, or 80% of the net coalbed production in the US (Ayers, 2002). The San Juan basin is the largest producer, 66% of total CBM production (20,006 Bcf) in the U.S, other basins contributed less: Powder River (12%), Black Warrior (9%), Central Appalachian (4%), Uinta (4%) and Raton (3%) (King and Long, 2007). San Juan basin being the most profitable among the all coal basin because of its high gas content, permeability, and thick coal seams (~1,000 feet total) (Halliburton, 2008). Coal of the San Juan basin is high volatile A bituminous or higher rank and bituminous coal commonly offers both high gas content and methane transmissibility (Gamson, Beamish and Johnson, 1993).

Many potential coalbeds have limited permeability in the absence of stimulation and thus are often marginal for economical coalbed methane. The methane content of the coal can be extracted profitably if the seam is dewatered and permeable paths establish between seam and wellbore (Rogers, 1994). It is common to stimulate the coalbed reservoir for economic extraction of coalbed methane (Rogers, 1994). There are several ways to stimulate the reservoirs: a) Vertical bore hole with multiple in-seam bore holes, b) Hydraulic fracturing of the coal seam, c) Open hole cavity completion and d) enhanced coalbed methane production via N<sub>2</sub> and/or CO<sub>2</sub> injection. The last option has the benefit of reducing the greenhouse gas emissions. However, the injectivity

of CO<sub>2</sub> in coal is very limited because of its inherently low permeability and swelling nature of the coal with CO<sub>2</sub> adsorption.

Microwaves are electromagnetic waves between 0.3 to 300 GHz and corresponding wavelengths ranging from 1m to 1 mm (Sutton, 1989). Microwaves have been utilized for improved coal grindability (Lester, Kingman and Dodds, 2005), rapid coke making (Lester, Kingman, Dodds and Patrick, 2006), coal drying (Lester and Kingman, 2004) and removal of pyrite from coal (Uslu and Atalay, 2004). High power microwave energy can produce changes in coal such as cracks and fractures (Wu, Lester, Kingman and Dodds, 2005).

Cleats and fractures are primary conduits for fluid flow in the coal permeability. Application of confining pressure has an effect on cleat permeability. Cleats/fractures tend to close under increasing confining pressure resulting into lower permeability (Gash, Volz, Potter and Corgan, 1993).

The objective of this study is to evaluate the potential of microwave in generating new fractures and increasing the cleat/fracture apertures under in situ conditions.

## **Chapter 2 : LITERATURE REVIEW**

### **2.1 COAL AS COALBED METHANE RESERVOIR**

Coal was formed from millions of years of swamp deposition under high pressure and high temperature in anoxic environments (Stach E., Mackowsky M.Th., Teichmuller M., Taylor G.H., Chandra D. and Teichmuller R., 1975). The warmer and wetter climate of Upper Carboniferous age assisted in growth of more flora and the dominant forest swamps (Stach E., Mackowsky M.Th., Teichmuller M., Taylor G.H., Chandra D. and Teichmuller R., 1975). Some of the coal swamps were created because of marine regression while others were created as a result of transgression (Stach E., Mackowsky M.Th., Teichmuller M., Taylor G.H., Chandra D. and Teichmuller R., 1975). Prolonged pressure and higher temperature resulted in the metamorphosis of parent organic material (humus) forming water logged peat bed (Van Geet and Swennen, 2001). Increasing compression forces, induced from continuous sediment deposition, forced water to leave the peat and at the same time allowed complex chemical and polymerization reaction in peat mass (Bustin, Cameron, Grieve and Kalkreuth, 1985; Stach E., Mackowsky M.Th., Teichmuller M., Taylor G.H., Chandra D. and Teichmuller R., 1975).

The development of lignite, bituminous, subbituminous and anthracite from peat occurs through 'coalification'. Higher temperature being dominant factor for more matured coal, however, pressure also plays an important role (Van Geet and Swennen, 2001). During this transformation, coal expels water, has reduced oxygen content and becomes enriched in carbon. Loss of moisture and burial stress decrease porosity and increase optical anisotropy parallel to the bedding planes (Van Geet and Swennen, 2001). During coalification, temperature has a greater effect than overburden pressure after a significant amount of moisture is lost, resulting in a less compressible lignite or subbituminous coal (Van Geet and Swennen, 2001). As the moisture

content decreased, the calorific value of the coal increased. Calorific value was further enhanced by thermal decomposition of hydroxyl (-OH), carboxyl (-COOH), methoxyl (-OCH<sub>3</sub>), carbonyl (>C=O) and ring oxygen (Stach E., Mackowsky M.Th., Teichmuller M., Taylor G.H., Chandra D. and Teichmuller R., 1975). Lignin and cellulose were transformed into humic acids and they were eventually transformed to form alkali-insoluble 'humines'(Stach E., Mackowsky M.Th., Teichmuller M., Taylor G.H., Chandra D. and Teichmuller R., 1975). As a result of this transformation, coal became black and lustrous during the gelification (vitrinization) stage of hard brown coal.

Coalbeds are commonly self-sourcing and low permeability (on the order of milli Darcy or  $10^{-16}$  m<sup>2</sup>) gas reservoirs. More than 98 % of the methane gas is located in the micropores of the coal-matrix depending on the gas pressure (Gray, 1987a). The concentration gradient of methane in coal matrix is responsible for its flow into the cleat system via diffusion after water removal and depressurization (Nandi and Walker Jr, 1970; Rogers, 1994). Coal is an important source rock as well as reservoir rock for coalbed methane. Coal acts as a source rock in coalbed methane reservoirs and may retain a fraction of the gas they generate (per unit volume) (Wang, Pang, Lu and Chen, 1997); however this fraction may represent two to seven times more gas than a similar size conventional gas reservoir (Levine, 1993; Rogers, 1994). Coal offers very high surface area (1 million sq ft/lb<sub>m</sub>) for natural gas adsorption, which results in adsorption density approaching that of liquid methane (Kuuskraa and Brandenburg, 1989; McElhiney, Koenig and Schraufnagel, 1989; Nandi and Walker Jr, 1970; Rogers, 1994). Economic success is influenced by three parameters: permeability, porosity, and gas content. Coalbed methane reservoir offers these three as cleats/macropores, micropores, and self-sourcing gas (Gray, 1987a; Gray, 1987b).

### **2.1.1 Porosity**

Three porosity types are present in coal: fracture porosity, phyteral porosity and matrix porosity (Gamson, Beamish and Johnson, 1993). Fracture porosity is often associated with bright coal banding,. However, microfractures are also present in maceral fragments from dull coals (Gamson, Beamish and Johnson, 1993). There are five types of fracture porosity (three macrofracture and five microfracture) present in coals described in the Table2-1 (Gamson, Beamish and Johnson, 1993). Cellular structures (lumen, splinters) of plants present in the coals offer the void space, acting as microcavities referred as phyteral porosity (Gamson, Beamish and Johnson, 1993). The large-sized pores contribute to the permeability (Gash, Volz, Potter and Corgan, 1993).These pores are of three types as shown in Table 2-1.

Table 2-1. Characterization of microstructures observed in coal using SEM.

Microstructures	Width of pathways ( $\mu\text{m}$ )	Length of pathway ( $\mu\text{m}$ )	Spacing ( $\mu\text{m}$ )	Orientation	Association
<i>Fracture Porosity</i>					
<i>Macrofracture</i>					
Face and Butt cleat	100-2000	100-	300-2000	Perpendicular to bedding	Restricted to bright
<i>Microfracture</i>					
Vertical microcleats	05-20.0	50-500	30-100	Perpendicular to bedding	Restricted to bright
Horizontal microcleats	0.5-2	50-300	10-May	Parallel to bedding	Restricted to bright
Blocky features	01-15.0	50-200	<100	Irregular	Restricted to bright
Conchoidal fractures	0.05-0.1	1-100	.05-.1	Irregular	Restricted to bright
Striae	0	5-100	.1-.3	Inclined 60-90 degree	Restricted to bright
<i>Phyteral Porosity</i>					
<i>Cavities associated with organic compound</i>	2.0-4.0	10-	1-20.0	Parallel to bedding	Restricted to dull
<i>Matrix Porosity</i>					
In between maceral fragments	0.05-50	0.05-50	0.05-50	Irregular	Restricted to dull
In between minute particles	0.01-0.05	0.01-0.05	0.01-0.05	Irregular	Restricted to dull
In between clays	0.1-2.0	1-20.0	Irregular	Parallel to bedding	Restricted to dull

Source: Gamson, P.D., Beamish, B.B. and Johnson, D.P., 1993. Coal microstructure and micropermeability and their effects on natural gas recovery. Fuel, 72(1): 87-99.

### 2.1.2 Permeability

Permeability is a critical parameter for economic viability of coalbed methane reservoirs. It is influenced by the frequency of natural fractures, their interconnections, degree of fissure aperture opening, direction of butt and face cleats, water saturations, burial depths, matrix

shrinkage upon desorption, and those in situ stress stimulations that affect the permeability (Rogers, 1994). Typical coal permeability is in the order of 1mD, though it varies with coal and gas used for permeability test (Gentzis, Deisman and Chalaturnyk, 2007). Permeability of the coal also varies with effective stress and pore pressure (Palmer and Mansoori, 1998). Cleats are systematic orthogonal fracture systems commonly perpendicular to bedding plane. Cleats and fractures offer pathways for migration of gas and water to the producing wellhead, and the presence/absence of cleats may enhance/retard the success of the coalbed methane production (Scott, 2002). Geological/tectonic forces, coupled with several other natural processes, lead to the formation of orthogonal cleat system during coalification. Endogenic stresses in coal, due to thermal maturation along with the concurrent tectonic stresses, are likely responsible for the observed orientation of cleats (Close, 1993; Laubach, Marrett, Olson and Scott, 1998; Laubach and Tremain, 1991; Pashin, 1998; Su, Feng, Chen and Pan, 2001). Their possible formation mechanisms have also been studied (Close and Mavor, 1991; Close, 1993; Laubach, Marrett, Olson and Scott, 1998; Levine, 1993; Pattison, Fielding, McWatters and Hamilton, 1996; Solano-Acosta, Mastalerz and Schimmelmann, 2007; Ting, 1978). Several hypotheses have been proposed e.g. intrinsic tensile forces (matrix shrinkage), fluid pressure and tectonic stress theories (Su, Feng, Chen and Pan, 2001). Coalification theory suggests that plant remains can be gelatinized under the effect of microbes, temperature and pressure, and they release large amount of fluids before becoming a plastic or semi-plastic material (Su, Feng, Chen and Pan, 2001). Fluid-release resulting in matrix shrinkage generates intrinsic tensile forces that may generate fractures. When tectonic stresses are weak and isotropic, mud-crack-like patterns will create reticular cleat pattern (Su, Feng, Chen and Pan, 2001).

Petroleum geologists postulate that coal microfractures are caused by fluid pressure transitions. (Zhang, Fang, Gao, Zhang and Jiang, 1999). During maturation, when hydrocarbons cannot be effectively released from the rock, abnormal high-fluid pressure can be created. When

this fluid pressure overcomes the yield-strength, fluid will be released by cracking the coal forming microfractures (Su, Feng, Chen and Pan, 2001). These may later 'heal' or close with overburden pressure (Su, Feng, Chen and Pan, 2001). When the fluid pressure exceeds the extrinsic effective normal stress and the fracture pressure of coal, the coal will be split along the direction of minimum stresses, and will develop into cleats along the direction of maximum stresses (Su, Feng, Chen and Pan, 2001) as shown in Figure 2-1. Face cleats extends in the direction of maximum stress while butt cleats extend along the direction of minimum stress (Su, Feng, Chen and Pan, 2001). Through-going cleats formed first and are referred to as face cleats; butt cleats end at intersections of through-going cleats that formed later (Kulander and Dean, 1993; Laubach and Tremain, 1991). When the fluid pressure is less than or equal to the effective normal stresses, the development of the cleat will terminate (Su, Feng, Chen and Pan, 2001). Face cleats are often considered extensional (opening mode) fractures, perpendicular to the least compressive principal stress that the coal was subjected to during the coalification, while, butt cleats are believed to form during relaxation of original stress field (Kulander and Dean, 1993). Face cleats form in response to coal that experiences a combination of hydraulic and high confining compressive pressure (Billings, 1954). The direction of butt cleat is approximately parallel to the axis of the original local compression (Hancock and Engelder, 1989).

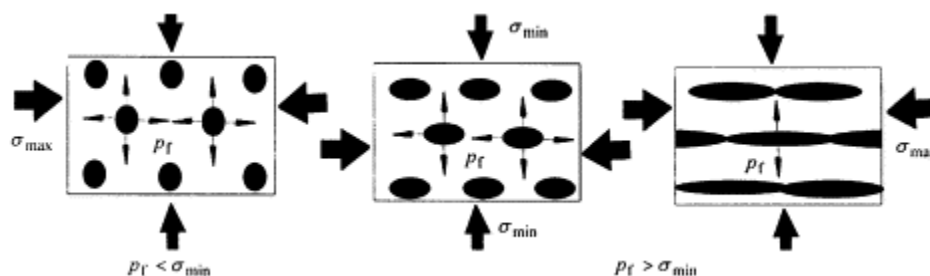


Figure 2-1. The mechanism of cleat formation under fluid pressure.  $\sigma_{max}$  is maximum stress,  $\sigma_{min}$  is minimum stress and  $P_f$  is the fluid pressure.

Source: Su, X., Feng, Y., Chen, J. and Pan, J., 2001. The characteristics and origins of cleat in coal from Western North China. *International Journal of Coal Geology*, 47(1): 51-62.

Tectonic stress theory explains the pattern of cleats in coal. During the long coalification period, several tectonic stresses worked on semi-plastic coal-mass. Strength and nature of these stresses determine the cleat pattern and their density as shown in Figure 2-2.

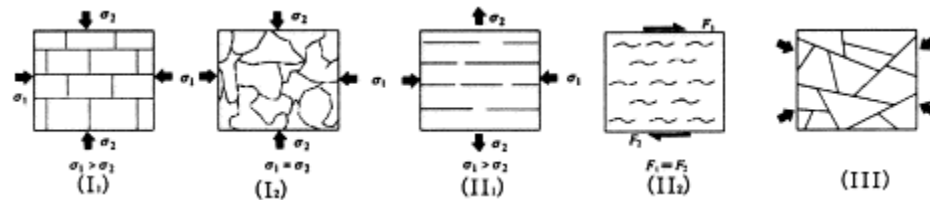


Figure 2-2. The network patterns of cleat: I<sub>1</sub> ( $\sigma_1 > \sigma_2$ ) reticular sub-pattern, I<sub>2</sub> ( $\sigma_1 = \sigma_2$ ) irregular reticular sub-pattern, II<sub>1</sub> ( $\sigma_1 > \sigma_2$ ) isolated straight sub-pattern, II<sub>2</sub> ( $\sigma_1 = \sigma_2$ ) isolated S pattern and III random pattern. Here  $\sigma_1$ = Maximum stress,  $\sigma_2$ =Minimum.

Source: Su, X., Feng, Y., Chen, J. and Pan, J., 2001. The characteristics and origins of cleat in coal from Western North China. *International Journal of Coal Geology*, 47(1): 51-62.

Cleat apertures may or may not contain authigenic minerals (commonly clays, quartz, and calcite) or organic material and resin (Daniels and Altaner, 1990; Spears and Caswell, 1986). In coalbed methane such minerals affect the diagenetic alteration of the cleat network due to precipitation of authigenic minerals and can fully occlude or preserve and open fracture pathways despite confining stress (much like a proppant), and thus reduces the ability of fractures to conduct fluid (Laubach, Marrett, Olson and Scott, 1998). In several coalbeds, paragenesis of cleat-filling minerals indicates that the development of fractures took place during coalification (Laubach, Marrett, Olson and Scott, 1998).

### 2.1.3 Inseam degasification

In active coal mining areas with high methane content or high outburst potential, coal seam degasification may be performed either prior to or during mining. Pre-mining drainage

method involves removing methane prior to mining a virgin coal seam. A continuous cleat system with moderate-to-high permeability is desirable for methane extraction (Markowski, 1998). The objective of pre-drainage is to maximize the rate of gas removal from the underground mining districts and hence minimize the gas flow into the mine airways (Creedy, Garner, Holloway and Ren, 2001). In gassy mines, the methane outbursts risk conditions becoming more common as mines reach deeper (Creedy, Garner, Holloway and Ren, 2001).

### ***2.1.3.1 Pre-mining drainage methods***

Pre-mining drainage involves drilling boreholes or bore wells from the surface into a virgin coal seam for the degasification of the seam. Pre-mining drainage is generally ineffective in low-permeability seams (Creedy, Garner, Holloway and Ren, 2001). Hydrofracture, blasting, and chemical reactions have been used in gassy Australian mines for increasing the permeability of coal (Creedy, Garner, Holloway and Ren, 2001). However, this is not typically sufficient for desirable production of coalbed methane. Pumps are installed for removing the water from the fractures and cleats to allow gas flow. Sometimes these pumps are also used to create a vacuum for better methane recovery (Creedy, Garner, Holloway and Ren, 2001). The following have been examined for increasing the permeability of a coal seam.

a) In-seam drainage from underground boreholes: This technique works in moderate-to-high natural permeability (Creedy, Garner, Holloway and Ren, 2001). If elevated methane flow occurs in coal drivages within virgin areas of a mine, the horizontal, in-seam boreholes are also likely to yield significant gas flow and hence, an underground pre-mining drainage scheme may be practical. The direction of drilling is also an important factor (Figure 2-3). Boreholes intersecting the main joints (cleats) in a coal seam at right angles may drain gas from larger

volume of coal than those drilled parallel to the face cleat direction (Creedy, Garner, Holloway and Ren, 2001; McCulloch, Deul and Jeran, 1974).

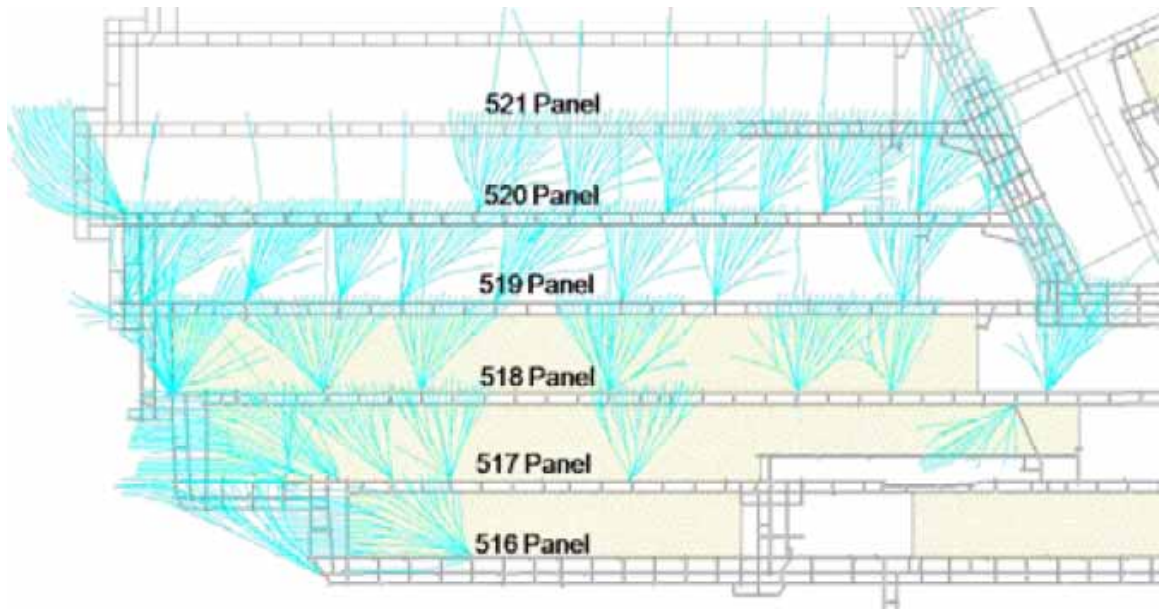


Figure 2-3. Typical layout of underground to in-seam boreholes relative to mine workings, drilled in a fan pattern from developed roadways

Source: Black, D.J., Aziz, N.I. and Florentin, R.M., 2010. Assessment of factors impacting coal seam gas production. 2010 International Coalbed and Shale Gas Symposium. University of Alabama, Tuscaloosa, AL.

For effective extraction of methane, the following parameters should be determined prior to the extraction.

- One challenge in the borehole drainage is the time available for drainage: In the case of pre-mining drainage, well-installation is done prior to mining activities so that whole in-situ methane can be extracted prior to mining or so that improved protocol allows for more rapid extraction.

In Australia the pre-degasification is extensive with different drilling patterns used for extraction depending on location (Creedy, Garner, Holloway and Ren, 2001; Florentin, Aziz, Black and Ngheim, 2010).

(i) Horizontal in-seam borehole: This method has particular success in longwall face mining (Creedy, Garner, Holloway and Ren, 2001). Depending on the mining and underground environmental constraints during development, boreholes are usually installed to function for periods of up to 12 months or greater than two years (Creedy, Garner, Holloway and Ren, 2001). In a typical arrangement horizontal boreholes are spaced 76m from the tail gate entry, perpendicular to the roadway for nearly full-length or retreat panel (Bustin and Clarkson, 1998).

(ii) Short boreholes in the mine roof: Short vertical boreholes are also drilled in the roof of headings to control emission of methane from the discrete fractures in gas-bearing sandstone (Creedy, Garner, Holloway and Ren, 2001). Where there is a frictional ignition risk in mechanized drivages, low angle boreholes are sometimes drilled in the roof to terminate ahead of the face in order to release the gas prior to mining (Creedy, Garner, Holloway and Ren, 2001).

(iii) Long horizontal in-seam borehole: In longwall panels horizontal boreholes, extending from shaft into the coal seam, are installed prior to development. Long, directionally steered in-seam boreholes can effectively reduce in-situ CBM contents of large coal volumes in advance of mining in low to high permeability of coals, as well as to drain faults and fissures containing free CBM (Thomas, 1994). Exploration is the primary purpose of these boreholes which give access to the coalbed methane.

The methane generated is used for power generation, town/industrial gas, mine site and chemical feedstock (Economic Commission, 2010). Gas engine generators are installed for producing power for mine use or grip supply.

### 2.1.4 Skin effect in coalbed reservoirs

The condition of near-wellbore region is critical in production of natural gas. Skin effect can be used as to characterize this region with steady state pressure differences that are proportional to the skin effect (Van Everdingen and Hurst, 1949). Mathematically, skin effect has no physical dimension and is analogous to the film heat transfer coefficient in heat transfer. Conveniently, the additional pressure drop associated with the skin effect is defined in terms of the same group of constants as the dimensionless solutions to the pressure drop in the porous medium. The well skin effect is thus a composite variable. In general, any phenomenon that causes a distortion of the flow would result in a positive value for the skin factor. Positive skin effect can be created by mechanical causes such as partial completion (i.e., a perforated height that is less than the reservoir height); by inadequate number perforations (again causing the distortions of the flow); by phase changes (relative permeability reduction to the main fluid); by turbulence and by damage to the natural reservoir permeability. Below is an equation for wellbore inflow

$$\frac{1}{r} \frac{\partial}{\partial r} \left( r \frac{\partial p}{\partial r} \right) = - \frac{q\mu}{\pi k h r_0^2} \text{ (Equation 2.1)}$$

$\rho$ ,  $q$ ,  $\mu$ ,  $k$ ,  $h$  and  $r_0$  represent density, flow, viscosity, permeability, height and wellbore radius.

Any phenomenon which can decrease the permeability of the reservoir around the wellbore will increase the skin effect. A negative skin effect denotes that the pressure drop in the near-wellbore zone is less than the pressure drop from the normal undisturbed reservoir mechanisms. Negative skin effect is usually due to acid fracturing or hydraulic fracturing, which increases the permeability (Economides, Hill and Ehlig-Economides, 1993). Production rate increases if the skin effect decreases. If drilling and completion decreases the permeability of the near wellbore region, then the skin factor is positive. Generally, hydraulic fracturing creates large

cracks near the wellbore region and a sudden increase may be observed in production rate. The combination of the following conditions affects the production rate for a hydrofracked well:- fracture conductivity, closure stress, proppant particle size, proppant concentration and proppant grain shape affects the production rate for a hydrofracked well (Gidley, Holditch, Nierode and Veatch, 1989). Wide and long range fractures are more conductive than narrow and short fractures. The stress transmitted from the earth to the proppant during fracture closure causes crushing of the proppant, reducing the particle size and increasing the surface the area of the proppant, both of which reduce the permeability of the propped fracture (Gidley, Holditch, Nierode and Veatch, 1989). Closure stress may also cause proppant particles to embed into the walls of a soft formation, thus decreasing the fracture width(Gidley, Holditch, Nierode and Veatch, 1989). There could be several mechanisms for positive skin factor in coalbed methane reservoir (Rogers, 1994) as discussed later on.

#### ***2.1.4.1 Particle Plugging of Pore Space***

Coal is friable and it may contain large variety of particle sizes, including very fine, fine, medium, large and very large size particles after completion. This complicated structure can be idealized as a collection of relatively large chambers, the pore bodies connected by narrower openings called pore throats. The permeability of the medium is controlled by the number and conductivity of pore throats. If the conductive pore throats are blocked by fine particles coming from the coal-matrix, then it results in significant reduction of permeability (Rogers, 1994). Fines could load the flowing fluid, increasing its viscosity and, consequently, increasing pressure drop as the more viscous fluid moves through the fracture (Rogers, 1994). Parting of the coal could create rubble and fines near the wellbore for a more tortuous flow path and further increasing the skin factor.

#### ***2.1.4.2 Fluid Damage***

Completion and fracturing fluid might damage the wellbore. The damage caused by the fluids is due either to a change in viscosity or to a change in relative permeability. Formation of emulsions can also cause damage, especially when the viscosity of the emulsion is very high (Rogers, 1994). A side effect of all fracturing operations, with gelled fluids, is the potential for formation damage from filtrate invasion at very high concentrations (Gall, Sattler, Maloney D.R. and Raible, 1988; Warpinski, Branagan, Sattler, Cipolla, Lorenz and Thorne, 1990). Adsorption and physical entrapment of polymer molecules in the coal obstructs butt and face cleats, tertiary fissures, and micropore openings to restrict methane desorption, diffusion, and Darcy flow (Rogers, 1994). Potential mechanisms that include sorption of gelled fluids or friction reducing agents over the surface of cleats may induce swelling and, therefore, may cause relatively significant reduction in permeability (Rogers, 1994). Moreover, this swelling is highly irreversible (Puri, King and Palmer, 1991). Contact of gels, friction reducers, and other polymers could be highly detrimental to coal permeability (Puri, King and Palmer, 1991). If highly effective filter cake can be formed around the wellbore, which only allows broken or filtered gelled fluids, then the damage to the permeability would be reduced to a degree. Gels and chemicals used during the hydraulic fracturing can substantially damage the permeability; however, this does not mean that hydraulic fracturing does not improve the productivity.

#### ***2.1.4.3 Mechanical Damage***

Physical crushing and compaction in the vicinity of a perforation is often unavoidable and depending on the type of the reservoir rock, may lead in substantial increase in skin factor. Collapse of the weak layers in a reservoir may also lead to mechanical damage. Uncontrolled

heavy turbulent flow may cause mechanical damage due to localized weakening of the sediment layers in a reservoir.

#### ***2.1.4.4 Biological Damage***

Some wells, particularly water injection wells, are susceptible to damage by bacteria in the near-wellbore zone. Anaerobic bacteria may grow and plug the pores (Economides, Hill and Ehlig-Economides, 1993). Byproduct of the biological activities may also produce and precipitate chemicals that can plug the pores. Biological type damages are a primary concern in biologically enhanced oil recovery methods. Biological damages are best prevented by treating injection waters with bactericides (Economides, Hill and Ehlig-Economides, 1993).

Water chemistry issues, environmental challenges in hydrofracking water disposal and access to large quantities of water during hydrofracking are challenges in stimulation approaches of coalbeds.

## **2.2 METHANE FLOW IN COALBED**

Coal, in a simplified sense for coalbed methane extraction, has dual porosity comprised of a macropore structure and a micropore structure (Krevelen, 1992; Rogers, 1994). Both are important for the transport and sorption properties of a coal seam (Ertekin and Sung, 1991). Figure 2-4 describes the most commonly used model for methane flow in coals (Rogers, 1994). Methane flow in coalbed is a three-step process: Desorption, Diffusion and Darcy's flow as shown in Figure 2-5.

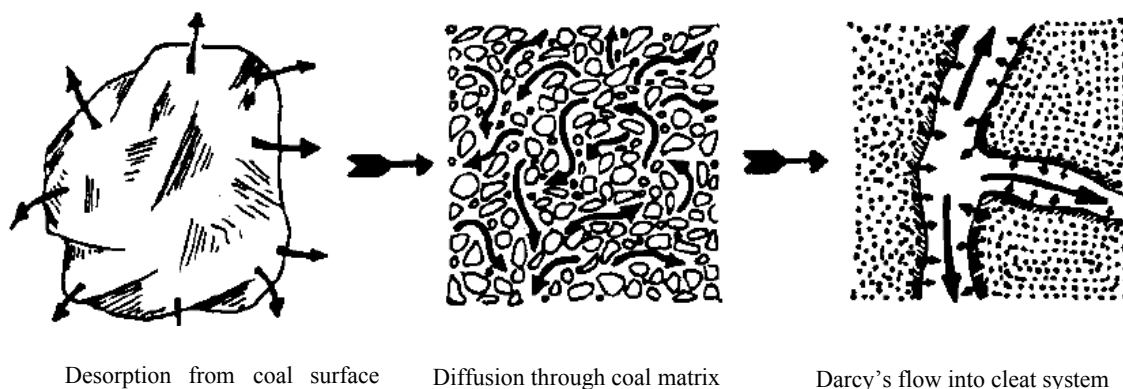


Figure 2-4. Schematic of methane flow dynamics in coals.

Source: Remner, D.J., Ertekin, T., Sung, W. and King, G.R., 1986. A Parametric Study of the Effects of Coal Seam Properties on Gas Drainage Efficiency. *SPE Reservoir Engineering*, 1(6): 633-646.

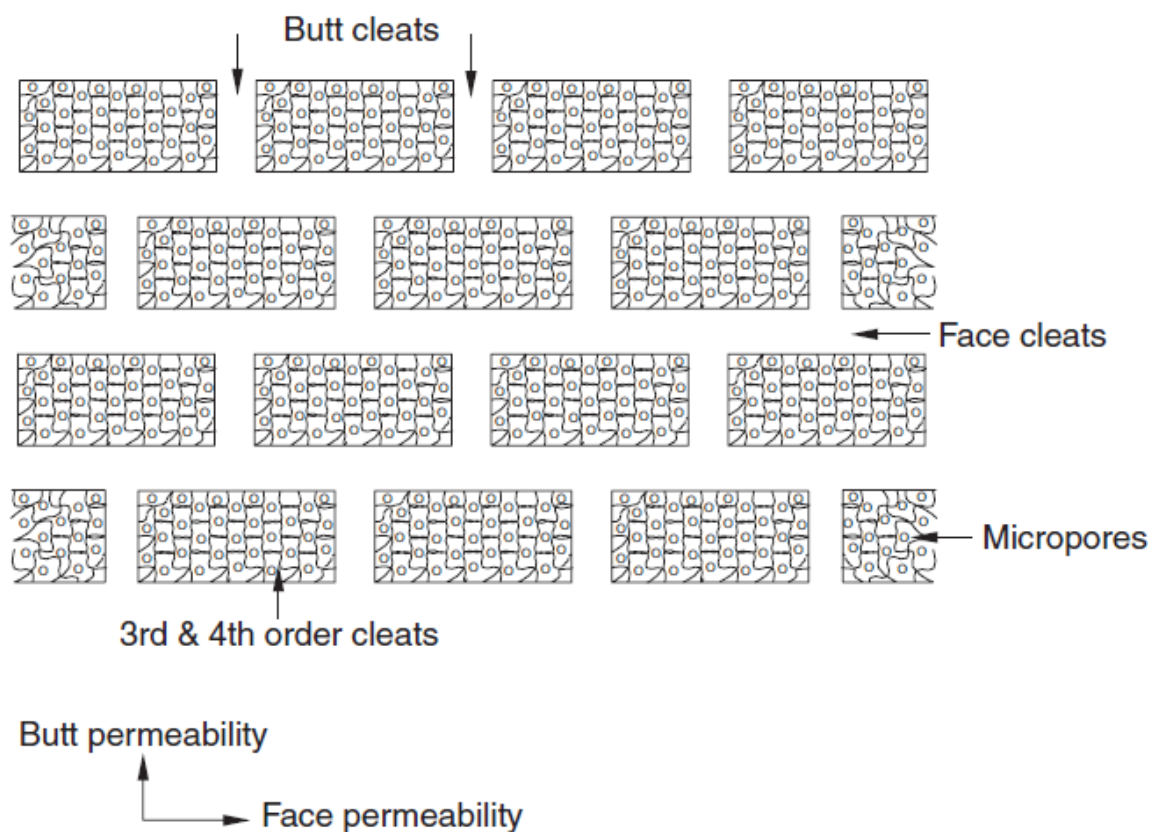


Figure 2-5. Plan view of coal fracture system in small units of coal matrix.

Source: McCulloch, C.M., Duel, M. and Jeran, P.W., 1974. Cleft in bituminous coalbeds. In: United States Bureau Mines. *U.S. Bureau Mines Report of Investigations*, pp. 74.

### 2.2.1 Desorption from micropores

Methane molecules remain adsorbed as liquid-like phase in the coal micropores (Kuuskraa and Brandenburg, 1989; McElhiney, Koenig and Schraufnagel, 1989; Nandi and Walker Jr, 1970). Adsorption due to weak Vander Waals forces allows methane to desorb readily at lower adsorption pressures (McCulloch, Deul and Jeran, 1974). Langmuir's theory for single-layer sorption can be used to approximate the equilibrium sorption isotherms (Langmuir, 1916). It assumes inelastic collisions between gaseous and solid molecules. At equilibrium condition, the rate of adsorption becomes equal to the rate of desorption. Langmuir derived this as equation 2.2.

$$V_E(p) = V_\infty p / (p + p_L) \text{ (Equation 2.2)}$$

Where  $V_E$  represents the amount of gas adsorbed at gas pressure  $p$ . The pressure constant  $p_L$  is a measure of residence time.  $V_\infty$  represents the maximum amount of gas that can be adsorbed.

### 2.2.2 Diffusion in coal matrix

Desorbed methane molecules from the coal's surface diffuse through the micropores via three mechanisms: bulk, Knudsen or surface diffusion. This could happen through a single mechanism or combination of mechanisms (Smith and Williams, 1984). Knudsen type diffusion occurs in capillaries with diameter less than the mean free path of gas molecules that move in the direction of lower concentration in the capillary. Smaller diameter capillaries and lower pressure of the gas are conducive to Knudsen flow (Rogers, 1994). If the adsorbed gas or pseudoliquid moves along the micropore surface somewhat like a liquid, then it is called surface diffusion. Bulk diffusion occurs within the gas phase, driven by concentration gradient, as adsorbate

molecules encounter gas-to-gas collisions. Larger pore diameters, larger molecules, and higher pressure are conducive to bulk diffusion.

Diffusion of methane can be described by Fick's law which may be applied to transport through microporous sphere using the following equation (Cussler, 1997; McElhiney, Koenig and Schraufnagel, 1989).

$$\frac{D}{r^2} \frac{\delta}{\delta r} \left( \frac{r^2 C}{r} \right) = \frac{\delta C}{\delta t} \quad (\text{Equation 2.3})$$

D is the effective diffusion coefficient at a radial distance r from the centre of the sphere at time t and gas concentration C. D is assumed to be constant for most calculations and its typical values for coal is in the order of  $10^{-9}$  (cm<sup>2</sup>/s)(Nandi S and Walker P, 1966) ; however, its value may change depending on temperature, pressure, pore length, pore diameter, and water content (Bird, Stewart and Lightfoot, 1960; Olague and Smith, 1989).

### 2.2.3 Darcy flow in fractures

After the diffusion of the gas through the micropores of the coal, transport of gas and water to the wellbore must follow through the network of fractures and cleats. Darcy's law governs the flow of fluids through the cleats. When the well is drilled, water may occupy the cleat space. Water must be removed in order to lower the pressure and to initiate desorption of methane molecule by making it oversaturated. Gas relative permeability rapidly improves significantly as the water saturation decreases (Rogers, 1994). Equation of the methane flow in fractures/cleats can be written as Equation 2.4.

$$-\left(\frac{1}{r}\right) \left(\frac{\partial}{\partial r}\right) \left[ \frac{r k p_a}{\mu p_a Z p_a} \left(\frac{\partial p_a}{\partial r}\right) \right] = \phi_a \frac{\partial}{\partial t} \left[ \frac{P_a}{Z p_a} \right] \quad (\text{Equation 2.4})$$

Total flow of methane from desorption to diffusion to Darcy's flow can be shown as in Figure 2-3.

#### **2.2.4 Effect of fracture characteristics on coalbed methane flow**

Cleat characteristics, including spacing and aperture, are important physical coal properties since their magnitudes directly affect the reservoir permeability. As the cleat spacing decreases while keeping cleat aperture constant, the permeability increases. However, vice versa is not true. If cleat spacing is decreased with fracture aperture increase, it would increase permeability. A correlation was developed between permeability and cleat aperture and cleat spacing for carbonate reservoirs (Lucia, 1983). Here  $k_s$  is permeability of the sample,  $w$  is cleat aperture and  $Z$  is spacing.  $K$  is a constant that depends upon the reservoir characteristics.

$$k_s = K\left(\frac{w^3}{Z}\right) \text{ (Equation 2.5)}$$

This model assumes that there is a series of planar fracture of constant width  $w$ , uniform height  $h$ , and spacing  $Z$ . The matrix is assumed to have negligible permeability. The sample width was assumed to be fracture spacing. This model is likely be the case of simple coal model described by other researchers (Harpalani and Schraufnagel, 1990). Cleats affect gas permeability more than bedding plane does.(Shimada, Zhang and Li, 2004).

### **2.3 COAL ANISOTROPY TO PERMEABILITY**

Coal often shows anisotropy; permeability may be 2.5-10 times greater in the face-cleat direction than in the butt-cleat direction (McCulloch, Deul and Jeran, 1974). Coal permeability is influenced by the in situ stress conditions. Cleat closure can occur with increasing pressure (overburden) resulting in the loss of the smaller cleats, and decreasing permeability by reducing the number of interconnections between pores and between major cleats, resulting into lower

permeability (Soeder). Coal's permeability to a gas decreases with decreasing gas pressure. However, increase in permeability can be observed for the coalbed methane reservoir due to the overwhelming effect of matrix shrinkage induced by significant desorption of methane and water removal (Harpalani and Schraufnagel, 1990). Cleats and bedding plane have a tendency to close under high hydrostatic pressure and it likely that the permeability of the deep coalbed methane reservoirs may be significantly low because of high overburden pressure (Shimada, Zhang and Li, 2004).

### **2.3.1 Effect of stress**

Permeability of coals is influenced by the stress regime. Direct observation of cleat structure with fluorescent resin showed preferential loss of the smaller aperture cleats, and reduced number of interconnections between the coal and the major cleat system, resulting in lower permeability under regionally representative coalbed methane stress conditions (1000 psi) (Soeder). The cleats have a tendency for aperture reduction and a tendency to close under high hydrostatic pressure (Gash, Volz, Potter and Corgan, 1993). Different lithotypes are responsible for the various methane capacities and anisotropic behavior of the coal (Clarkson and Bustin, 1996; Crosdale, Beamish and Valix, 1998; Karacan and Mitchell, 2003; Pone, Halleck and Mathews; Ting, 1987). The abundance and orientation of macroscopic fracturing as well as type, size, shape, density, orientation, distribution, and connectivity of microstructure is dependent upon lithotype (Clarkson and Bustin, 1997). Cleat spacing is wider in dull lithotypes than it is in bright lithotypes (Stach E., Mackowsky M.Th., Teichmuller M., Taylor G.H., Chandra D. and Teichmuller R., 1975). Higher coalbed gas production rate is expected with more cleats (lower cleat spacing) at same permeability regime (Cui and Bustin, 2005). More research is required to understand the coal cleat anisotropy for fracture generation and cleat aperture enhancement.

### **2.3.2 Effect of gas content on strength of coal**

The effect of gas sorption on the strength of the coal has been studied by a number of researchers. Theoretically, the force of attraction between the two solid coal surfaces will be replaced by that between two adsorbed gas films with weaker Van der Waal's fields than the original solid coal surface (Aziz and Ming-Li, 1999). Consequently, the strength of coal would be reduced. The adsorption capacity of coal is strictly dependent on the composition of coal. Different macerals present in the coal affect its adsorption capacity and therefore the strength of the coal. It is expected that macerals/lithotypes will have an effect on the artificial fracturing and the extent of fracturing pattern.

### **2.3.3 Composition**

During bituminization, mobile products (gas or crude oil) are lost and other aromatization and condensation of the solid residual products (coals or kerogen of petroleum-source rocks) take place. Thermal and biochemical decomposition of lignin and cellulose into complex aromatic and aliphatic compounds resulted in higher carbon content mass. Differential degree of bituminization, strengths of lignin and cellulose, physical structure of plants and deposition condition gave rise to inhomogeneity. The duller lithotypes are less prone to artificial fracturing during handling and preparation (Clarkson and Bustin, 1997) and have lower grindability (Hower, 1998).

#### ***2.3.3.1 Macerals***

Coal is not a homogeneous substance but consists of various constituents. The term 'macerals' describes the shape as well as the nature of the microscopically recognizable

constituents of the coal (Stach E., Mackowsky M.Th., Teichmuller M., Taylor G.H., Chandra D. and Teichmuller R., 1975). Mainly, macerals are classified in three groups. All macerals have the suffix 'inite' .e.g. liptinite. Table 2-2 gives the division of macerals (Bustin, Cameron, Grieve and Kalkreuth, 1985; Stach E., Mackowsky M.Th., Teichmuller M., Taylor G.H., Chandra D. and Teichmuller R., 1975).

Table 2-2. Summary of macerals of hard coals.

<b>Group Maceral</b>	<b>Maceral</b>	<b>Origin</b>	<b>Submaceral</b>
<b><i>Vitrinite</i></b>	Telinite	Woody tissues, Bark, Leaves, etc.	Telinite 1 Telinite 2
	Collinite	Cell fillings (structureless)	Collinite Telocollinite Gelcollinite Desmocollinite Corpocollinite
	Vitrodetrinite	Plant or humic-peat	
<b><i>Exinite</i></b>	Sporinite	Polen, Spores	
	Cutinite	Cuticles	
	Resinite	Resin, Waxes	
	Alginite	Algae	
	Liptodetrinite	Degraded from Liptintic macerals	
<b><i>Inertinite</i></b>	Micrinite	Secondary maceral, related to liptinite	
	Macrinite	Oxidation of gelified plant	
	Semifusinite	Woody tissues	
	Fusinite	Woody Tissues	Pyrofusinitite
			Degraddofusinite
	Sclerotinite	Fungal mycelia/spores	Fungosclerotinite
	Inertodetrinite		

Source: Stach E., Mackowsky M.Th., Teichmuller M., Taylor G.H., Chandra D. and Teichmuller R., 1975. Stach's Textbook of Coal Petrology, Stuttgart

*Vitrinite* : is the most frequent and most important maceral group in bituminous coal (Stach E., Mackowsky M.Th., Teichmuller M., Taylor G.H., Chandra D. and Teichmuller R., 1975). Cellular structures derived from vegetable material are sometimes visible under vitrinite under the microscope. Fractures in the vitrinite bands occur angularly and conchoidally and

sometimes grooved conchoidal (Stach E., Mackowsky M.Th., Teichmuller M., Taylor G.H., Chandra D. and Teichmuller R., 1975). Details of fracture in coal are discussed in following section. Reflectance of the vitrinite is intermediate in comparison to other maceral group. Vitrinite exhibits bireflectance, which can be observed to a certain degree even in the high-volatile coal (Stach E., Mackowsky M.Th., Teichmuller M., Taylor G.H., Chandra D. and Teichmuller R., 1975). It is lowest in high-volatile coals and increases with rank. Compared with exinite, vitrinite has a high degree of brittleness. The Vicker's hardness decreases with increasing rank (Van Geet and Swennen, 2001).

*Exinite*: consists of sporine, cutine, suberine, resins, waxes, fats and oils of vegetable origin (Stach E., Mackowsky M.Th., Teichmuller M., Taylor G.H., Chandra D. and Teichmuller R., 1975). Exinites are distinguished from vitrinite by higher hydrogen content in low rank coal (Stach E., Mackowsky M.Th., Teichmuller M., Taylor G.H., Chandra D. and Teichmuller R., 1975).

*Inertinite*: The fusibility of Inertinite macerals is very weak or nil in comparison to vitrinite and exinite group. The word "inert" indicates less reactive nature during carbonization. The characteristic optical property of Inertinite macerals is their high reflectance (Bustin, Cameron, Grieve and Kalkreuth, 1985).

#### **2.3.3.2 Lithotypes**

Macerals do not occur in isolation, but rather, they are associated with one another in different proportion and variable amount of mineral matter and moisture. They are distinguished macroscopically in material of hand specimen size. As per ICCP handbook, lithotype is "the

macroscopically recognizable bands (Vitrain, Clarain, Durain and Fusain) of humic coals ” (ICCP, 1963). Table 2-3 shows macroscopic details of lithotypes.

Table 2-3. Types and lithotypes of bituminous coals.

<b>Coal Type</b>	<b>Lithotype</b>	<b>Composition</b>	<b>Macroscopically recognizable features</b>
<i>Humic Coal</i>	Vitrain	Rich in Vitrinite	Bright, black, usually brittle, frequently with fissures
	Clarain	Vitrinite, Exinite, Inertinite	Semi-bright, black, very fine stratified
	Durain	Exinite or Inertinite	Dull, black or grey-black, hard, rough surface
	Fusain	Rich in Fusite	Silky lusture, black, fibrous, soft, quite friable
<i>Sapropelic Coal</i>	Cannel Coal	Little/No Alginite, Small Vitrinite, High Inertinite	Dull or slightly greasy lusture, black, homogeneous, unstratified , very hard. Conchoidal fracture, black streak
	Boghead coal	Alginite, Liptinite	Cannel coal, brownish appearance, brown streak

Source: Stach E., Mackowsky M.Th., Teichmuller M., Taylor G.H., Chandra D. and Teichmuller R., 1975. Stach's Textbook of Coal Petrology, Stuttgart.

### **2.3.3.3 Microlithotypes**

Bands of lithotypes distinguished under the microscope are termed as ‘microlithotype’. Microlithotype can be regarded as genetic units if they occur in relatively large thickness, details can be found elsewhere (Stach E., Mackowsky M.Th., Teichmuller M., Taylor G.H., Chandra D. and Teichmuller R., 1975). Vitrite, clarite, durite and trimacerite are major microlithotype observed in bituminous coals. Thus the coal is inherited by the lithotypes and macerals.

#### **2.3.3.4 Water**

Coals hold more or less residual water when mined. In particular, low-rank coals contain a number of oxygen functional groups resulting in material with hydrophilicity, and this is the primary reason for their water content being as much as 30-60 wt % on a wet basis (Mahajan and Walker, 1971) . It is a widely recognized fact that the coals have gel-like structures that can shrink and swell in response to water loss and uptake, respectively (Hayashi, Norinaga, Kudo and Chiba, 2001). A portion of sorbed water interacts with oxygen functionalities via hydrogen bonds and thereby contributes to the three-dimensional structure of the macromolecular coal network (Mahajan and Walker, 1971). Water sorbed on/in coal matrix can be classified into three types on the basis of crystallization characteristics, free water, bound water and non freezing water (Norinaga, Kumagai, Hayashi and Chiba, 1997).

#### **2.3.4 Effect of CO<sub>2</sub> adsorption in coal seam**

The CO<sub>2</sub>-induced swelling of coal is thought to be responsible for reduced injectivity during enhanced coalbed methane operations or CO<sub>2</sub> sequestration (Durucan and Shi, 2009; Fokker and Van der Meer, 2004; Mazumder, Wolf, Elewaut and Ephraim, 2006; Pone, Halleck and Mathews, 2009b; Reeves, 2003; van Bergen, Krzystolik, van Wageningen, Pagnier, Jura, Skiba, Winthagen and Kobiela, 2009). Fluid flows through coal via the fracture network or cleat system (Close, 1993; Gray, 1987a). Yet, the faces of these coal cleats are the maceral combinations that form identifiable lithotype bands in the coal seam, visible to the naked eye. It seems probably that these lithotypes will impact the following characteristics of the coal: water storage (Unsworth, Fowler and Jones, 1989), hydrophobicity and therefore, ease of water removal (Arnold and Aplan, 1989), porosity (Clarkson and Bustin, 1996) methane storage

capacity (Crosdale, Beamish and Valix, 1998), mineral matter content (Lamberson and Bustin, 1993), cleat frequency (Smyth and Buckley, 1993), and thus degree of swelling or contraction. More details are available in Appendix.

## 2.4 ENHANCED COALBED METHANE

Coalbed methane is being recovered by means of reservoir pressure depletion. While this method is simple and effective, it is not efficient. Reduction in reservoir pressure lowers the energy of the fluid to flow to the wellbore. Low rate of production and overall low recovery limit the success of the CBM reservoir. Despite the low permeability, coal has extensive cleat and natural fracture system as shown in Figure 2-6. Artificial fracturing may enable the connection between the natural cleat system and wellbore, connecting more drainage area to it. It also reduces the diffusion time for methane molecule to reach the fracture system. There are few methods which have been used for the stimulation of coalbed methane.

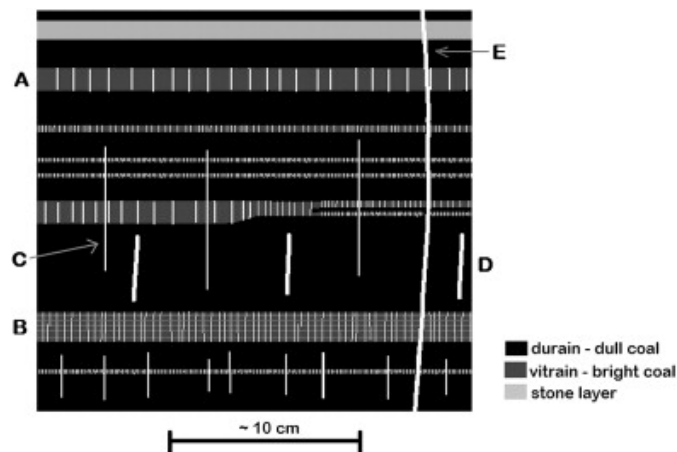


Figure 2-6. Illustration of the extensive four major cleat classes in coal.

Source: Dawson, G.K.W. and Esterle, J.S., Controls on coal cleat spacing. *International Journal of Coal Geology*, 82(3-4): 213-218.

### 2.4.1 Coalbed Methane Stimulation Techniques

a) *Vertical bore hole with multiple horizontal in-seam bore hole*: Directional drilling is done from a single vertical borehole (Creedy, Garner, Holloway and Ren, 2001). Sometimes, slant hole drilling is done intersecting the all in-seam boreholes (Kennedy, 2002). Horizontal bore holes are done in the directions perpendicular to the plane of maximum fracturing for maximum collecting of gas from the seam. Increased low-pressure contact area of the coal seam increases the gas productivity (Creedy, Garner, Holloway and Ren, 2001).

c) *Coal seam fracturing*: High pressure hydraulic fracturing or coiled tubular fracking is practiced for developing fractures inside the coal seam.

d) *Open hole cavity method*: Repeatedly pressurizing and de-pressurizing a coal seam with compressed air removes coal particles and forms a cavity. This method has been developed as an alternative to hydro-fracking, but its application appears to be limited to relatively weak, permeable coal seams (Kelso, 1994).

e) *CO<sub>2</sub> and N<sub>2</sub> injection in coal seam*: In this method mixture of CO<sub>2</sub> and N<sub>2</sub> is injected in to the coal seam for sweeping out the CH<sub>4</sub> from the coal seam. CO<sub>2</sub> stimulates desorption of CH<sub>4</sub> from the coal seam (Gale and Freund, 2001).

### 2.4.2 Coalbed methane stimulation

Each stimulation method has advantages and disadvantages. Highly developed hydraulic fracturing in conventional reservoirs and low permeability has made this technique common in certain coalbed methane reservoirs (Rogers, 1994). adjustments in conventional hydraulic fracturing have made it successful for coalbed stimulation (Rogers, 1994). These adjustments include:

1. Surface of coal adsorbs chemicals of fracturing fluid
2. Presence of extensive natural fracture network requires higher treating pressure
3. Fracturing fluid leaks deep into the fracture
4. Excessive water requirements
5. Young's modulus is low and promotes fines generation
6. Horizontal fracture occur in very shallow coals

7. Screen out of the fracture due to excessive fluid leakages
8. Instability , rubble at wellbore

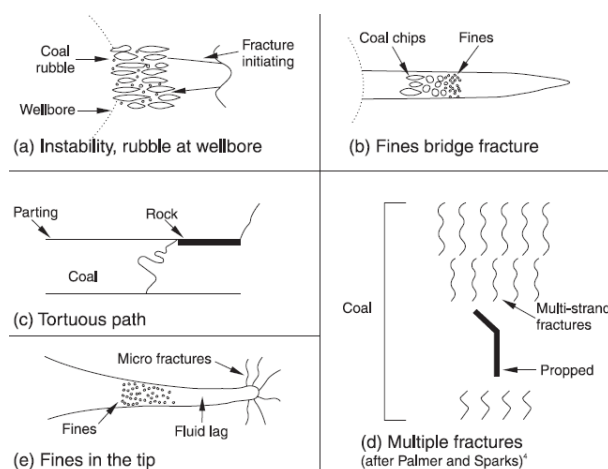


Figure 2-7. Schematic representation of hydraulic fractured coal and issues associated.

Source: Rogers, R.E., 1994. Coalbed Methane: Principles and Practice. PTR Prentice Hall, Englewood Cliffs, N.J.

High treating pressure, fracture breakout, fluid damage, excessive fine generation and permanent permeability damage of the coal in hydraulic fracturing has limited the success of hydraulic fracturing. Unconventional fracturing methods addressing the issues of hydraulic fracturing need to be investigated. Swelling of coal in the case of enhanced methane recovery assisted with CO<sub>2</sub> sweep or CO<sub>2</sub> sequestration in unminable coal seam has posed the barrier in the success of both. Swelled coal offers low permeability and the rate of extraction or CO<sub>2</sub> sequestrations are low (Reucroft and Sethuraman, 1987). Very large reduction in permeability has been observed after few hours of CO<sub>2</sub> exposure to coal in laboratory examinations (Smith and Jikich, 2009). It is thus desirable to have an alternative stimulation approach. A method is thus needed for increasing the gas release rate from coal seams. *“Increasing field permeability in coal seams requires new ideas and greater research effort”* IEA Coal Research (Creedy, Garner, Holloway and Ren, 2001). Inducing fractures in coal with microwave energy along in-seam bore

has the potential to increase the extraction rate and thus the economics and production of coalbed methane.

## 2.5 MICROWAVE APPLICATION TO COAL

The heating property of microwave energy has been in use since late 1940's. Focus was shifted towards exploitation of microwave properties at industry level for paper/wood dryer, liquid evaporation and thaw (Meredith, 1997). Microwaves were applied as pyrolysis agent of oil shales in 1973 (Chanaa, Lallemand and Mokhlisse, 1994). Morphological examination of shale samples suggested that the pyrolysis of the shale created a network of fissures increasing porosity (Chanaa, Lallemand and Mokhlisse, 1994). Microwave energy can be fine-tuned for those components that are receptive (lossy) to microwave energy, so most of the electromagnetic energy can be utilized for targeted material. Microwave heating does not depend on conduction as in conventional heating. Microwave can penetrate the sample to a certain depth and results in volumetric heating (inside out) which gives rise to very rapid heating (Bogdal and Prociak, 2007). Microwave induced differential heating in heterogeneous ore, not only helps in generating new fractures but also changes the grains, increasing the pore volume (Chanaa, Lallemand and Mokhlisse, 1994; Kingman, Corfield and Rowson, 1999). Selective heating of a component depends upon its dielectric permittivity ( $\epsilon_0$ ) and loss factor ( $\epsilon''$ ). There are several components of coal lump, viz. organic carbon, pyrites, mineral content and water (both as pore water and bound water). Ability of a material to adsorb electromagnetic energy is  $\epsilon_0$  while  $\epsilon''$  is responsible for converting absorbed electromagnetic energy into heat (Lester and Kingman, 2004). Few workers have used microwave energy for improved coal grindability, rapid coke making, coal breakage and removal of pyrite from coal (Lester, Kingman and Dodds, 2005; Lester, Kingman, Dodds and Patrick, 2006; Uslu and Atalay, 2004). The power adsorbed per unit volume of material, known

as power density  $P_d$ , is dependent on the dielectric properties of the material and can be represented by

$$P_d = 2\pi f \epsilon_0 \epsilon'' |E|^2 \text{ (Equation 1.2)}$$

Where  $f$  is the frequency and  $|E|$  the magnitude of the electric field.

Dry coal is commonly a poor absorber of microwave energy as it possesses lot of organic carbon which has very low loss factor (less than 0.25 at 25°C, 2.45GHz) (Marland, Han, Merchant and Rowson, 2000) and hence the organic coal could be considered as microwave transparent (Uslu and Atalay, 2004). This is not the case for certain minerals found in coal. Power absorption at various frequencies on coal/pyrite mixtures concludes that frequencies of 5GHz gave the greatest differential heating between pyrite and coal (Zavitsanos, 1978). Improved differential heating could be achieved at higher frequencies (Uslu and Atalay, 2004). The Larger the microwave transparency, the greater is the penetration depth, creating excellent skin-depth which allows uniform volumetric heating in large volumes. These characteristics have been used in several coal-cleaning and beneficiation studies primarily for the coal drying and improved grindability as will be discussed below.

The maximum amplitude of Electric and Magnetic fields are separated by the half wavelength of electromagnetic microwaves as shown in Figure 2-6. The position and characteristics of the samples might have an effect on its heating profile (Sutton, 1989).

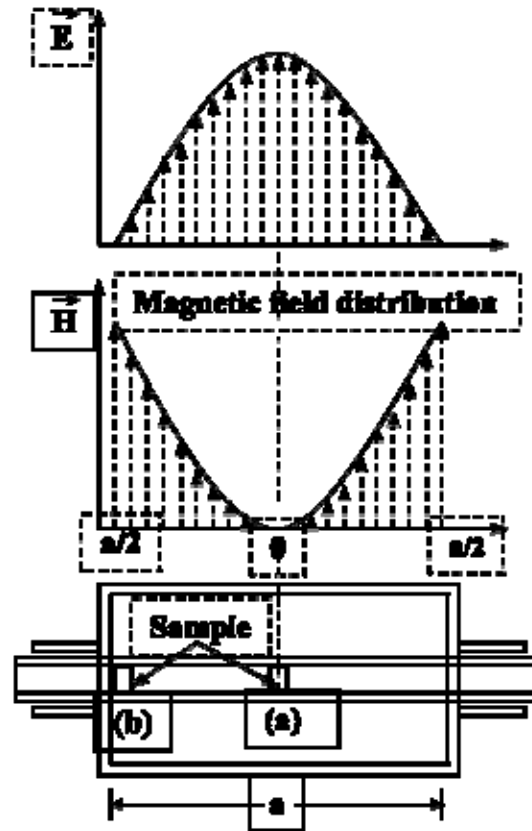


Figure 2-8. . Magnetic and Electric field distribution profile in a waveguide. The half wavelength of the microwave is  $a/2$ .

During microwave exposure, pyrites are excited by the magnetic field present in the microwave energy (Viswanathan, 1990). They may act as hot-spots for fracture initiation due to local thermal stress development between pyrite and the coal-matrix (Rowson, 1990). Microwave induced differential heating in heterogeneous ore not only helps in generating new fractures (Kingman, Lester, Wu, Mathews and Bradshaw, 2007) but also changes shale at grain level by increasing the pore volume (Chanaa, Lallemand and Mokhlisse, 1994; Kingman, Corfield and Rowson, 1999). Polar molecules, such as water, are highly affected by microwaves. Water may achieve super-heating in coal structures during the microwave exposure (Lytle, Choi and Prisbrey, 1992).

### **2.5.1 Rapid coke making**

Microwaves have been explored for the production of coke from an industrially non-suitable coking coal (Lester, Kingman, Dodds and Patrick, 2006). Multimode microwave was used to heat a high volatile bituminous coal at different sized cut and different treatment times. Devolatilisation started in one minute and the structural changes were observed by several different techniques and were similar to those in conventional coke making process (Lester, Kingman, Dodds and Patrick, 2006). Heating the coal to higher temperature increases the aromaticity of the carbon material (Honda, 1959). Loss of volatile component during the pyrolysis and reordering of the carbon structures allow higher conductivity and therefore higher level of heating from the microwave energy (Lester, Kingman, Dodds and Patrick, 2006). The degree of anisotropy, the intrinsic reactivity and dielectric properties of the sample heated for 70 min is similar to that of conventionally prepared commercial cokes (Lester, Kingman, Dodds and Patrick, 2006). The time taken to generate the graphitized coke-like material with highly anisotropic appearances is surprisingly short (under 2h) compared with the conventional methods (Lester, Kingman, Dodds and Patrick, 2006). High volatile coals are considered to be unsuitable for conventional coke making, but they are suitable with the microwave coke-making method (Lester, Kingman, Dodds and Patrick, 2006).

### **2.5.2 Improved pyrite separation from coal**

Desulphurization by magnetic separation followed by microwave heating has been investigated for faster pyrite separation (Uslu and Atalay, 2004). The inorganic sulfur occurs in raw coal mainly in pyritic and sulfate form. The separation of fine pyrite from coal is difficult by conventional magnetic separation methods. The performance of magnetic separation in removing

mineral pyrite from coal can be improved by increasing the pyrite's magnetic susceptibility. However, the problem of heating pyrite in coal is that energy is wasted by also heating the coal (Uslu and Atalay, 2004). A selective microwave method has been used to heat the pyrite by microwaves at sufficiently high-energy density to heat quickly for minimum heat loss to the coal.

The heat from the microwave absorption is dissipated by the surrounding material. The pyrite volume in coal is low and pyrite particles in coal are disseminated. Pure coal particles and other poor microwave absorber materials in coal such as calcite, siderite and quartz dissipate the heat absorbed by pyrite. Therefore, adding effective microwave-absorbing material to coal was essential for increasing the medium temperature to sufficiently heat pyrite and convert it to magnetic products for desulfurization by subsequent magnetic separation (Uslu and Atalay, 2004). The Addition of magnetite, which is an excellent microwave absorber, enhanced the microwave heating and pyritic sulfur removal by magnetic separation. With the addition of 5% magnetite, pyritic sulfur contents of coal was reduced by 55%, by magnetic separation at 2 Tesla following the microwave heating. A decrease (22%) in ash values and an increase (20%) in calorific value were also obtained (Uslu and Atalay, 2004).

### **2.5.3 Improved economics of grindability (comminution)**

High power microwave treatment of coals for very short residence times may produce the physical changes, such as cracks and fissures, in the coal mass both at the surface and interior (Kingman, Lester, Wu, Mathews and Bradshaw, 2007). It has been found that an average of 69%, 38% and 29% improvement in terms of specific breakage of rate for milling for 8s, 16s and 32s respectively in the ballmill have been achieved for bituminous coals following microwave exposure (Kingman, Lester, Wu, Mathews and Bradshaw, 2007). X-ray Computed Tomography

(CT) studies demonstrated new fracture generation through a coal core (Lester, Kingman and Dodds, 2005). Increasing the electric field strength increases the induced physical structural changes; high power densities produce a pressure increment across each coal particle which is significantly greater than the rate of escape of the resultant steam (Kingman, Lester, Wu, Mathews and Bradshaw, 2007). Thus, while high heating is achieved with microwave exposure, it does not necessarily reduced moisture content when the coal is exposed to short bursts of microwaves. Thus the observed increase in grindability is not related to moisture loss.

## **2.6 OPTICAL MICROSCOPY AND X-RAY CT QUANTIFICATION OF CLEATS**

Cleats in coal have been of interest to the coal mining community to design efficient coal extraction, and degasification systems. Quantitative data are mostly limited to the orientation and spacing information. Few data exist on apertures, heights, lengths, connectivity and the relation of cleat formation to diagenesis. These are important characteristics for permeability. Optical microscopy on polished coal surfaces has been used for evaluating the cleat characteristics including: aperture, length, orientation, and extent. Optical microscopy enables very accurate measurement of the features of the surface, but it is destructive, typically requiring resin impregnation and a highly-polished surface. Scanning electron microscopy also has been used for higher resolution determination of microcleats in cuttings (Wolf, Codreanu, Ephraim and Simons, 2004). The following optical techniques have been investigated: infrared photography, interferometer and high resolution automated optical microscopy (Cloke, Lester, Allen and Miles, 1995; Diamond, McCulloch and Bench, 1975). However, these techniques are limited to two dimensional analysis, not three-dimensional characterizations of fractures and cleats. Three-dimensional analyses could not be rendered unless the desired plane of the samples are obtained by cutting at the required location, which is destructive, and any information gained is also

limited to that slice location. Thus a non-destructive technique is more desirable in situations where pre- and post-comparisons are necessary.

X-ray CT is an often non-destructive technique for volumetric visualization. It produces a digital image that is a map of the X-ray attenuation in a slice through the object. These slices are stacked, digitally, allowing 3D rendering of the volume. This non-destructive technique (Yao, Liu, Che, Tang, Tang and Huang, 2009) has been used in the determination of mineral dispersion for coal cleaning potential (Lin, Miller, Cortes and Galery, 1991; Moza and Neavel, 1986), shrinking and fracturing accompanying thermal drying (Mathews, Pone, Mitchell and Halleck, 2009; Sarunac, Levy, Ness, Bullinger, Mathews and Halleck, 2009), transitions with devolatilization and combustion (Mayolotte, Lamby, Kosky and St. Peters, 1981), shrinking and swelling with gas sorption/desorption (Karacan and Okandan, 2000; Mazumder, Wolf, Elewaut and Ephraim, 2006; Pone, Halleck and Mathews, 2009a; Van Geet and Swennen, 2001), cleat system determination (Pyrak-Nolte, Montemagno and Nolte, 1997) and fluid flow gas uptake and degassing (Karacan, 2003; Saites, Guo, Mannhardt and Kantzas, 2006), coal compression (Pone, Halleck and Mathews, 2010) coking (Mayolotte, Lamby, Kosky and St. Peters, 1981), and solvent swelling (Niekerk, Halleck and Mathews). There have been several advances in X-ray CT reconstructions, slicing, microfocus, calibration, and reduction in acquisition times that enables geologists to study complex phenomenon in a spatial diverse environment. The technique provides visualization and concurrent quantification.

Early work on fracture porosity often required contrast-enhancing agents for these lower resolution X-ray CT medical units. Either Woods metal was used in a destructive manner or Xe gas was utilized. Wood's metal injection technique aids in measuring the effective cleat porosity of a coal core and capturing the geometry of the cleat network. A low- melting- point alloy is injected into the sample subjected to a confining pressure. The sample is heated to 95°C and molten alloy (Bismuth-42.5%, Lead-37.7%, Tin-11.3% and Cadmium-8.5%) is injected into the

sample with the help of a pressure generator (Pyrak-Nolte, Haley and Gash, 1993). Nitrogen backpressure is applied and maintained during the cooling of the sample. Metal and sample are allowed to cool in order to solidify the injected alloy inside the fracture network. The cleat volume can be determined from the volume injected inside the sample and visualized with X-ray CT. The geometry of the cleat network can be examined with X-ray CT (Pyrak-Nolte, Haley and Gash, 1993). Alloy shrinkage and capillary forces that prevent access result in some error in volumetric determination of the cleat structure (Pyrak-Nolte, Haley and Gash, 1993).

Similarly, cleat porosity has been examined by the injection of xenon gas into the sample at room temperature (Maylotte, Kosky, Lamby, Spiro, Bartges, Davis and Bensley, 1984). Here however the contrast aid does not destroy the sample. Xenon is often utilized because of its relatively inert nature and higher X-ray absorption. Thus, it aids X-ray CT attenuation differences. The penetration of xenon gas into the coal was performed by exposing the coal core to xenon (22 psi) at one end and monitoring the gas exiting the opposite face by following the pressure rise in a closed system of known volume. The penetration of gas within the coal was monitored and images from the X-ray CT were obtained for cleat porosity (Van Geet and Swennen, 2001); (Maylotte, Kosky, Lamby, Spiro, Bartges, Davis and Bensley, 1984). The images show the non-uniform nature of the penetration of the xenon into the coal. This behavior suggested that the xenon penetrated into the plane by a network of fine cracks. As the xenon diffused into the coal away from the crack more xenon was introduced into the voxel containing the crack, and into neighboring voxels and, consequently, the CT attenuation numbers on the difference image increased. Xe injection has shown success in mapping the fracture/cleat network in three dimensions with X-ray CT techniques. Image subtractions with progressive diffusion in the coal enable visualization of the Xe diffusion profile in coal cleats and fractures in three dimensions (Maylotte, Kosky, Lamby, Spiro, Bartges, Davis and Bensley, 1984). Advances in X-ray CT resolution now allow cleat volume to be estimated without the aid of contrasting agents.

## 2.7 SUMMARY

Coal seam degasification in gassy mines improves the mine's safety, productivity, and greenhouse footprint. It reduces the risk of outburst, coal mine methane explosion, ventilation cost, green house gas emission, while providing a cleaner source of energy for electricity generation or as a transportation fuel. Many unminable coal seams have potential for coalbed methane extraction. Despite a natural fracture system (cleats) present in the coal, coalbeds often have low permeability. This low permeability limits the applicability of coalbed methane extraction or CO<sub>2</sub> sequestration. Coalbeds are often stimulated to aid in methane extractions. Hydraulic fracturing is the most common approach used. Open hole cavity or N<sub>2</sub>/CO<sub>2</sub> mixture injection haven been explored for enhanced coalbed methane extraction. However, there are limitations and challenges for each of each stimulation approach. An alternative approach is desirable.

Microwaves have been used for several applications in coal, viz. improved grindability, pyrite separation, rapid coal coking, and coal drying. Improved coal grindability was thought to occur due to physical changes (porosity/fractures) in the coal matrix. No significant moisture loss was observed in the coal so these physical changes were not due to coal drying. However, no work has examined microwave applications to coal under hydrostatic stress conditions to improve permeability through cleat aperture enhancements and the induction of fractures in coal. It is desirable to observe the existing fracture system pre- and post-microwave exposure. This requires non-destructive 3D volumetric observations. Modern X-ray CT examinations have been utilized to examine the cleat system in coal non-destructively. Semi-quantitative data can be obtained for the fracture volume with this approach. Confidence is increased however if optical microscopy or alternative approach is used in calibration of cleat aperture. Significant gains in microscope

automation now allow significant field of view observations at high-resolution via the stitching of multiple micrographs to generate mosaics of the coal surface. Unfortunately, no microwave transparent pressure vessel is commercially available to allow microwave exposure under hydrostatic stress.

The objective of this research is to evaluate the potential of microwaves in improving permeability or wellbore cleat system connectivity through the proxy of generating new fractures or cleat aperture enhancements of Appalachian bituminous coal core while the coal is under simulated in situ stress.

## Chapter 3 : METHODS

### 3.1 COAL SAMPLE

A vertical orientation bituminous coal core of 50 mm diameter from Pittsburgh-seam was obtained. Total moisture in the coal was determined as per the ASTM standards D3302 (ASTM, 2010). This coal core was divided in to two cores of approximately equal length (54 mm). Coal cores were kept in argon filled foil multilaminated bags to limit any moisture loss or coal “weathering” (Glick, Mitchell and Davis, 2005). One of the cores has an apparent vertical fracture/cleat as shown in Figure 3-1.



Figure 3-1. Pittsburgh seam bituminous coal core with inherent fracture/cleat.

### 3.2 MICROWAVE AND X-RAY TRANSPARENT VESSEL

Given the size of microwave-cavity and restriction of microwave transparency of the pressure vessel a true simulator of the in situ stress condition is difficult to manufacture. No commercial system is available for such requirement. Hence a relatively simple system was designed and fabricated in the lab. Microwave- and X-ray-transparent high strength vessel was fabricated for applying microwave bursts to stressed coal core. This microwave-transparent

pressure vessel simulated hydrostatic stressed coal seam in lab. Hydrostatic conditions were created for the coal sample by pressurizing this vessel with Nitrogen. Pressure was kept at 1000 psi to simulate the depth of 1875 feet deep coal mine (refer appendix). The material selected for the pressure vessel was 16,000 psi tensile strength glass-filled (20% silicate glass) polycarbonate of grade V (strength calculation supplied in Appendix A). Vessel was fabricated in the machine shop as per the designing specification. Dielectric permittivity ( $\epsilon_0$ ) and loss factor ( $\epsilon''$ ) of the polycarbonate were tested in the lab and it was confirmed that this polycarbonate was microwave transparent at 2.45 GHz (refer to Figure 3-2).

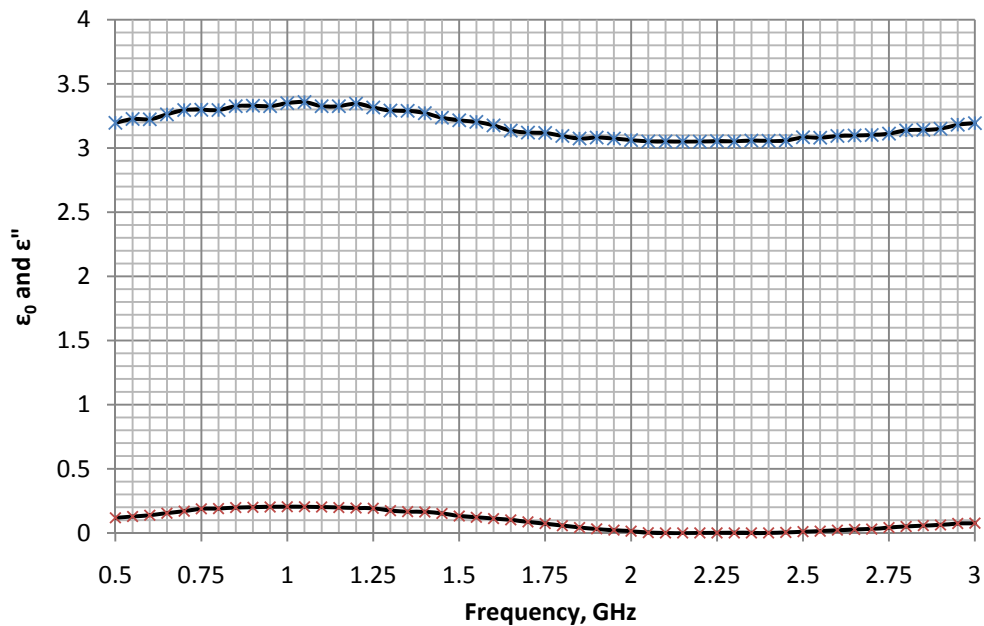


Figure 3-2. Variation of permittivity coefficient and loss constant with frequency.

The zero dielectric loss-factor at a frequency of 2.45 GHz suggests that there would be no microwave energy loss due to the vessel and thus all the energy would be available to impact the coal. Coal cores were exposed to short-bursts of microwave energy at 15 kWh for 3 seconds at National Centre for Industrial Microwave Processing (NCIMP), University of Nottingham, UK.

X-ray CT volumetric image reconstructions were obtained for the sample prior to and after the microwave exposure. In the case of the sample exposed at simulated hydrostatic stress, a high strength polycarbonate microwave-transparent vessel was fabricated to contain the core (Figure 3-3). The core holder consisted of two parts, a long-threaded portion which contained a pressure relief valve (1000 psi) and a gas charging port. The square-cut buttress thread went half the length of the holder to ensure appropriate safety with high-pressure gas.

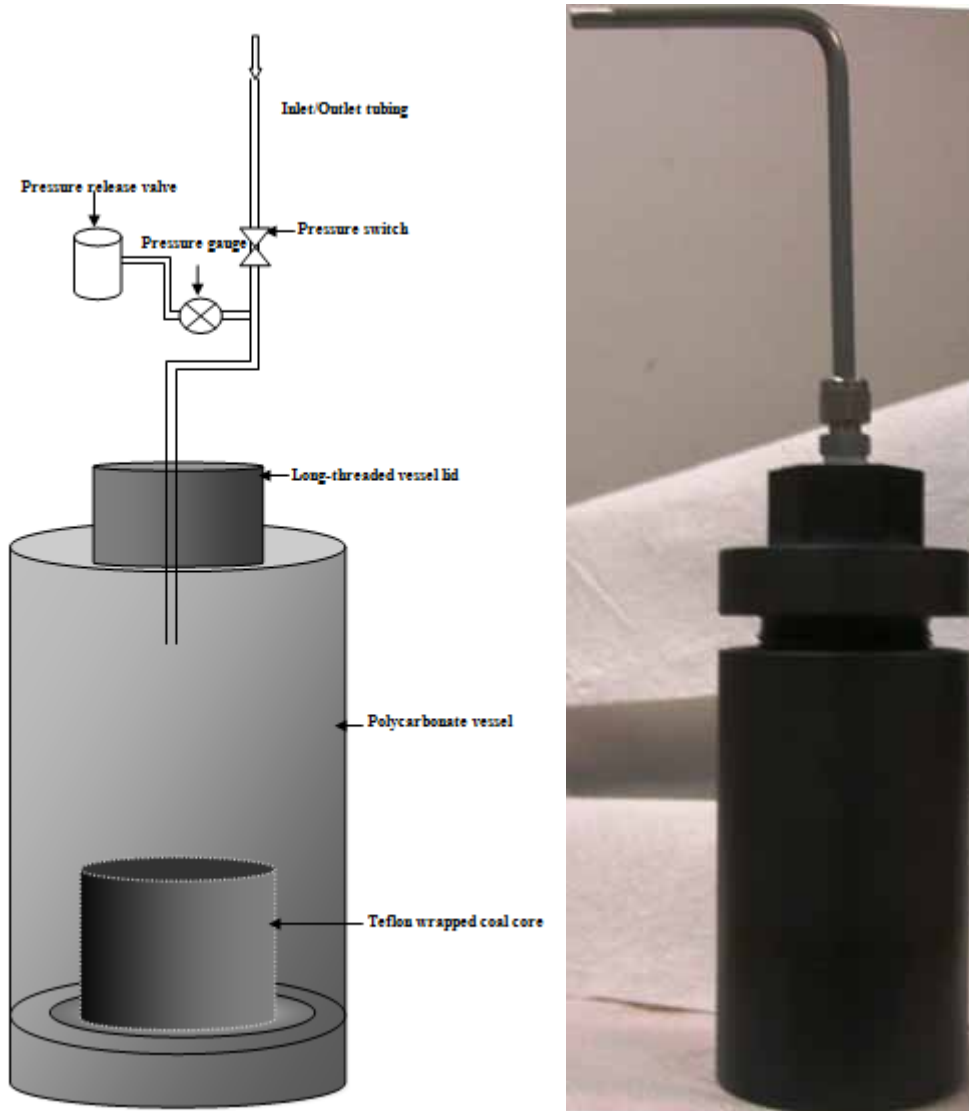


Figure 3-3. Schematic and photograph of microwave and X-ray transparent polycarbonate vessel containing coal core.

The core sat on the bottom on the holder with argon gas pressurized the surrounding space at 1000 psi. Pressurizing and depressurizing were performed slowly to lower the residual stresses and eliminated the chances of new fracture generation except the microwave-bursts. Given the

diffusion coefficient of argon in coal ( $10^{-9}$  cm<sup>2</sup>/sec) (Nandi S and Walker P, 1966), mathematical modeling suggests that no significant diffusion can take place in coal core through the fracture network with argon over the time scale employed here. It can be assumed that the effective pore pressure is zero as developed by argon gas diffusion. The vessel was allowed to cool before degassing. The vessel was hand carried in a hard-sided foam filled camera-carrying case between the Penn State and Nottingham locations.

### 3.3 X-RAY COMPUTED TOMOGRAPHY

X-ray Computed Tomography (CT) is radiographic technique for digitally viewing the reconstructed 3-dimensional nature of an object from a set of one- or two- dimensional X-ray image projections from various angles. When X-ray beam passes through an object, it becomes attenuated through thorough photoelectric absorption and Compton scattering. The attenuation coefficient is given by Beer's Law in terms of the initial and attenuated X-ray intensity and thickness of the object.

$$\left(\frac{I}{I_0}\right) = e^{-\mu x} \text{ (Equation 3.1)}$$

Where I is attenuated X-ray intensity at a distance x, while I<sub>0</sub> represents initial X-ray intensity. Linear attenuation coefficient ( $\mu$ ) is primarily a function of X-ray energy and the density and atomic number of the material being imaged.

All transmission CT-devices are based on the same principle: the object is positioned in between an X-ray source and X-ray detector. The CT requires a rotational motion of the sample relative to the source-detector system. X-ray attenuations are measured by detectors and are used to reconstruct the attenuation numbers in two dimensions by obtaining one- dimensional projections at different angles for one slice. Stacked two dimensional data represent three

dimensions of the object. This technique is non-destructive in nature but has certain limitations in terms of size, length and diameter.

There has been a rise in the application of X-ray CT for the study of coal. X-ray CT has been used for analyzing various phenomenon, Coal cleaning and drying, pyrolysis and combustion, cleats and fractures, Carbon dioxide sequestration in coal, petrography, solvent swelling and particle handling. There has been extensive use of X-ray CT in cleat fracture analysis. X-ray computed tomography has been used for cleat observation with the help of Wood's metal injection (Pyrak-Nolte, Montemagno and Nolte, 1997). Here the cleat aperture enhancement and new fracture induction of coal cores under hydrostatic pressure were evaluated using the X-ray CT technique.

An industrial X-ray CT (Universal HD-600, OMNI-X) scanner was used to obtain high-resolution coal volumetric reconstructions at 160 kV energy level with 120 or 150 mA current. Temperature was maintained via a specialized air handling system at  $76^{\circ}\text{F} \pm 1^{\circ}\text{F}$ . Volumetric scans, containing multiple stacked slices, were taken in 0.06 mm thick cross-sectional layers. Images were stored in a three dimensional matrix of voxels. Each voxel represents a volumetric element of  $0.056 \times 0.056 \times 0.06$  mm and consists of CT number (an X-ray attenuation number) that is related to the material density and atomic number.

### **3.4 HIGH-ENERGY MICROWAVE BURSTS**

Polar molecules, such as water, are highly affected by microwaves. If the resonant frequency of the molecule corresponds to the microwave frequency, then that molecule vibrates with high amplitude oscillations resulting in the breakage of the bond that binds that molecule to the material (Mahadevan, 2002; Meredith, 1997).

Industrial microwave available at NCIMP, Nottingham were used at 15Kw power and total exposure of 3 seconds to the coal core. Schematic in Figure 3-4 shows a typical industrial microwave set-up.

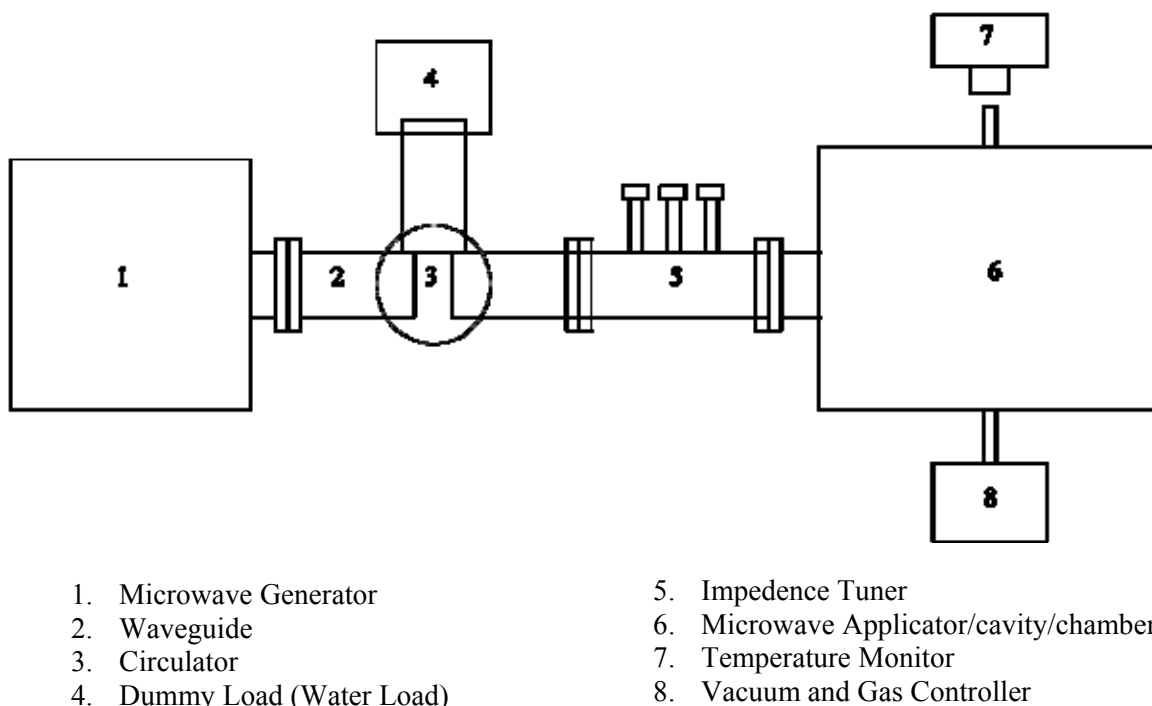


Figure 3-4. Schematic of typical industrial microwave set-up available at NCIMP, Nottingham,UK.

Microwaves are generated in an electromagnetic wave generator called a magnetron. This device works in the density modulated mode, rather than the current modulated mode (Meredith, 1997). This means that the microwaves work on the basis of clumps of electrons flying ballistically through them, rather than using continuous stream. A magnetron is the most common source of microwave used for industrial and research applications, and are economical and efficient. Frequency can be made precise adjusted within a set range band, and the microwave efficiency is about 65-70%.

These microwaves are propagated through a rectangular brass pipe- shaped cavity. If microwave oscillation is set up at one end of a waveguide, its electric fields cause electric currents to flow in the Cu/Al walls. In turn these currents induce new electric and magnetic fields in the waveguide, oscillating with the same frequency as the original microwave. The result is that the microwave travels along the pipe. There is some small loss of energy due to the electrical resistance of the Cu/Al, but the microwave intensity that arrives at the far end of the pipe/waveguide (length ~ few inches to few feet) is almost as large as the intensity fed in at the beginning (Meredith, 1997). Because The size of the waveguide must be a multiple of the wavelength of the wave, waveguides are only practical for electromagnetic waves in the microwave range, with wavelengths on the scale of a few centimeters (Bogdal and Prociak, 2007). Circulator and Dummy load of water are attached to the waveguide to absorb the reflected microwaves from the exposure chamber. An impedance tuner is also attached to the waveguide for fine tuning of the frequency propagated. The coal sample is placed in the cavity for microwave exposure within a walk-in microwave container.

The moisture, determined from core cuttings, was 1.7% as-received. Thus no moisture removal or enhancements were made. Moisture flashing to steam and isolated high-energy water molecules are thought to be responsible for the microwave influence in short-bursts that generate new fractures and enhance existing cleat apertures.

### **3.5 OPTICAL MICROSCOPY**

Optical microscopy performed at Nottingham University utilized Zeiss microscope S100 (Carl Zeiss, Jena, Germany) equipped with Zeiss Axicam HRC Color camera (Carl Zeiss, Jena, Germany) to acquire the images of cut coal sections following X-ray CT observations. An oil immersion objective lens of 32X and eyepiece of 10X were used for magnification. The stage of

the microscope was programmed for movement in the horizontal plane with software-automated controls. AxioVision software was used for auto stitching of the small surface-capture into a 10mmX10mm mosaic. These mosaics were stitched into a surface map with the aid of DoubleTake software.

Following microwave exposure, cores were impregnated with an epoxy resin at room temperature vacuum oven until bubbling stopped and the resin was allowed to set overnight. In the case of the pressure vessel, resin impregnation occurred within the vessel to avoid handling damage to the coal. Selective surfaces, from X-ray CT observations, of the cores were cut and hand-polished. Surface mosaics were obtained using optical microscopy under oil to aid in maceral contrast. Cleat aperture, lengths, and orientation were obtained from image analysis using Photoshop with the ForeaPro4 plugin. Maceral and micro-lithotype analysis were also performed.

For fracture/cleat volumetric determinations from X-ray data, the exterior of the coal core was removed via cropping each slice of the volumetric reconstruction using combination of Adobe Photoshop with ForeaPro4 and Graphic Converter software. Slice rotations were also performed to better match core orientations. Avizo software was used for 3-D visualization and quantification of cleat/fracture volumes and aperture sizes. For determining the threshold number value to distinguish between cleat/fracture and coal, apertures obtained from AVIZO were calibrated with optical microscopy observations.

## Chapter 4 : RESULTS AND DISCUSSION

### 4.1 FRACTURE CREATION AND APERTURE ENHANCEMENT

#### 4.1.1 Threshold number selection

The combination of X-ray CT and optical microscopy was used in the determination of the fracture volumes. The fracture volume (%) is defined as follows.

$$\text{Fracture volume (\%)} = \left( \frac{\text{Fracture Volume in coal core}}{\text{Volume of the coal core}} \right)$$

This volume (%) is dependent on the threshold value selected to distinguish void/coal in the X-ray CT reconstructions (Figure 4-1 and Figure 4-2). The quantitative aspect is dependent on selecting the appropriate CT threshold number value.

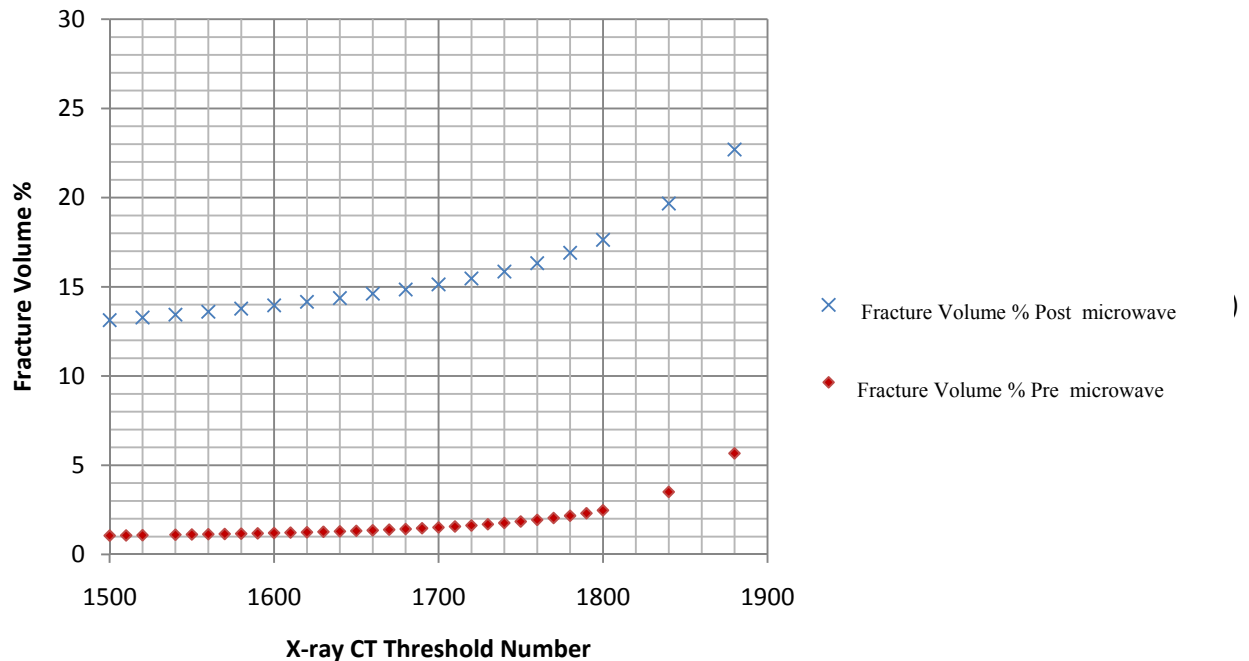


Figure 4-1. Variation of Fracture volume percentage of the coal core pre- and post- microwave bursts under no stress with X-ray CT threshold number.

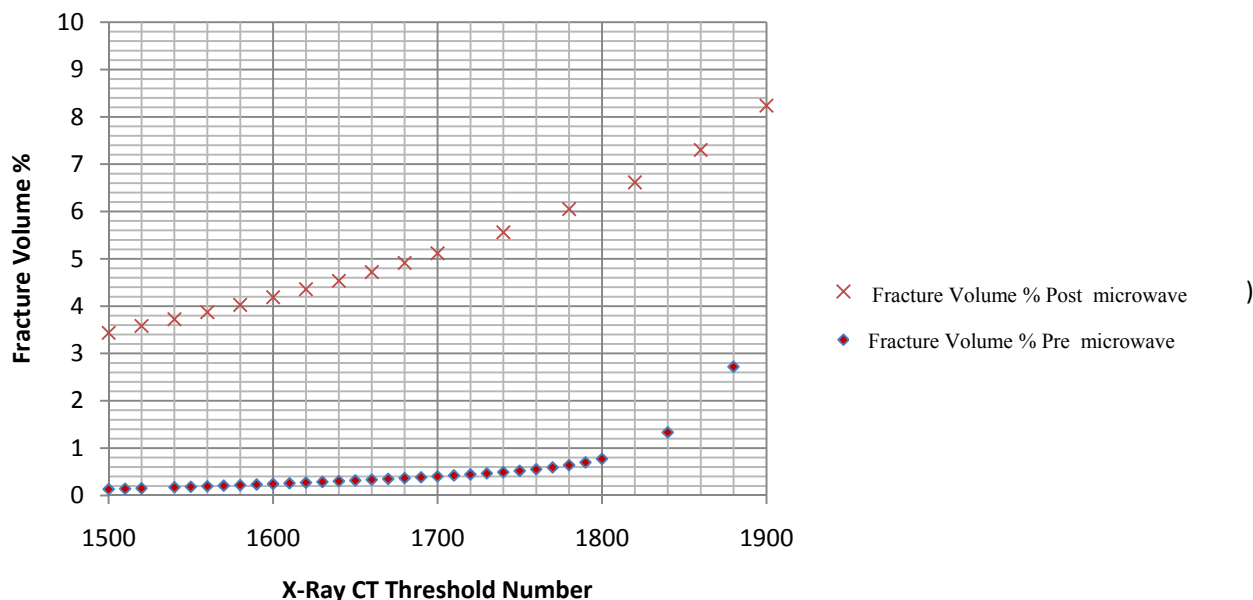


Figure 4-2. Variation of fracture volume percentage of the coal core pre- and post- microwave bursts under hydrostatic stress with X-ray CT threshold number.

The coal core volume increased after the microwave bursts, hence the fracture volume is relative to the new volume. The fracture volume increases with X-ray CT threshold number (coal determination) and there is a steep rise in the volume percentages after certain CT threshold number for the raw coal. However, following the microwave exposure significant increase in volume was observed along with a change in the threshold to CT volume relationship. There is a greater change in volume with CT number increase that occurs over a wider range than the raw coal (Figures 4-1, 4-2). If the microwave exposure induced multiple microfractures, below the resolution of the X-ray CT resolution used, the fracture volume becomes more sensitive to CT number. However in both cases the fracture volumes in post-microwave bursts are higher than pre-microwave bursts. To obtain the appropriate threshold value the system was calibrated with the optical microscopy observations. A single large fracture was selected, at slice number 559, and its aperture measured at multiple locations, both optically and with X-ray CT. The optical work being performed by hand polishing the coal surface and the appropriate X-ray CT slice was

selected and compared. A comparison of the polished surface and virtual slice is shown in Figure 4-3. Both show an obvious fracture spanning the upper region. The average aperture for this single fracture was in the range of  $0.41 \pm 0.01$  mm with optical microscopy (higher resolution) with duplicate values being obtained at a CT threshold number of 1750. This value was used in fracture volume and fracture mapping for both cores.

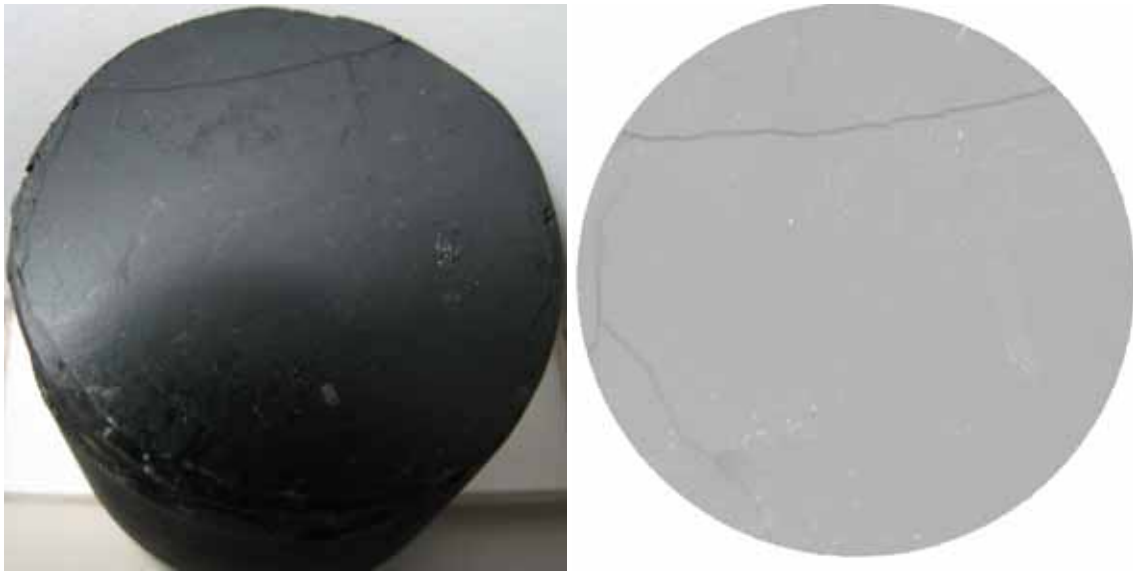


Figure 4-3. Photograph of hand polishing coal surface (right) and X-ray CT reconstruction at the same location (559<sup>th</sup> slice) for the microwave-exposed while stressed coal.

#### **4.1.2 Fractography and fracture volume determination**

Figure 4-4 shows a virtual vertical slice from the volumetric reconstruction of the core (exposed under stress) pre- and post-exposure. From this and other slices (not shown), the induced fractures tended to be contained mostly in the horizontal (bedding) plane- similar to an earlier observation (Kingman, Lester, Wu, Mathews and Bradshaw, 2007). Lithotypes planes tend to be weaker locals in coal and hence have higher tendency to fracture in situations such as

comminution. In hydrofracking, vertical fractures are common, but horizontal fractures may occur when the depth is lower (<100 feet) (Davidson, Sloss and Clarke, 1995). Most of the butt cleats are parallel to deposition planes while the cleat system is vertical to the deposition plane. Fractures/cleats present in the vertically drilled coal sample prior to microwave exposure were mostly in the vertical plane (one lesser horizontal fracture in one core).

After exposure, new fractures were induced in the core without application of stress during exposure, as expected. However, new fractures were also present (three vertical and six horizontal) in the case of the sample exposed while under simulated hydrostatic stress. Both cores had aperture enhancements to the existing cleats. Thus, existing cleats/fractures were enhanced by microwave exposure and new fractures were also created. The cores deformed during exposure with noticeable volumetric expansion, being greater at the core top in both cases. In the case of the core that was exposed while under simulated hydrostatic stress the expansion was likely limited by the enclosing pressure vessel, 1 mm relief on both sides. The pressure vessel was designed to accommodate the cores obtained and the spacing of 1 mm is appropriate for primary face cleat apertures to better represent the actual in situ conditions where horizontal expansion is limited to coal displacement into the cleat system.

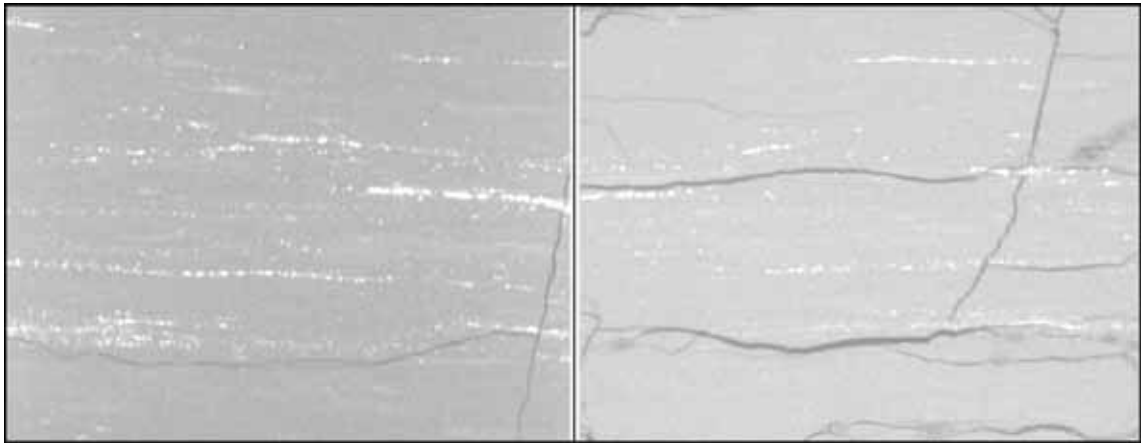


Figure 4-4. . X-ray CT volumetric reconstructions of slices showing a horizontal fractures and a cleat before (left) and induced fracture with enhanced apertures for existing fracture/cleats after microwave exposure for adjacent core regions (right).

A fracture map of coal core before and after microwave exposure without stress conditions was obtained from X-ray CT volume reconstructions by selecting the coal matrix to be transparent and the fracture surface a contrasting color. This is shown in Figure 4-5 for the unconfined core. It is obvious that there are new fractures generated after the high-energy microwave bursts. The core has been fractured at several places in the horizontal plane. Although there are also new fractures in the vertical plane, they are not as extensive.

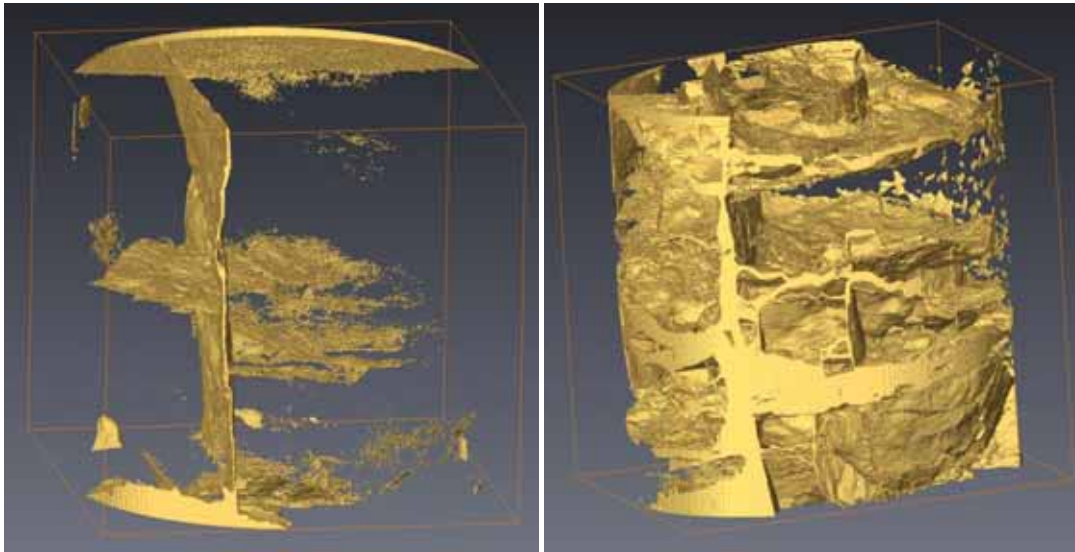


Figure 4-5. Fracture map of the unconfined coal core before (left) and after (right) microwave exposure.

The nature of induced fractures was similar under simulated hydrostatic stress conditions but the extent of fracturing was less. There were new fractures in both the vertical and horizontal planes (Figure 4-6). The confining gas pressure may act to restrict cleat expansion and retard/prevent fractures; hence the evaluations performed here tested if microwaves can induce fractures at in situ- like conditions. Here it has been confirmed, for the first time, that microwaves are able to generate new fractures under hydrostatic stressed condition used here (consistent with reasonable coalbed methane extraction depths in the U.S. i.e. 1875 feet) (Gray, 1987a).

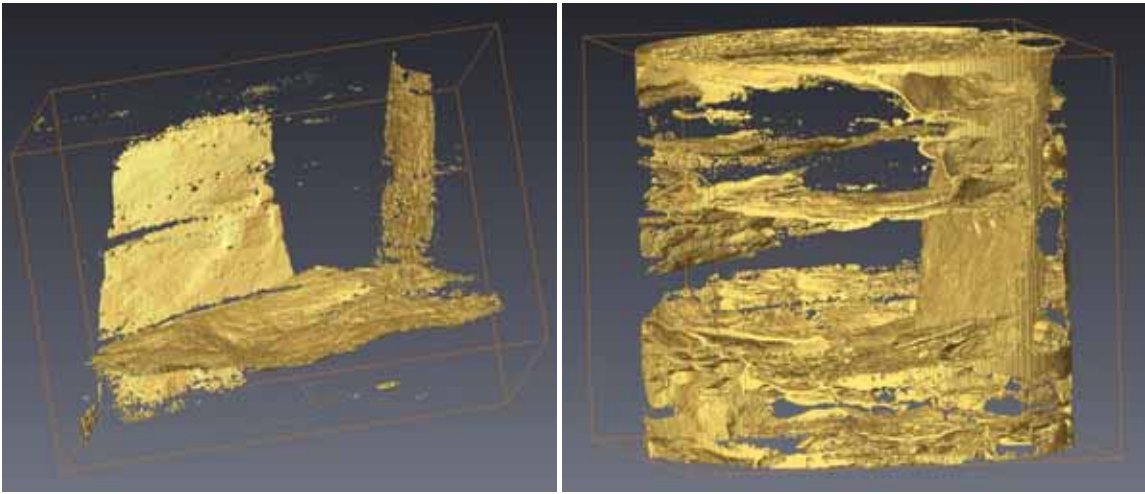


Figure 4-6. Fracture map of hydrostatically confined (1000 psi) coal core before (left) and after (right) microwave exposure. Coal matrix is transparent.

The expectation was for fractures to be generated in the vertical planes similar to the natural process; however, the new fractures generated from the microwave bursts were more frequently in the horizontal/bedding plane. This relationship is likely to be stress dependant as in the case of hydrofracking where at lower stress (shallower depth) vertical fractures may occur. Pre- and post-microwave fracture apertures along pre-existing fractures exposed with and without hydrostatically stressed conditions during exposure are shown in Figures 4-5 and 4-6. Normalized length is used for the comparison between pre and post measurement; as the fracture volume increased, the core expanded. The normalized length does assume proportional expansion rather than spatially-specific expansion observed. However, as the aperture enhancements are spectacular the error is minimal. The apertures are measured perpendicular to the fracture wall in that plane i.e. the minimum distance between the fracture wall in particular slice at certain location. The aperture enhancements were not uniform between fractures or necessarily along fractures. The expansion ranged from approximately 400% to 100%. At the core edges, lost material is responsible for the larger gain observed in fracture 1. The gains are less extensive in

the core that was stressed during exposure, where the gain may have been 250% for the single existing cleat. Error bars are generous, reflecting the resolution of the X-ray CT experiment at these conditions. Following microwave exposure, the cleat aperture was remarkably uniform with regard to aperture, despite the cleat originally having a less uniform aperture distribution.

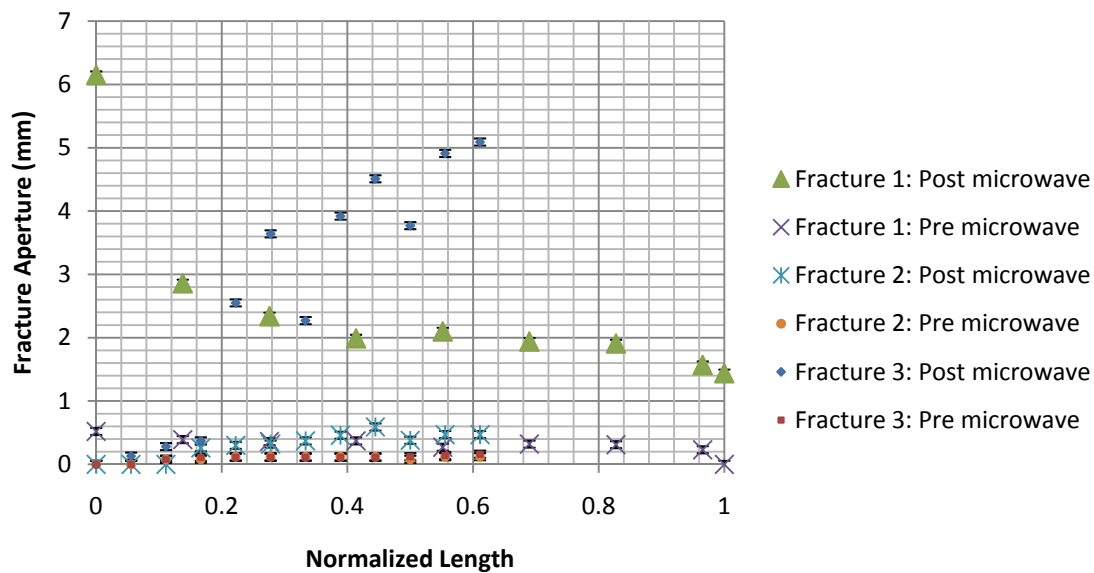


Figure 4-7. Fracture apertures before and after microwave exposure without confining stress during exposure.

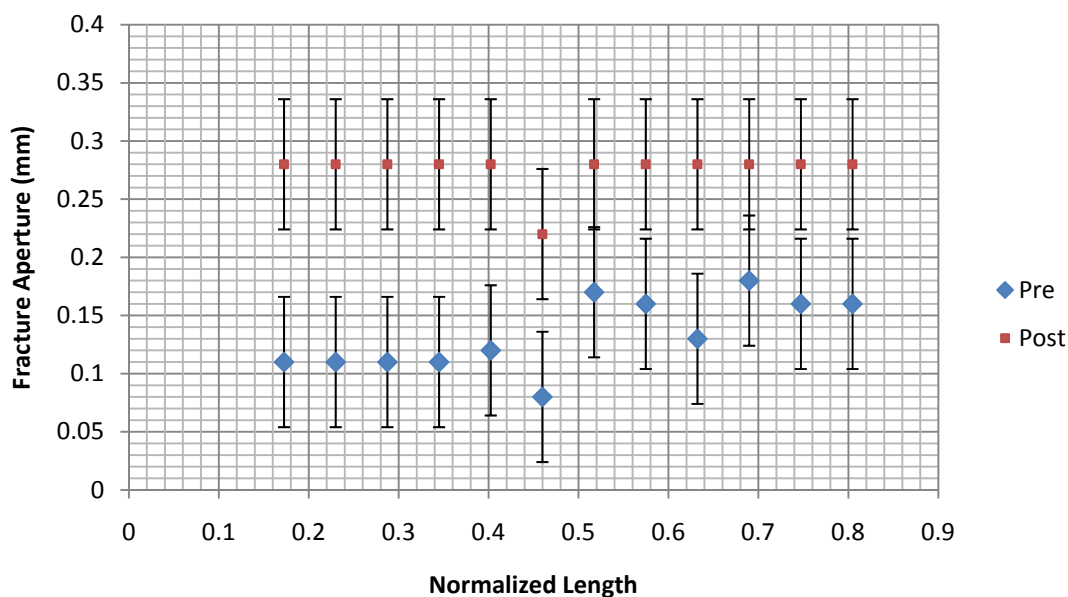


Figure 4-8. Fracture apertures before and after microwave exposure under hydrostatic stressed (1000 psi) conditions.

The fracture aperture distributions of two nascent fractures created by microwave exposure, under simulated hydrostatic stress conditions, are shown in Figure 4-9. The fracture had been occluded by the particles/fines generated during fracturing; occasionally the fracture apertures may be reduced due to coal slippages. The Core had expanded in the horizontal and vertical directions after the microwave exposure. However, it is unlikely that the occlusion occurs throughout the fracture (may be slice specific) and, indeed, may aid in preventing fracture closure/healing. In comparison, natural cleats tend to have uniform more aperture distributions beyond the length scales explored here. It was observed that some coal particles have dropped into the fractures and clogged the fractures at some places Figure 4-9. These particles may act as natural proppant if fracturing is carried out under in situ conditions. Alternatively, excessive fine generation is undesirable due to fracture plugging.

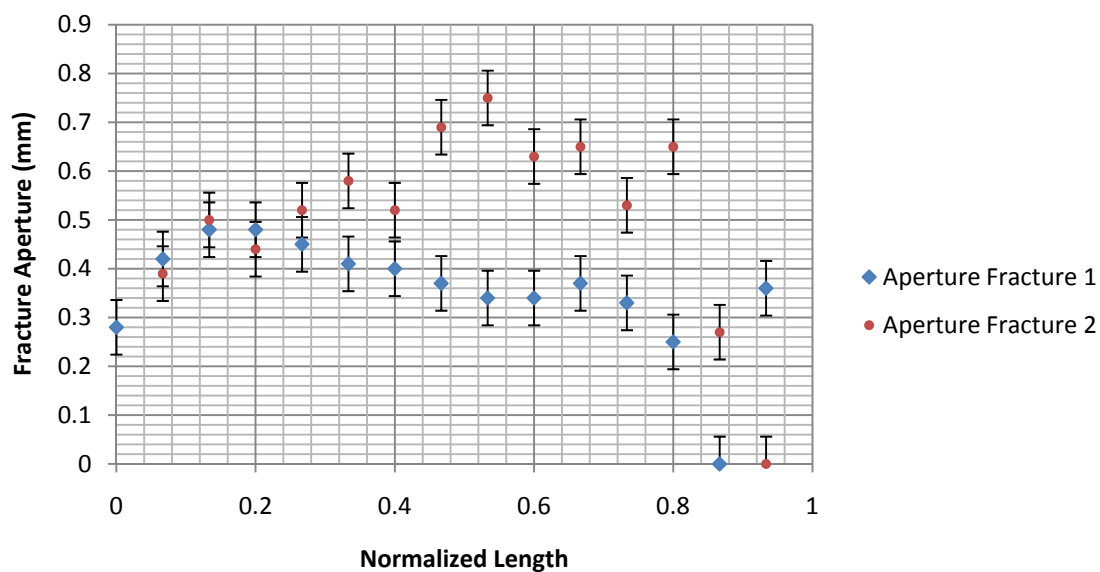


Figure 4-9. Fracture apertures of new generated fractures after microwave exposure under hydrostatic stressed (1000 psi) conditions.

Fracture aperture distribution for three newly generated fractures has been shown in the Figure 4-10 which suggests that the microwave fracturing is heterogeneous. Fracture apertures show a range of values that could be affected by fracture initiation/termination location, lithotypes, cleat propensity (length of fracture), moisture content, mineral influences, or some combination thereof.

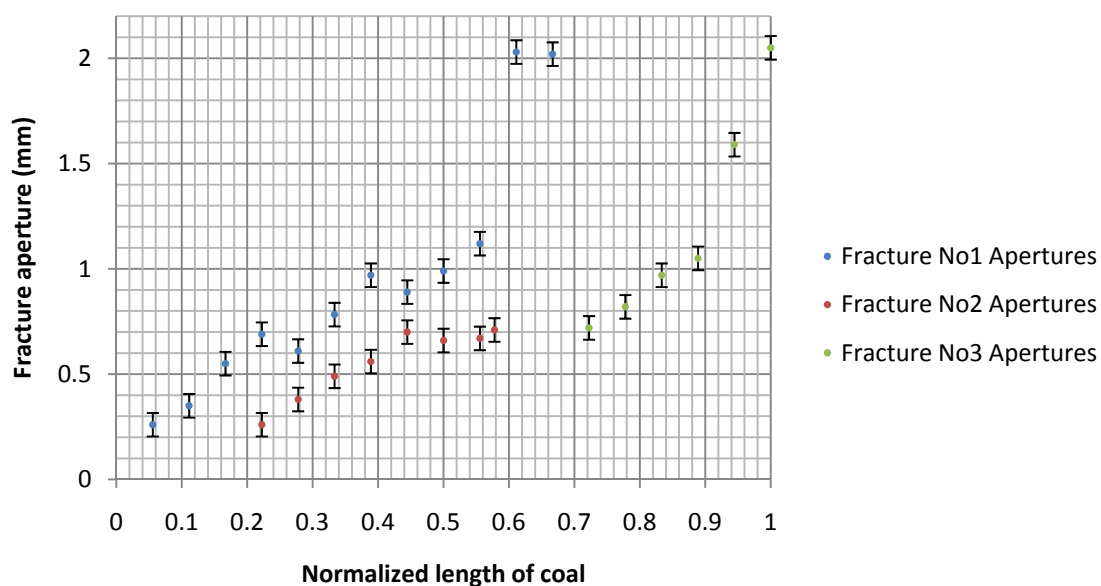


Figure 4-10. Fracture apertures of newly generated fractures in horizontal plane after microwave exposure under no stress.

The fracture volume increases from 1.8% to 16.1% for the core not exposed under stress, determined by X-ray CT. The core under 1000 psi gas pressure during microwave exposure increased to a lesser degree from 0.5% to 5.5%. Here it was likely constrained by the pressure vessel which only provided 1 mm gap between the 50 mm diameter core and the vessel. Vertical expansion of the core was not likely to have been hindered by the vessel, as the clearance was >10 mm. However, lithotype and maceral /mineral matter compositions may differ between the two cores, reflecting coal's heterogeneous nature despite being adjacent to the same core. Or the simulated hydrostatic pressure may have also affected the fracture generation and aperture enhancements. Regardless, the fracture and aperture gains are expected to significantly enhance permeability in tight coals either for methane extraction or carbon dioxide injection.

### 4.1.3 Role of lithotypes and surface porosity

The anisotropic nature of the induced fractures of the coal is likely dependent on the presence of lithotypes. Lithotypes are expected to have different fracturing strength, fracturing tendency, type and direction of failure, moisture content, porosity, and mineral content. Hence lithotypes are expected to play a role in artificial fracturing by microwave exposure. Optical microscopy was utilized in deciding the role of the microlithotype during the artificial microwave fracturing process. An oil immersion lens was utilized to aid contrast among the microlithotypes. An automated stage, coupled to an optical microscope, was used to capture the polished surface of the post-microwave core at selected location and mosaics were produced. Five of these micrographs were assembled with Double-Take software, capturing a portion of the polished surface (Figure 4-12) with high-resolution: 600 pixels per mm (11346 x 5848 pixels total) representing an area of 153.53 mm<sup>2</sup>. The resin was false-coloring blue to aid in identification. This area was selected as the likely initiation location for some major induced fractures, as determined from X-ray CT observations (greatest aperture generation). Furthermore, due to the greater resolution, additional microfractures are likely to be observed and this was indeed the case. These microfractures will not contribute significantly to the permeability (small aperture size) but are expected to significantly aid in degasification (reduction of diffusion length) and carbon dioxide injectivity in those regions. Figure 4-11 shows fracture distribution of the selected region of Figure 4-12, if the apertures are classified as shown in Table 4. The region is shown in Figure 4-13.

Table 4-1. Relative classification of fractures identified in Figure 4-10.

Aperture Range (mm)	>1	1-0.1	0.1-0.01	0.01-0.001
Classification	Large	Medium	Small	Very Small

There are a significant number of very small microfractures while large fractures are very few in number in the field of view. This was expected as cleat distribution frequencies are often power-law distributions: far more small cleats than larger cleats (Solano-Acosta, Mastalerz and Schimmelmann, 2007).

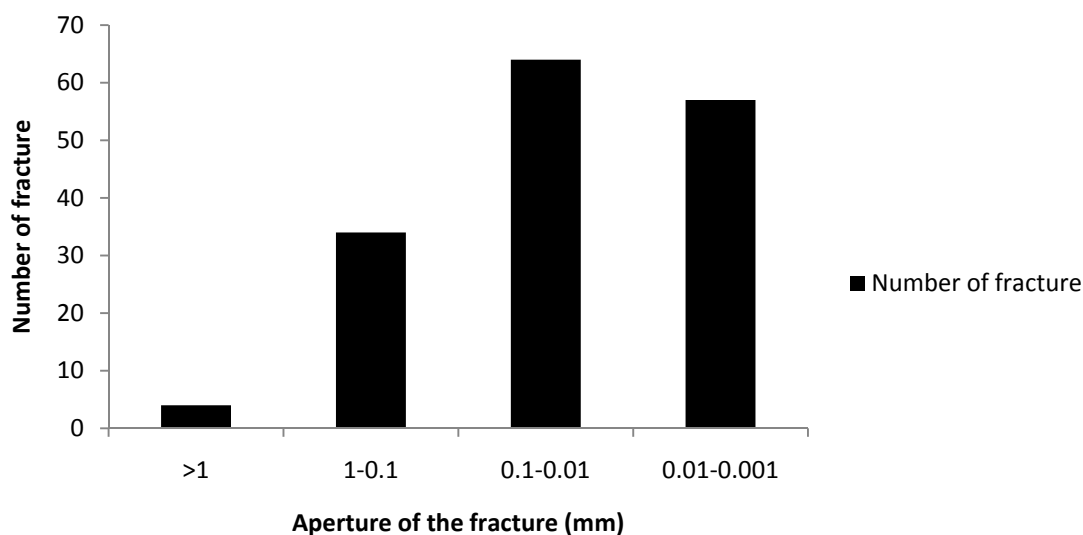


Figure 4-11. Number of fractures in various aperture ranges observed by optical microscope.

The fracture area was 24% of the (coal) region of view (Figure 4-13). New fractures were likely initiated at the highly-reflecting macerals at this location. Many of the induced fractures propagated through vitrinite bands within the lithotype and merged into the existing cleat system. The fractures in the top right hand region appear to cross along and across the fusinite or semifusinite banding. Inherently inertinite lithotypes are friable, and can shatter through thermal shock (Stach E., Mackowsky M.Th., Teichmuller M., Taylor G.H., Chandra D. and Teichmuller R., 1975). In Figure 4-13, the widest fractures appear between inertinite domains. However more work is needed to determine if this is a controlling fracture mechanism or simply the weakest location in this coal? In terms of microlithotype composition, the thicker vitrinite bands readily fracture along and across the bands (Dawson and Esterle). Vitrinite bands are often more fractured

in banded coal than other lithotype bands and this feature is used in the vitrain definition. Vitrains glassy nature likely contributes to its effective fracturing..

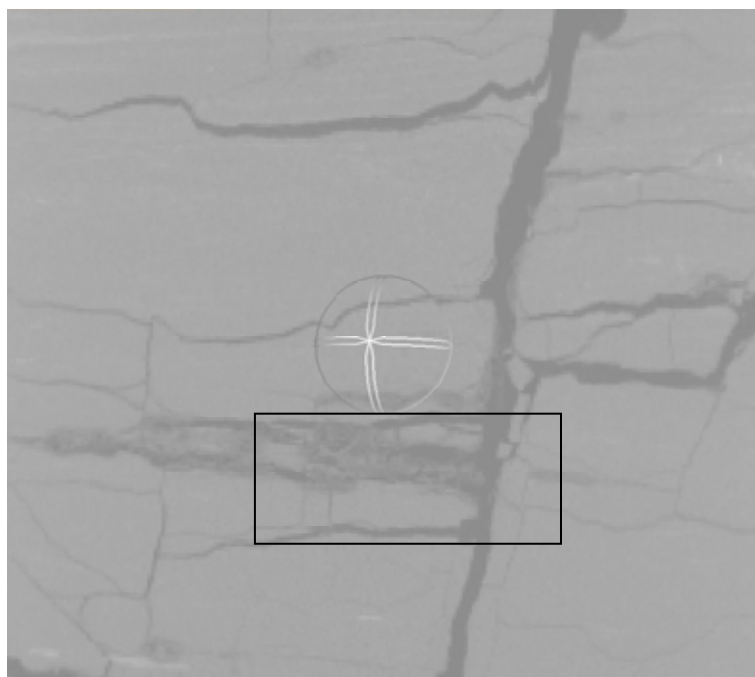


Figure 4-12. Surface of the coal obtained from X-ray CT reconstructions at the desired location. Black color shows epoxy filled fracture surfaces. Highlighted portion is focused in the Figure 4-13.

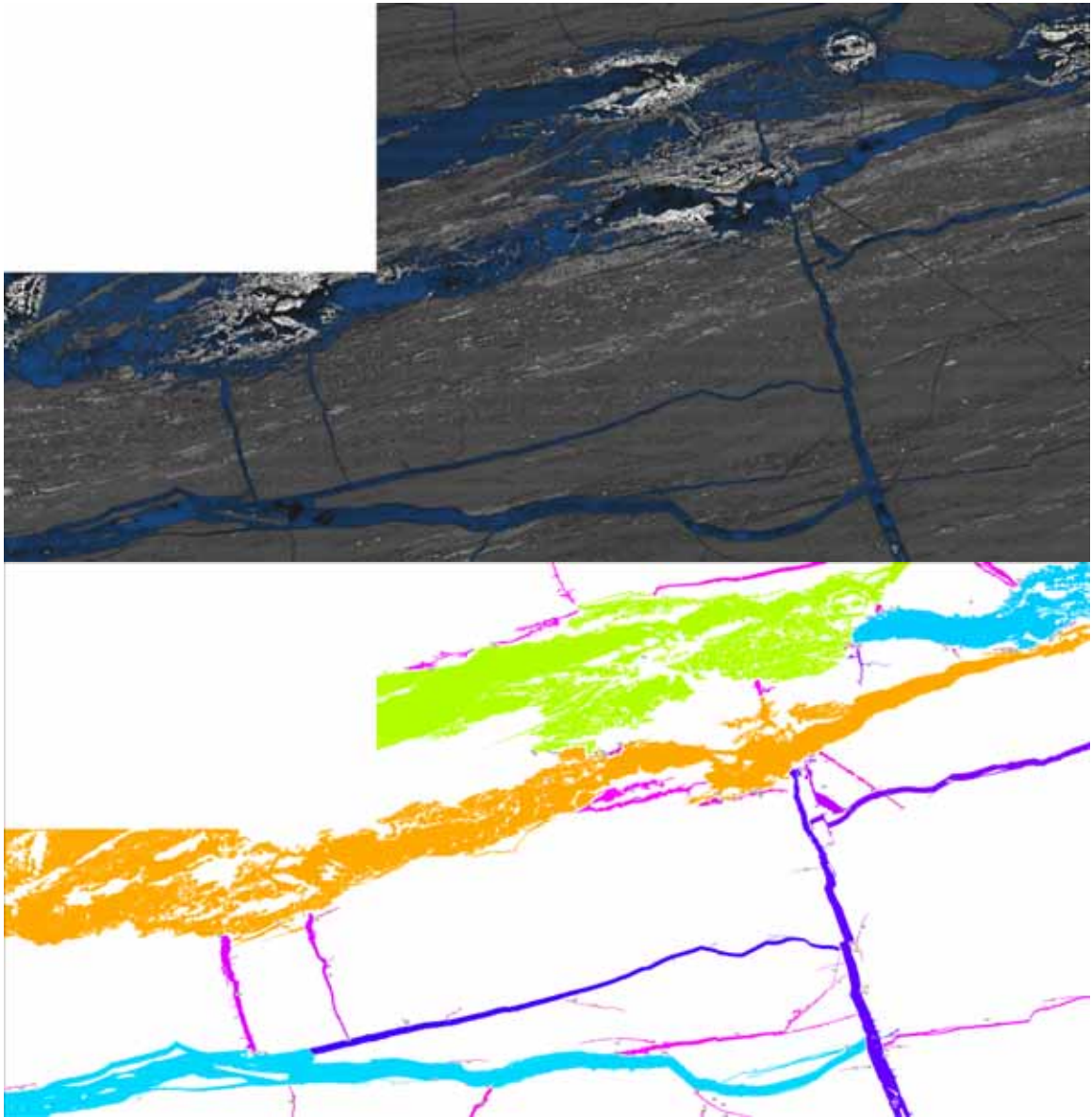


Figure 4-13. Mosaic of micrographs obtained from the vertical bituminous coal surface following microwave exposure. Cleats and fractures are false-colored in blue (upper) and false coloring by their aperture (lower).

It is likely that mineral grains will not only absorb microwave energy but also will generate fractures around the mineral/coal interface that will aid in comminution for extracted coals or will impede fracture propagation. This was explored with additional optical microscopy at an additional site in the core that was confined during exposure. Figure 4-14 shows 4 micrographs

containing mineral/fracture interactions. A fracture passing through one of the mineral grains is shown in the upper left image Figure 4-14 (a). It is noticeable that the fracture in the upper right image passes a pyrite grain that appears to have generated porosity around its exterior Figure 4-14(b). This is presumably due to temperature and thermal expansion. The fracture has circumvented the mineral grains at the surface and then proceeded further. Upper right image in Figure 4-14(b), fracture has circumvented a pyrite particle while in upper left image the fracture has propagated through the heavy inclusion.

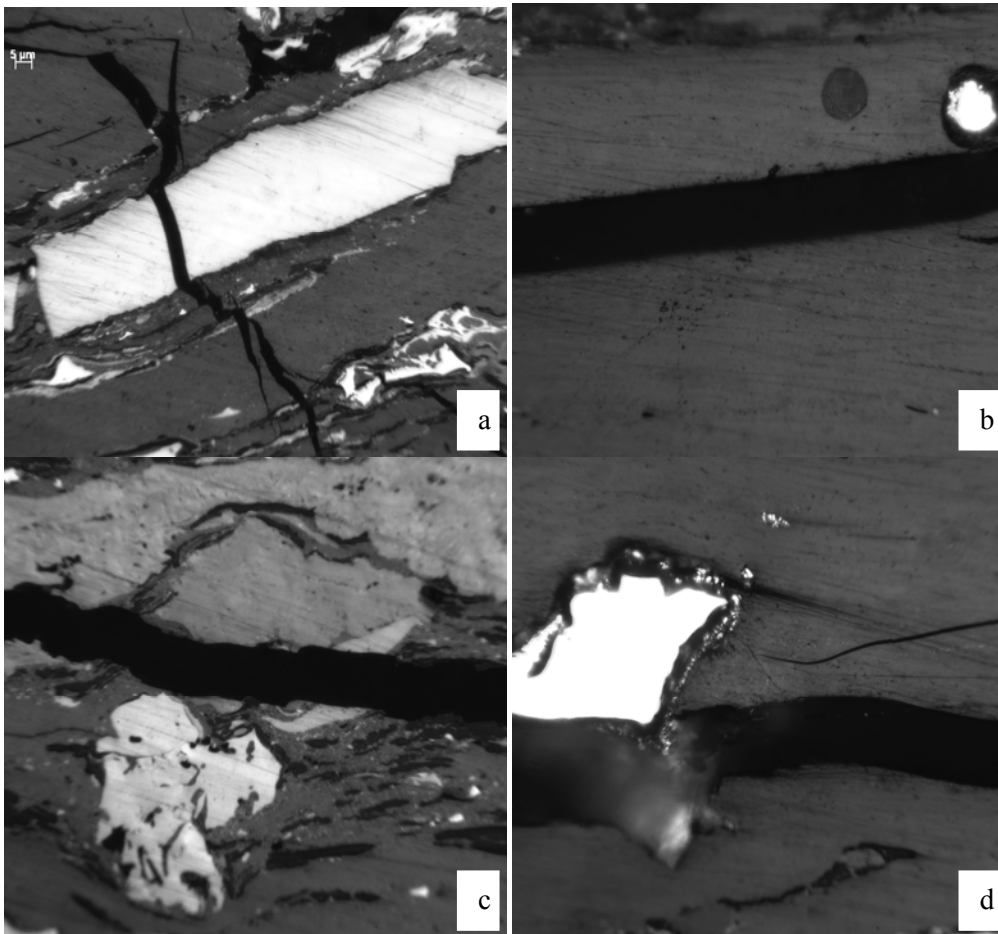


Figure 4-14. Fracture and mineral grain interactions for the coal stressed while exposed.

#### **4.2 POTENTIAL MECHANISMS OF MICROWAVE-INDUCED FRACTURES**

It is unclear if it is the bulk water in macropores or the more widely dispersed bound water in micropores that is responsible for the majority of the fracturing. However, high micropore methane pressure is thought to be one of the cleat formation mechanisms (Rogers, 1994). Alternatively, high macropore surfaces may yield steam condensation sites and limit the duration of the enhanced stress. In the field, the presence of methane reduces the strength of coal (Aziz and Ming-Li, 1999) and the fracturing may be enhanced beyond these observations. Microscopy observation of the hydrostatically stressed core (during microwave exposure) suggests that the microwave-induced fractures are of type I mode opening (Laubach, Marrett, Olson and Scott, 1998).

In addition, it can be postulated that the water present in the lithotype rapidly converts into super-heated steam during microwaving at high power densities. The super-heated steam develops pressure differential inside the pore network of the coal generate potential sites for fracture generation. These fractures propagate in the weak lithotype banding until they intersect the natural fracture system where they terminate. Elevated pore pressure is one of the proposed mechanisms for opening-mode fracture creation (in a compressive stress state) when hydrocarbon gas generation is sufficient.

#### **4.3 POTENTIAL APPLICATION OF MICROWAVE ENERGY FOR ECBM**

Microwave induced fracturing can be utilized in horizontal drilling where the microwave burst fractures would grow perpendicular to the bedding and, therefore, allow more access to the methane degasification or CO<sub>2</sub> injection. A Microwave generator can be attached to the drill bit and the proximal wellbore region can be exposed to short bursts of high-energy microwaves.

There is extensive borehole network in the underground mining as shown in Figure 2-3. These boreholes can be used as access to the in-seam coal for microwave bursts. Microwave generator and antenna can be sent to the desired location via these boreholes. High-energy microwave exposure to the coal would have higher connectivity and larger drainage area and, as a result, reduce skin factor. A low skin factor would allow higher productivity and reduced pressure drop in the wellbore region. However, more work is required to decide the optimum moisture content of the coal seam for better production with microwave bursts. Should it be done as soon as seam is exposed or at some later stages of dewatering?

Reduced diameter drill bit can be used if the coal is fractured during the drilling by the microwave bursts. However, safety issues in the employment of microwave fracturing technique have not been addressed. Highly fractured coal lumps or particles can be removed during the retreat of the bit. Economic viability of this technique requires more work.

## Chapter 5 : SUMMARY AND CONCLUSIONS

The potential of microwave exposure was evaluated, for the first time, in developing new fractures and cleat aperture enhancement in bituminous coal under hydrostatic stress. Bituminous coal cores under both the absence and presence of simulated hydrostatic stress were exposed to short-bursts of high-energy microwaves. A X-ray and microwave transparent vessel was fabricated to allow both microwave exposure under stress and X-ray CT observations. The hydrostatic stress being simulated with 1000 psi argon gas pressure. A 15kw multi mode cavity microwave chamber was used to provide high-energy microwave bursts to the coal cores for a total of 3 seconds under stressed and unstressed condition. Exposure of microwave energy to coal generated new fractures and enhanced the existing natural fracture apertures for the unstressed core. For the first time, similar fracture enhancements (fracture creation and aperture enhancements) were observed in a coal core under simulated hydrostatic stress.

Fracture volume was determined with X-ray computed tomography. The fracture volume increased from 1.8% to 16.1% in the unstressed coal core while it increased from 0.5% to 5.5% in the case of stressed coal core under hydrostatic condition. Cleat aperture enhancement were observed for both cores being on the order of 400% for unstressed core and lower values of around 100% for the single cleat in the cores while exposed under stress. The 1mm relief between coal and pressure vessel likely restricted the fracture enhancement and expansion, similarly to the in situ conditions. The induced fractures have various orientations but at these conditions they tended to be more horizontal and often these were contained within certain lithotypes. The role of the lithotypes in the microwave fracturing was investigated via optical microscopy. Thicker vitrinite bands readily fractured along and across these lithotype bands. Fractures were mode I openings in nature, and they propagated through the glassy (brittle) lithotypes often terminating at the cleat system. Induced fractures often circumvented certain minerals such as pyrite but able

to cleave small clay particle. In the region examined, greater induced volume in the inertinite region was thought to be fracture initiation site.

It is expected that the water present in the coal formed high energy water molecules or steam. It is unclear if it is the bulk water in macropores or the more widely dispersed bound water in micropores that is responsible for the induced enhancements in fracture volume. These highly energetic water molecules may duplicate high methane pressure which is thought to be one of the cleat formation mechanisms. Alternatively, high energy steam may generate localized stress disruptions resulting in fracturing. It is important to note that these experiments were performed without methane present in the coal. The presence of methane lowers the strength of coal and it should be expected that the fracturing may be more extensive with microwave exposure.

Thus, microwave exposure may aid in increased connectivity and enhanced-flow between horizontal wellbore and coal for enhanced coalbed methane production (injectivity) or in-seam degasification for greenhouse gas (CH<sub>4</sub>) reduction prior to coal extraction. New fractures and enhancements to cleat/fracture apertures would make an impact in productivity during extraction of methane or injection of CO<sub>2</sub> during sequestration.

## **FUTURE WORK**

This study was a preliminary evaluation of the potential of high-energy microwaves to generate or enhance new fracture in hydrostatically stressed coal. This was performed with one coal at one stress condition. By increasing the sampling the effect of microwave frequency, power, exposure time, coal gas content, moisture content, temporal and spatial spacing of exposure, mineral matter and macerals, composition can be evaluated and the process optimized. Fines generation, safety of microwave exposure in active coal seams, and fire/explosion risks will also need to be evaluated before demonstration phase could proceed.

Microwaves are likely to have penetration depth ranging in meters. The penetration depth of microwaves- in different types of coal under various in situ conditions- may vary and require more research and study. Optimum level of moisture that should present in the coal for maximum impact of microwave high-energy bursts would optimize the time of microwave exposure. Optimum utilization of extensive borehole network in underground coal mine working for microwave bursts needs to be investigated. Borehole frequency, length and spatial location with respect to coal deposition should be studied for better utilization of infrastructure. The integration of all parameters with economics would predict the economic viability of this technique in coalbed methane reservoirs.

## **ACKNOWLEDGEMENTS**

Funding for this project is provided through the "Ultra-Deepwater and Unconventional Natural Gas and Other Petroleum Resources Research and Development Program" authorized by the Energy Policy Act of 2005. This program, funded from lease bonuses and royalties paid by industry to produce oil and gas on federal lands, is specifically designed to increase supply and reduce costs to consumers while enhancing the global leadership position of the United States in energy technology through the development of domestic intellectual capital. RPSEA is under contract with the U.S. Department of Energy's National Energy Technology Laboratory to administer several elements of the program. RPSEA is a 501(c)(3) nonprofit consortium with more than 150 members, including 24 of the nation's premier research universities, five national laboratories, other major research institutions, large and small energy producers and energy consumers. The mission of RPSEA, headquartered in Sugar Land, Texas, is to provide a stewardship role in ensuring the focused research, development and deployment of safe and environmentally responsible technology that can effectively deliver hydrocarbons from domestic resources to the citizens of the United States. Additional information can be found at [www.rpsea.org](http://www.rpsea.org).

## REFERENCES

- Arnold, B.J. and Aplan, F.F., 1989. The hydrophobicity of coal macerals. *Fuel*, 68(5): 651-658.
- ASTM, International, 2010. D3302/D3302M - 10, Standard Test Method for Total Moisture in Coal.
- Ayers, W.B., Jr., 2002. Coalbed gas systems, resources, and production and a review of contrasting cases from the San Juan and Powder River Basins. *AAPG Bulletin*, 86(11): 1853-1890.
- Aziz, N.I. and Ming-Li, W., 1999. The effect of sorbed gas on the strength of coal – an experimental study. *Geotechnical and Geological Engineering*, 17(3): 387-402.
- Billings, M.P., 1954. *Structural Geology*. Prentice Hall, New Jersey, 1-514 pp.
- Bird, R.B., Stewart, W.E. and Lightfoot, E.N., 1960. *Transport Phenomena*. John Wiley & Sons, Inc., Newyork.
- Bogdal, D. and Prociak, A., 2007. *Microwave-Enhanced Polymer Chemistry and Technology 1*. Blackwell, Poland, 275 pp.
- Bustin, R.M., Cameron, A.R., Grieve, D.A. and Kalkreuth, W.D., 1985. *Coal petrology - its principles, methods, and applications*, 243 pp.
- Bustin, R.M. and Clarkson, C.R., 1998. Geological controls on coalbed methane reservoir capacity and gas content. *International Journal of Coal Geology*, 38(1-2): 3-26.
- Chanaa, M.B., Lallemand, M. and Mokhlisse, A., 1994. Pyrolysis of Timahdit, Morocco, oil shales under microwave field. *Fuel*, 73(10): 1643-1649.
- Clarkson, C.R. and Bustin, M.R., 1996. Variation in micropore capacity and size distribution with composition in bituminous coal of the Western Canadian Sedimentary Basin : Implications for coalbed methane potential. *Fuel*, 75(13): 1483-1498.

- Clarkson, C.R. and Bustin, R.M., 1997. Variation in permeability with lithotype and maceral composition of Cretaceous coals of the Canadian Cordillera. *International Journal of Coal Geology*, 33(2): 135-151.
- Cloke, M., Lester, E., Allen, M. and Miles, N.J., 1995. Automated maceral analysis using fluorescence microscopy and image analysis. *Fuel*, 74(5): 659-669.
- Close, J. and Mavor, M., 1991. Influence of coal composition and rank on fracture development in Fruitland coal gas reservoirs of the San Juan Basin. In: S. Schwochow, D.K. Murray and M.F. Fahy (Editors), *Rocky Mountains Association Geol. Field Conf.*, pp. 109–121.
- Close, J.C., 1993. Natural fractures in coal. In: B.E. Law and D.D. Rice (Editors), *AAPG Studies in Geology*. American Association of Petroleum Geologists, Tulsa, OK, USA, pp. 119-132.
- Creedy, D.P., Garner, K., Holloway, S. and Ren, T.X., 2001. A review of the worldwide status of coalbed methane extraction and utilization, UK Department of Trade and Industry.
- Crosdale, P.J., Beamish, B.B. and Valix, M., 1998. Coalbed methane sorption related to coal composition. *International Journal of Coal Geology*, 35(1-4): 147-158.
- Cui, X. and Bustin, R.M., 2005. Volumetric strain associated with methane desorption and its impact on coalbed gas production from deep coal seams. *AAPG Bulletin*, 89(9): 1181-1202.
- Cussler, E.L., 1997. *Diffusion: Mass Transfer in Fluid Systems* Cambridge University Press, Cambridge, UK, 579 pp.
- Daniels, E.J. and Altaner, S.P., 1990. Clay mineral authigenesis in coal and shale from the anthracite region, Pennsylvania. *American Mineralogist*, 75(7-8): 825-839.
- Davidson, R.M., Sloss, L.L. and Clarke, L.B., 1995. *Coalbed Methane Extraction*. IEA Coal Research.

- Dawson, G.K.W. and Esterle, J.S., 2010. Controls on coal cleat spacing. *International Journal of Coal Geology*, 82(3-4): 213-218.
- Diamond, W.P., McCulloch, C.M. and Bench, B.M., 1975. Estimation of coal cleat orientation using surface joint and photo linear analysis U.S. Bureau of Mines, Pittsburgh.
- Durucan, S. and Shi, J.Q., 2009. Improving the CO<sub>2</sub> well injectivity and enhanced coalbed methane production performance in coal seams. *International Journal of Coal Geology*, 77(1-2): 214-221.
- Economic Commission, 2010. Best practice guidance for effective methane drainage and use in coal mines 978-92-1-117018-4, Geneva.
- Economides, M.J., Hill, A.D. and Ehlig-Economides, C., 1993. *Petroleum Production System*. PTR Prentice Hall, Englewood Cliffs, NJ, 83 pp.
- Energy Information Administration, Department of Energy, 2009. *International Energy Outlook 2009*.
- Ertekin, T. and Sung, W., 1991. Structural properties of coal that control coalbed methane production. In: D.C. Peters (Editor), *Geology in coal resource utilization*, Energy Minerals Division. American Association of Petroleum Geologists, Fairfax, VA, pp. 105-124.
- Florentin, R., Aziz, N., Black, D. and Ngheim, L., 2010. Stored gas recovery in coal by nitrogen injection 2010 International Coalbed and Shale Gas Symposium. University of Alabama, Tuscaloosa, AL.
- Fokker, P.A. and Van der Meer, L.G.H., 2004. The injectivity of coalbed CO<sub>2</sub> injection wells. *Energy & Fuels*, 29: 1423-1429.
- Gale, J. and Freund, P., 2001. Coal-Bed methane enhancement with CO<sub>2</sub> sequestration worldwide potential. *Environmental Geosciences*, 8(3): 210-217.

- Gall, B.L., Sattler, A.R., Maloney D.R. and Raible, C.J., 1988. Permeability damage to natural fractures caused by fracturing fluid polymers, SPE Rocky Mountain Regional Meeting. SPE, Casper, Wyoming.
- Gamson, P.D., Beamish, B.B. and Johnson, D.P., 1993. Coal microstructure and micropermeability and their effects on natural gas recovery. *Fuel*, 72(1): 87-99.
- Gash, B.W., Volz, R.F., Potter, G. and Corgan, J.M., 1993. The effects of cleat orientation and confining pressure on cleat porosity, permeability and relative permeability in coal, International Coalbed Methane Conference, University of Alabama, Tuscaloosa.
- Gentzis, T., Deisman, N. and Chalaturnyk, R.J., 2007. Geomechanical properties and permeability of coals from the Foothills and Mountain regions of western Canada. *International Journal of Coal Geology*, 69(3): 153-164.
- Gidley, J.L., Holditch, S.A., Nierode, D.E. and Veatch, R.W., 1989. Recent Advances in Hydraulic Fracturing, 12. SPE, Richardson, TX.
- Glick, D.C., Mitchell, G.D. and Davis, A., 2005. Coal sample preservation in foil multilaminate bags. *International Journal of Coal Geology*, 63(1-2): 178-189.
- Gray, I., 1987a. Reservoir engineering in coal seams: Part 1-The physical process of gas storage and movement in coal seams. *SPE Reservoir Engineering*, 2(1): 28-34.
- Gray, I., 1987b. Reservoir engineering in coal seams: Part 2- Observation of gas movement in coal seams. *SPE Reservoir Engineering*, 2: 35-40.
- Halliburton, 2008. Economics of Coalbed Methane Recovery. *Coalbed Methane: Principles and Practices*. Halliburton, 461-490 pp.
- Hancock, P.L. and Engelder, T., 1989. Neotectonic joints. *Geological Society of America Bulletin*, 101(10): 1197-1208.
- Harpalani, S. and Schraufnagel, R.A., 1990. Shrinkage of coal matrix with release of gas and its impact on permeability of coal. *Fuel*, 69(5): 551-556.

- Hayashi, J.-i., Norinaga, K., Kudo, N. and Chiba, T., 2001. Estimation of Size and Shape of Pores in Moist Coal Utilizing Sorbed Water as a Molecular Probe. *Energy & Fuels*, 15(4): 903-909.
- Honda, H., 1959. The change in magnetic properties in carbonization and graphitization of coal, Third Conference on Carbon. Pergamon, Buffalo.
- Hower, J.C., 1998. Interrelationship of coal grinding properties and coal petrology. *Minerals & Metallurgical Processing*, 15(3): 16.
- ICCP, 1963. International Handbook of Coal Petrography. Centre de la Recherche Scientifique, Paris, France.
- Karacan, C.Ö., 2003. Heterogeneous sorption and swelling in a confined and stressed coal during CO<sub>2</sub> injection. *Energy & Fuels*, 17(6): 1595-1608.
- Karacan, C.Ö. and Mitchell, G.D., 2003. Behavior and effect of different coal microlithotypes during gas transport for carbon dioxide sequestration into coal seams. *International Journal of Coal Geology*, 53(4): 201-217.
- Karacan, C.Ö. and Okandan, E., 2000. Fracture/cleat analysis of coals from Zonguldak Basin (northwestern Turkey) relative to the potential of coalbed methane production. *International Journal of Coal Geology*, 44(2): 109-125.
- Kelso, B.S., 1994. Geologic controls on open-hole cavity completions in the San Juan basin. *Quarterly Review of Methane from Coal Seams Technology*, 3&4: 1-6.
- Kendell, J., 2007. Natural Gas Annual 2006, Energy Information Administration, Washington D.C.
- Kennedy, A., 2002. R&D in Oilwell Drilling. *GeoDrilling International*, 10(2).
- King, B. and Long, G., 2007. US Coalbed Methane: Past, Present and Future. Energy Information Administration.

- Kingman, S., Lester, E., Wu, T., Mathews, J.P. and Bradshaw, S., 2007. The potential of coal microwaving in power stations to improve grindability International Conference on Coal Science and Technology. The University of Nottingham, England, Nottingham, England.
- Kingman, S.W., Corfield, G.M. and Rowson, N.A., 1999. Effects of microwave radiation upon the mineralogy and magnetic processing of a massive Norwegian Ilmenite ore. *Magnetic and Electrical Separation*, 9(3): 131-148.
- Krevelen, D.W.V. (Editor), 1992. *Coal: Topology-Physics-Chemistry-Constitution*. Elsevier, The Netherlands, 73-104 pp.
- Kulander, B.R. and Dean, S.L., 1993. Coal-cleat domains and domain boundaries in the Allegheny Plateau of West Virginia. *AAPG Bulletin*, 77(8): 1374-1388.
- Kuuskräa, V.A. and Brandenburg, C.F., 1989. Coalbed methane sparks a new energy industry. *Oil and Gas Journal*, 87(41): 49-56.
- Lamberson, M.N. and Bustin, R.M., 1993. Coalbed methane characteristics of Gates Formation coals, Northeastern British Columbia: Effect of maceral composition. *AAPG Bulletin*, 77(12): 2062-2076.
- Langmuir, I., 1916. The constitution and fundamental properties of solids and liquids. *Journal of the American Chemical Society*, 38.
- Laubach, S.E., Marrett, R.A., Olson, J.E. and Scott, A.R., 1998. Characteristics and origins of coal cleat: A review. *International Journal of Coal Geology*, 35(1-4): 175-207.
- Laubach, S.E. and Tremain, C.M., 1991. Distribution and origin of regional coal fracture (cleat) domains in Upper Cretaceous Fruitland Formation coal; possible effects on coalbed stimulation and methane production. *AAPG, Tulsa, OK, United States (USA)*, 75(3): 618.
- Lester, E. and Kingman, S., 2004. The effect of microwave pre-heating on five different coals. *Fuel*, 83(14-15): 1941-1947.

- Lester, E., Kingman, S. and Dodds, C., 2005. Increased coal grindability as a result of microwave pretreatment at economic energy inputs. *Fuel*, 84(4): 423-427.
- Lester, E., Kingman, S., Dodds, C. and Patrick, J., 2006. The potential for rapid coke making using microwave energy. *Fuel*, 85(14-15): 2057-2063.
- Levine, J.R., 1993. Coalification: the evolution of coal as source rock and reservoir rock for oil and gas. *AAPG Study in Geology*, 38: 39-77.
- Lin, C.L., Miller, J.D., Cortes, A.B. and Galery, R., 1991. Coal washability analysis by X-ray computed tomography. *International Journal of Coal Preparation and Utilization*, 9(3): 107 - 119.
- Lucia, F.J., 1983. Petrophysical parameters estimated from visual descriptions of carbonate rocks: a field classification of carbonate pore space. *Journal of Petroleum Technology*, 35(3): 629-637.
- Lytle, J., Choi, N. and Prisbrey, K., 1992. Influence of preheating on grindability of coal. *International Journal of Mineral Processing*, 36(1-2): 107-112.
- Mahadevan, V., 2002. Versatility of microwave applications to processing: coal and ores, National Symposium of Sustainable Mining Technology: Present and Future. Anna University, India.
- Mahajan, O.P. and Walker, P.L., 1971. Water adsorption on coals. *Fuel*, 50(3): 308-317.
- Markowski, A.K., 1998. Coalbed methane resource potential and current prospects in Pennsylvania. *International Journal of Coal Geology*, 38(1-2): 137-159.
- Marland, S., Han, B., Merchant, A. and Rowson, N., 2000. The effect of microwave radiation on coal grindability. *Fuel*, 79(11): 1283-1288.
- Mathews, J.P., Pone, J.D.N., Mitchell, G.D. and Halleck, P.M., 2009. High resolution X-ray computed tomography observations of thermal drying of lump sized bituminous coal, International Conference on Coal Science and Technology, Cape Town, South Africa.

- Maylotte, D.H. et al., 1984. Application to X-ray computed tomography to coal studies, Symposium On Structure And Chemistry Of Carbonaceous Materials, Newyork.
- Maylotte, D.H., Lamby, E.J., Kosky, P.G. and St. Peters, R.L., 1981. Computed tomography of coal during pyrolysis, International Conference of Coal Science, Oviedo, Spain, pp. 612.
- Mazumder, S., Wolf, K.H.A.A., Elewaut, K. and Ephraim, R., 2006. Application of X-ray computed tomography for analyzing cleat spacing and cleat aperture in coal samples. International Journal of Coal Geology, 68(3-4): 205-222.
- McCulloch, C.M., Deul, M. and Jeran, P.W., 1974. Cleat in bituminous coalbeds, US Bureau Mines Report of Investigations, pp. 1-25.
- McElhiney, J.E., Koenig, R.A. and Schraufnagel, R.A., 1989. Evaluation of coalbed methane reserves involves different techniques. Oil and Gas Journal, 87(44): 63-72.
- Meredith, R., 1997. Engineers Handbook of Industrial Microwave Heating. Institution of Electrical Engineers, 350 pp.
- Moza, A.K. and Neavel, R.C., 1986. Estimation of coal washability using X-radiography. Fuel, 65(4): 547-551.
- Nandi S, P. and Walker P, L., 1966. Diffusion of Argon from coals of different rank, Coal Science. Advances in Chemistry. AMERICAN CHEMICAL SOCIETY, pp. 379-385.
- Nandi, S.P. and Walker Jr, P.L., 1970. Activated diffusion of methane in coal. Fuel, 49(3): 309-323.
- Niekerk, D.V., Halleck, P.M. and Mathews, J.P., Solvent swelling behavior of Permian-aged South African vitrinite-rich and inertinite-rich coals. Fuel, 89(1): 19-25.
- Norinaga, K., Kumagai, H., Hayashi, J.I. and Chiba, T., 1997. Type of water associated with coal. Energy & Fuels, ACS Publications.
- Olague, N.E. and Smith, D.M., 1989. Diffusion of gases in American coals. Fuel, 68(11): 1381-1387.

- Palmer, I. and Mansoori, J., 1998. How permeability depends on stress and pore pressure in coalbeds: A new model. *SPE Reservoir Evaluation & Engineering*.
- Pashin, J.C., 1998. Stratigraphy and structure of coalbed methane reservoirs in the United States: An overview. *International Journal of Coal Geology*, 35(1-4): 209-240.
- Pattison, C.I., Fielding, C.R., McWatters, R.H. and Hamilton, L.H., 1996. Nature and origin of fractures in Permian coals from the Bowen Basin, Queensland, Australia. Coalbed methane and coal geology in *Geological Society Special Publications*, 109: 133-150.
- Pone, J.D.N., Halleck, P.M. and Mathews, J.P., 2009a. Methane and Carbon Dioxide sorption and transport rates in coal at in-situ conditions. *Energy Procedia*, 1(1): 3121-3128.
- Pone, J.D.N., Halleck, P.M. and Mathews, J.P., 2009b. Sorption capacity and sorption kinetic measurements of CO<sub>2</sub> and CH<sub>4</sub> in confined and unconfined bituminous coal. *Energy & Fuels*, 23(9): 4688-4695.
- Pone, J.D.N., Halleck, P.M. and Mathews, J.P., 2010. 3D characterization of coal strains induced by compression, carbon dioxide sorption, and desorption at in-situ stress conditions. *International Journal of Coal Geology*, 82(3-4).
- Puri, R., King, G.E. and Palmer, I.D., 1991. Damage to coal permeability during hydraulic fracturing, Coalbed Methane Symposium. University of Alabama, Alabama, AL.
- Pyrak-Nolte, L.J., Haley, G.M. and Gash, B.W., 1993. Effective cleat porosity & cleat geometry from the Wood's Metal porosimetry, International Coalbed Methane Symposium Alabama. The University of Alabama, Tuscaloosa.
- Pyrak-Nolte, L.J., Montemagno, C.D. and Nolte, D.D., 1997. Volumetric imaging of aperture distributions in connected fracture networks. *Geophys. Res. Lett.*, 24(18).
- Reeves, S.R., 2003. Enhanced CBM recovery coalbed CO<sub>2</sub> sequestration assessed. *Oil and gas Journal*, 101(27): 49.

- Reucroft, P.J. and Sethuraman, A.R., 1987. Effect of pressure on carbon dioxide induced coal swelling. *Energy & Fuels*, 1(1): 72-75.
- Rogers, R.E., 1994. *Coalbed Methane: Principles and Practice*. PTR Prentice Hall, Englewood Cliffs, N.J.
- Rowson, N.A., 1990. Desulphurization of coal using low power microwave energy *Minerals Engineering*, 3.
- Saites, F., Guo, R., Mannhardt, K. and Kantzas, A., 2006. A coal characterization and transport phenomenon in coalbed, CHISA, Novotneho Lavka, Czech Republic.
- Sarunac, N. et al., 2009. A novel fluidized bed drying and density segregation process for upgrading low-rank coals. *International Journal of Coal Preparation and Utilization*, 29(6): 317 - 332.
- Scott, A.R., 2002. Hydrogeologic factors affecting gas content distribution in coal beds. *International Journal of Coal Geology*, 50(1-4): 363-387.
- Shimada, S., Zhang, M. and Li, H., 2004. Anisotropy of gas permeability associated with cleat pattern in a coal seam of the Kushiro coalfield in Japan. *Environmental geology*, 47(1): 45-50.
- Smith, D.H. and Jikich, S.A., 2009. Permeability, elastic, and carbon dioxide-sorption properties of Upper Freeport coalbed cores from a carbon dioxide sequestration/enhanced coalbed methane field project, Coalbed and Shale Gas Symposium. University of Alabama, Tuscaloosa, Alabama.
- Smith, D.M. and Williams, F.L., 1984. Diffusional effects in the recovery of methane from coalbeds. *SPE Journal*, 24(5): 529-535.
- Smyth, M. and Buckley, M.J., 1993. Statistical analysis of the microlithotype sequences in the Bulli Seam, Australia, and relevance to permeability for coal gas. *International Journal of Coal Geology*, 22(3-4): 167-187.

- Soeder, D.J., 1991. The effects of overburden stress on coalbed methane production. *Geology in Coal Resource Utilization*. TechBooks, Sponsored by American Association of Petroleum Geologists, Energy Minerals Division, Fairfax, VA.
- Solano-Acosta, W., Mastalerz, M. and Schimmelmann, A., 2007. Cleats and their relation to geologic lineaments and coalbed methane potential in Pennsylvanian coals in Indiana. *International Journal of Coal Geology*, 72(3-4): 187-208.
- Spears, D.A. and Caswell, S.A., 1986. Mineral matter in coals: cleat minerals and their origin in some coals from the English midlands. *International Journal of Coal Geology*, 6(2): 107-125.
- Stach E. et al., 1975. *Stach's Textbook of Coal Petrology*, Stuttgart.
- Su, X., Feng, Y., Chen, J. and Pan, J., 2001. The characteristics and origins of cleat in coal from Western North China. *International Journal of Coal Geology*, 47(1): 51-62.
- Sutton, W.H., 1989. *Microwave processing of ceramic materials*. American Ceramic Society, 68(2): 376-386.
- Talkington, C.C. and Schultz, K.H., 2004. An overview of the global coal mine methane industry, *International Coalbed Methane Conference*, Tuscaloosa, AL.
- Thakur, P.C., 2006. Advancing mine safety and energy production through coalbed methane production, *Coal Mine Gas Drainage and Monitoring techniques*, China, pp. 145-153.
- Thomas, L., 1994. *Handbook of Practical Coal Geology*. *Geological Journal*, 29, 289-290 pp.
- Ting, F.T.C., 1978. Origin and spacing of cleats in coal beds. *Mechanical Engineering*, 100(1): 101-101.
- Ting, F.T.C., 1987. Optical anisotropism and its relationship with some physical and chemical properties of coal. *Organic Geochemistry*, 11(5): 403-405.
- U.S.-E.P.A., 2000. *Emissions & Generation Resource Integrated Database (eGRID)*.

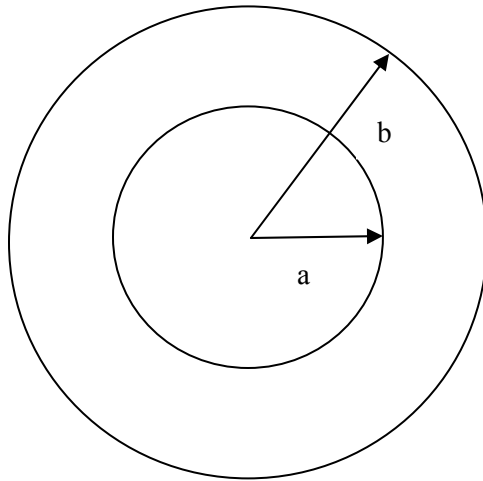
- Unsworth, J.F., Fowler, C.S. and Jones, L.F., 1989. Moisture in coal: 2. Maceral effects on pore structure. *Fuel*, 68(1): 18-26.
- Uslu, T. and Atalay, Ü., 2004. Microwave heating of coal for enhanced magnetic removal of pyrite. *Fuel Processing Technology*, 85(1): 21-29.
- van Bergen, F. et al., 2009. Production of gas from coal seams in the Upper Silesian Coal Basin in Poland in the post-injection period of an ECBM pilot site. *International Journal of Coal Geology*, 77(1-2): 175-187.
- Van Everdingen, A.F. and Hurst, W., 1949. The application of the Laplace transformation to flow problems in reservoirs. *Petroleum Transactions, AIME*, 186: 305-324.
- Van Geet, M. and Swennen, R., 2001. Quantitative 3D fracture analysis by means of microfocus X-ray computer tomography ( $\mu$ CT): An example from coal. *Geophys. Res. Lett.*, 28(17): 3333-3336.
- Viswanathan, M., 1990. Investigation on the effect of microwave pre-treatment on comminution/beneficiation and desulphurisation of coals 11th International Coal Preparation Congress, Tokyo, pp. 151-155.
- Wang, Y., Pang, X., Lu, S. and Chen, Z., 1997. Quantitative evaluation of coal as source rocks. *Natural Resources Research*, 6(4): 245-249.
- Warpinski, N.R. et al., 1990. Case Study of a Stimulation Experiment in a Fluvial, Tight-Sandstone Gas Reservoir. *SPE Production Engineering*, 5(4): 403-410.
- Wolf, K.-H.A.A., Codreanu, D.B., Ephraim, R. and Siemons, N., 2004. Analysing cleat angles in coal seams using image analysis techniques on artificial drilling cuttings and prepared coal blocks. *Geologica Belgica*, 7(3): 105.
- Wu, T., Lester, E., Kingman, S. and Dodds, C., 2005. Quantification of the influence of microwave pre-treatment on coal breakage, 13th International Conference on Coal Science and Technology, Okinawa, Japan.

- Yao, Y. et al., 2009. Non-destructive characterization of coal samples from China using microfocus X-ray computed tomography. *International Journal of Coal Geology*, 80(2): 113-123.
- Zavitsanos, P.D., 1978. Coal Desulfurization Using Microwave Energy. Report No. EPA-600/7-78-089.
- Zhang, H., Fang, C., Gao, X., Zhang, Z. and Jiang, Y., 1999. *Petroleum Geology*. Petroleum Industry Press, Beijing: 1-345.

## APPENDIX

### Pressure Vessel Construction Calculations

The vessel was considered as a pressurized thick-walled cylinder and all the calculations were carried out as hoop stress developing in the thick cylinders (Green, 1998).



Assuming that outside pressure  $P_b = 0$

The radial pressure which is compressive

$$\sigma_{rr} = \frac{a^2 P_a (r^2 - b^2)}{r^2 (b^2 - a^2)}$$

The tangential stress is tensile. The maximum value of tensile stress is of concern

$$\sigma_{\theta\theta} = -\frac{a^2 P_a (r^2 + b^2)}{r^2 (b^2 - a^2)}$$

As failure processes occurs usually from inside locations; for  $r = a$

$$\sigma_{\theta\theta} = -\frac{P_a (r^2 + b^2)}{(b^2 - a^2)}$$

Solving this equation for parameter, the variable has the value as follows:

$$a = b \sqrt{\frac{\sigma_{\theta\theta} - P_a}{\sigma_{\theta\theta} + P_a}}$$

Now,  $\sigma_{\theta\theta} \leq T$  for sustainable design. Here T= Tensile Strength of material

Polycarbonate strength is quoted as more than 10,000 psi from the manufacturer. Exact value, which is 16,000 psi for Grade 5 polycarbonate from this manufacturer, is available by calling customer service. To be on the safe side, a value of 9,000 psi was used for calculations. Pressure will be 1000 psi but for a factor of safety 3;  $P_a = 3000 \text{ psi}$  was considered.

$$\sigma_{\theta\theta} = T = 9000 \text{ psi}, P_a = 3000 \text{ psi and } b = 37 \text{ mm}$$

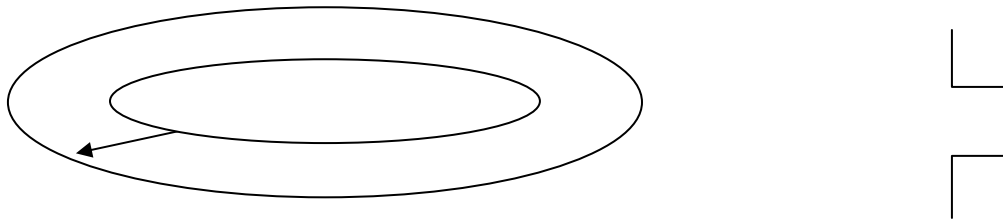
By putting these values in the equation above

$$a = b \sqrt{\frac{\sigma_{\theta\theta} - P_a}{\sigma_{\theta\theta} + P_a}} \text{ i.e.}$$

$$a = 37 \sqrt{\frac{9000 - 3000}{9000 + 3000}} = 26 \text{ mm}$$

$$\text{Thickness (t) of the vessel, } t = b - a = (37 - 26) \text{ mm} = 9 \text{ mm}$$

**Thread design:** 9 mm thick wall cylinder will be having internal threads for attaching a microwave transparent, gas (Nitrogen) delivery pipe. This pipe has outer thread for running over internal threads of a pressure vessel. Shearing strength of the



Thread has been designed to avoid shear failure of the threads. To ensure this, shearing force offered by all threads should be greater than the blow-off force exerted by the pressure vessel.

(P/2) is considered to be 0.05 inch.

$$\begin{aligned} \text{Blow off force} &= \text{Pressure inside the vessel} * \text{Area of vessel} = 3000 * (\pi r^2) \\ &= 3000 * \pi (0.98)^2 \text{ pounds} \dots \dots \dots \text{(A)} \end{aligned}$$

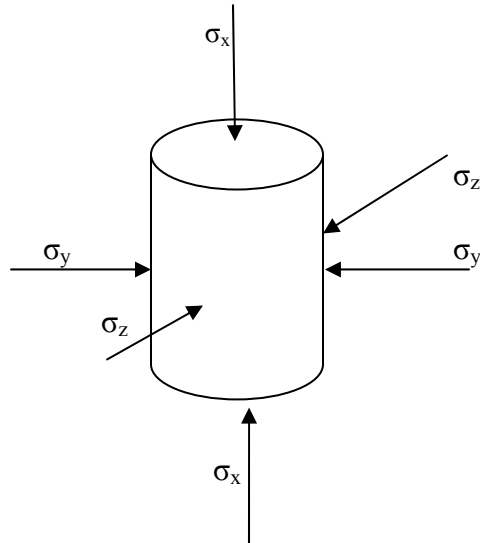
*Shear force offered by all threads*

$$\begin{aligned} &= (\text{Shearing strength} * \text{Shearing area per thread} \\ & * \text{number of threads}) \\ &= \left( 6000 * 2 * \pi * \left( r - \left( \frac{P}{2} \right) \right) * \left( \frac{P}{2} \right) * \text{number of threads} \right) \text{ pounds} \\ &= (6000 * 2 * \pi * (0.98 - 0.05) * (0.05) * \text{number of threads}) \text{ pounds} \\ & \dots \dots \dots \text{(B)} \end{aligned}$$

Making equation A and B

Number of threads comes out to be = 6.

### Equivalent stress calculation



Here  $\sigma_y = \sigma_z = \sigma_x$  are stresses in X, Y and Z directions. To maintain the hydrostatic conditions they are kept equal.

$$\sigma_y = \sigma_z = \nu \sigma_x = \rho g h = 2300 * 9.81 * (1875 / 3.28) * 0.000145 \text{ Psi} = 1875 \text{ Psi}$$

$\rho$ ,  $g$  and  $h$  represent density, gravity and depth respectively in MKS units.

$$\text{Hydrostatic Stress: } \sigma_X \frac{1+2\nu}{3} = \frac{1875(1+2*0.29)}{3} \sim 1000 \text{ Psi}$$

# **LITHOTYPE INFLUENCES ON (AN IDEALIZED) COAL CLEAT SURFACE DEFORMATION BY CARBON DIOXIDE INDUCED SWELLING**

Hemant Kumar, J. Denis N. Pone, Gareth D. Mitchell, Phillip M. Halleck, Jonathan P. Mathews,

126 Hosler Building, Department of Energy and Mineral Engineering & The EMS Energy

Institute, The Pennsylvania State University, University Park, PA 16802

[jmathews@psu.edu](mailto:jmathews@psu.edu) (814) 863 6213

## **ABSTRACT**

Coal cleats, which are the flow-pathway for gases into and out of coal, have a range of apertures. Carbon-dioxide-induced coal swelling is thought to be responsible for reduced injectability observed in field and laboratory experiments. However, we expect differences in the capacities, and thus in the degree of swelling, for different bands within coal. In this study the influence of lithotypes (coal bands observable to the naked eye) on swelling was investigated directly utilizing an optical profilometer. This approach uses optical interferometry to rapidly, and non-destructively determine surface typography. A polished bituminous coal surface (proxy for a cleat surface), constrained in all other sides by a steel jacket, was exposed to CO<sub>2</sub> at 15-atmospheres initial gas pressure for 6-7 days. Following exposure, the surface typology was examined immediately. Any relative deformation was likely captured before significant contraction due to the slow desorption of CO<sub>2</sub>, the limited exposed surface, and the relative speed of the optical profilometer technique. Thus, although the observations are limited to the surface of the coal, it reflects the behavior of the bulk. Generally, the surface typology was unchanged after CO<sub>2</sub> exposure. However, in some regions greater swelling reduced or extended the typology differences as certain lithotypes swelled to a greater extent than their neighbors. However, the

magnitude of these differentials (for example the differential of the relative heights of vitrain and clarain bands) was only 1 micron. It is thought that as the lithotypes are intimately associated with each other, a preferential swelling by one lithotype band will be attenuated by its neighbors. Thus, differential swelling is not thought to be important in permeability reduction.

## **INTRODUCTION**

The CO<sub>2</sub>-induced swelling of coal is thought to be responsible for reduced injectivity during enhanced coalbed methane operations or CO<sub>2</sub> sequestration (Durucan et al., 2009; Fokker et al., 2004; Mazumder et al., 2006; Reeves, 2003; van Bergen et al., 2009). The flow of fluids, in coal, is via the fracture network or cleat system (Close, 1993; Gray, 1987). Yet, the faces of these coal cleats are the maceral combinations that form identifiable lithotype bands in the coal seam, visible to the naked eye. It seems probable that these lithotypes will impact the degree of: water storage (Unsworth et al., 1989), hydrophobicity and , thus, the ease of water removal (Arnold et al., 1989), change in porosity (Clarkson et al., 1996; Clarkson et al., 1997; Lamberson et al., 1993; Smyth et al., 1993) and , thus, also the change in methane storage capacity (Beamish et al., 1998; Crosdale et al., 1998), mineral matter content (Lamberson et al., 1993), cleat frequency (Smyth et al., 1993), and, thus, the degree of swelling or contraction. Indeed, it is already clear from X-ray computed tomography techniques that differential swelling of lithotypes occurs under sequestration conditions (Karacan, 2003; Pone et al., 2009). Observations of solvent-swelling of individual coal particles can also show dramatically different swelling extents, presumably linked to lithotypes (Gao et al., 1999; Gao et al., 2009; Van Niekerk et al., 2007). Thus, is it possible for extensive swelling of certain lithotypes to close off a local cleat system resulting in permeability reduction? The distinction between this and the current understanding of permeability reduction being certain lithotypes, rather than the whole coal, could be responsible or at least more responsible for some of the observed permeability reduction. Alternatively, mineral dissolution

followed by cleat closure or mineral re-precipitation could also play a role in permeability reduction (Schroeder et al., 2001), but it is not discussed here. One important distinction between individual particle swelling and coal monolith swelling is the degree of association between lithotypes. If lithotypes are intimately associated with each other, a preferential swelling by one lithotype band will be attenuated by its neighbors. Thus, differential swelling in narrow bands may be small and hence a suitable analytical approach is necessary.

To evaluate lithotype swelling a polished coal surface, contained different lithotypes, from a horizontal core was prepared. This surface served as a proxy for a cleat face. The 2.4 cm diameter coal core was placed within a stainless steel pellet mould, commonly used for petrographic pellet creation (ASTM, 1995), and hence was constrained on all sides apart from the one exposed polished face. The surface was investigated directly utilizing an optical profilometer. This approach uses optical interferometry to rapidly, and non-destructively determine surface typography. A graphite rod was glued to the bottom of the pellet mould plate, to provide a surface calibration point as it was not expected to swell with CO<sub>2</sub> exposure. Surface deformation, due to exposure to 15 atmospheres of CO<sub>2</sub>, was measure immediately after gas pressure release. Additionally, an obvious coal cleat from a bituminous Kentucky coal was examined with transmitted light.

## **EXPERIMENTAL**

The coal used in this experiment was a bituminous coal from Kentucky. Details on the sample are available elsewhere (Pone et al., 2008). Figure 1 shows the experimental setup of the coal core, held in a pellet holder, within a pressurized reactor. The 2.4 cm diameter, roughly 2.4 cm long dry core was placed within a thick steel jacket with a steel plug closing one end. A hydraulic ram was used to push the plug and core to be in-line with the upper exposed surface of the steel jacket.

This setup limited swelling to only in one direction to better simulate the in situ conditions of coal cleat face. The core, and hence the polished coal surface were orientated so the bedding plane was visible and multiple lithotype bands were observed. The surface was polished in the usual manner for optical petrography of coal (ASTM, 1995). The gold surface, to allow optical interferometry was an atomic gold layer, spluttered on within a vacuum in a manner similar to the preparation of SEM samples. The coal core was dried overnight before the gold surface was deposited to remove any influence of water in the surface deformation (contraction with water loss, CO<sub>2</sub> uptake capacity or rate, and resultant swelling (Clarkson et al., 2000; Goodman et al., 2004; Jahediesfanjani et al., 2007; Roy et al., 1995)). The cores were exposed to

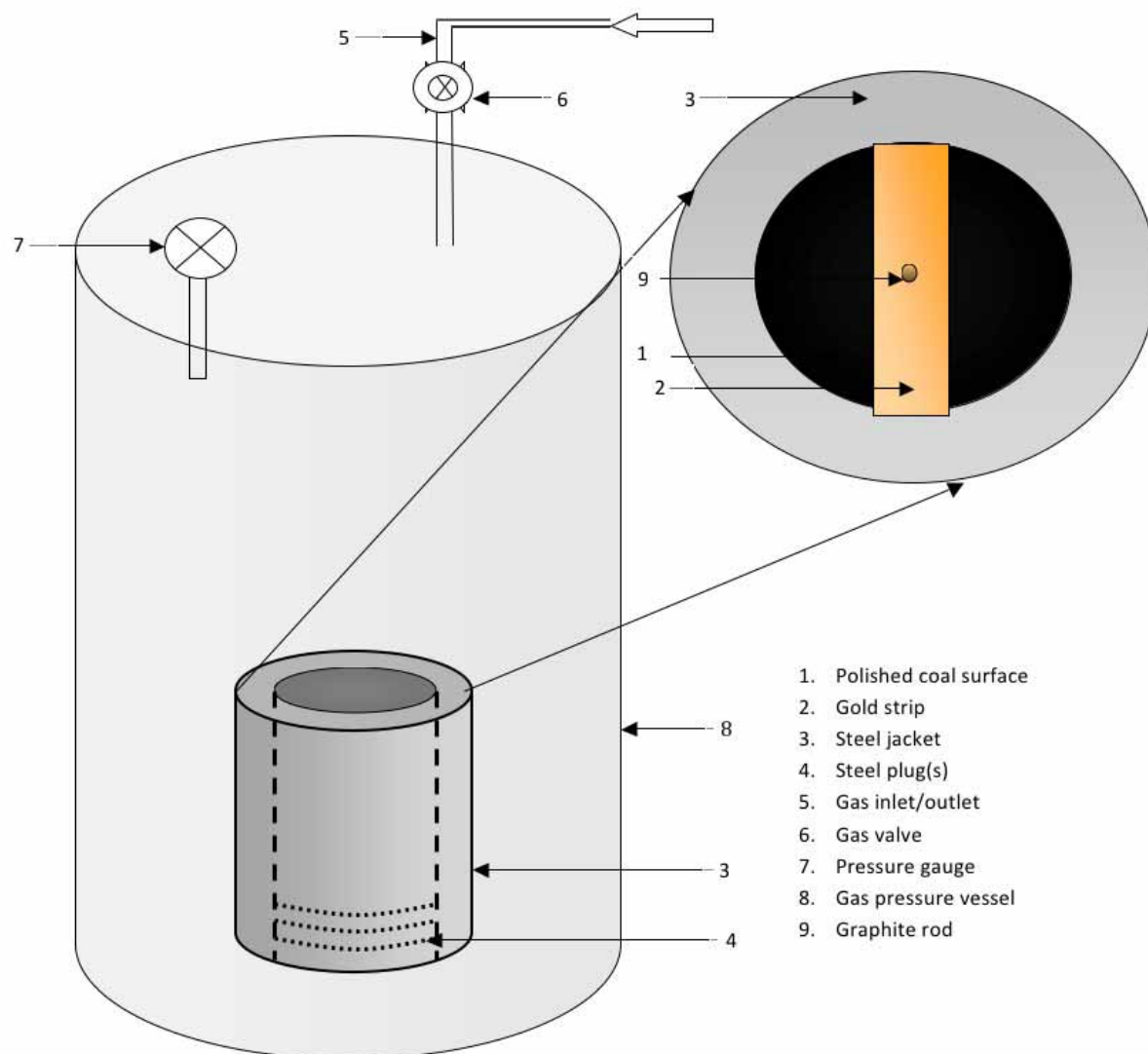


Figure 1. Experimental setup with the coal core within a steel pellet mould, within a CO<sub>2</sub> pressurized vessel. A strip, or the whole surface, is gold coated to aid light reflection.

carbon dioxide for 6-7 days at 1.5 MPa (15 atmospheres) of gas pressure. The gas was released and the optical profilometry was performed immediately with a Wyko NT1100. In interferometry, a light beam is split into two paths. One path of light impinges on the specimen surface and is reflected. The other is reflected from a reference mirror. Reflections from these surfaces are recombined and projected onto an array detector. When the path differences are on the order of

wavelengths of light, interference occurs. This interference contains information about the surface topology. Vertical resolutions of 0.1 microns were measurable. The field of view included a graphite core that was placed in a central drill hole in the core and was glued to the bottom plate of the pellet mould to provide a stable reference point. Unfortunately, a pencil “lead” was used in error and the extent of swelling will not be reported due to possible swelling of the clays within the “lead” (Romanov, 2008). It was however, still possible to determine differential swelling within lithotype regions. The field of view, with x2.5 objective and x 0.5 viewer lenses, was 3.7 x 4.9 mm.

## **RESULTS**

The polished and gold-coated surface of the coal is shown in a “3D” view in Figure 2. The topology of the surface is magnified and shown at a different scale than the x-y plane. The “graphite” is partially shown in the top region of the micrograph. As expected, the coal surface is relatively smooth from the polishing process but with the surface being slightly elevated in places. This is likely due to subtle differences in the micro-hardness of the lithotypes. Quantification of the relative height differential across this field of view is on the order of 4-9 micron only, depending on location (avoiding holes). These differences are visually enhanced with an automated, image specific, false-coloring. Figure 2 also shows the same region

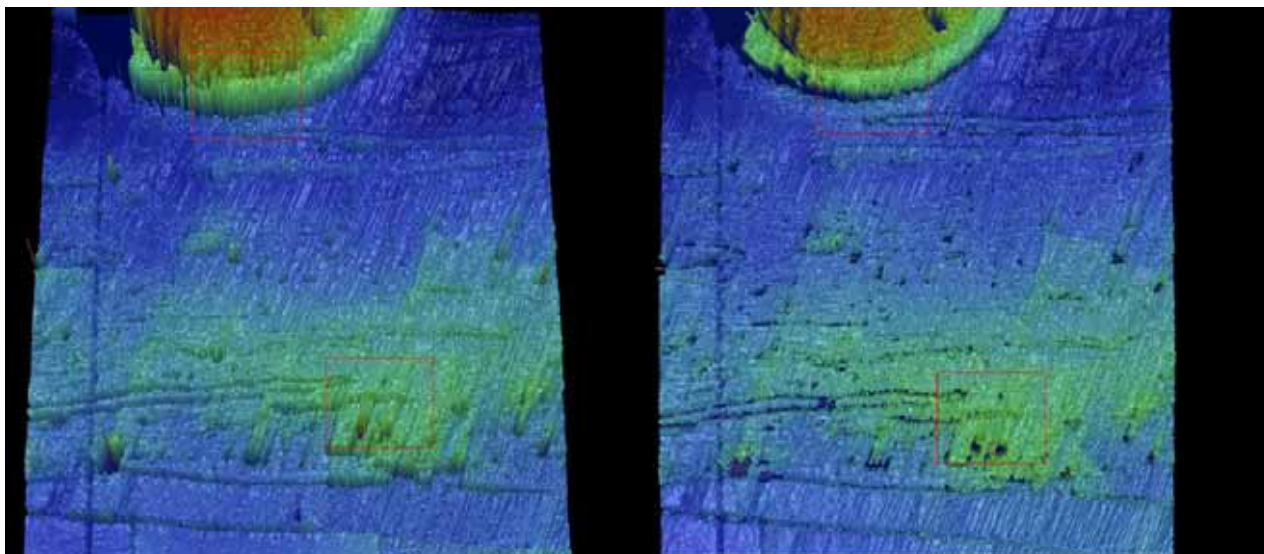


Figure 2. A polished coal surface, before (left-hand-side) and after 6 days of to CO<sub>2</sub> exposure, shown in a false-colored “3D” view with exaggerated vertical displacement. Typology changes are evident in the marked regions. The upper region is the “graphite” rod.

after 6-days of exposure. Quantification of the surface deformation across the coal regions of the plot, again avoiding holes, was only  $0.9 \pm 0.2$  microns with increase in height in the vitrain region close to the graphite rod and a reduction in the relative heights of vitrain and clarain (higher region). Thus, although differential lithotype swelling occurred, the presence of adjacent lithotypes likely attenuated the swelling extent, or both lithotypes swelled to remarkably similar degrees. This latter postulation seems unlikely. Solvent swelling of maceral concentrates versus raw coals also show an attenuation for swelling for raw coal in comparison to maceral concentrates (Milligan et al., 1997). An inertinite band was also observed (not shown) and adjacent clarain swelled to a greater extent, as expected (Milligan et al., 1997), with 0.5 micron differential.

A lithotype “map” is shown in Figure 3. The coal had an obvious thick vitrain band across the bottom portion of the pellet. The remaining portion containing clarain with thin bands of inertinite and vitrain. Mineral (pyrite) particles were also observed. Figure 2 is from the center region of the pellet surface capturing the “graphite” rod and clarain into the vitrain band (below the central rod).

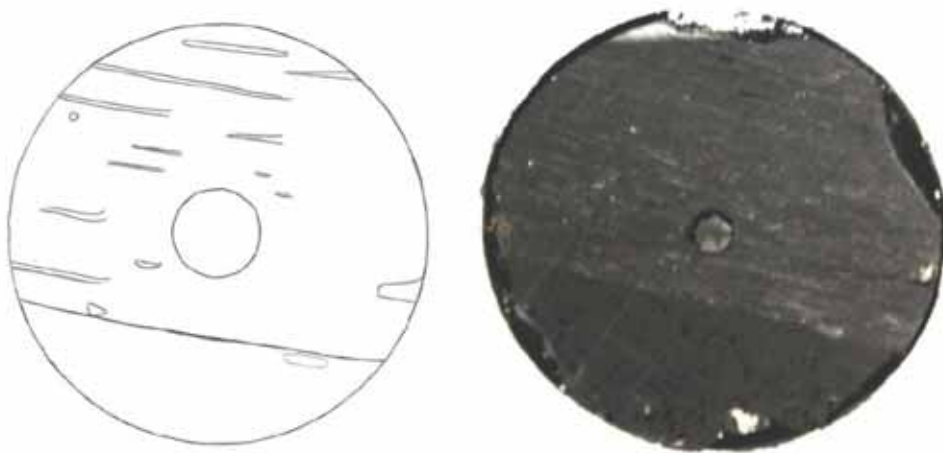


Figure 3. Sketch of lithotype boundaries and a photograph of the polished coal surface before gold coating.

An additional false-colored coal “3D” surface, of another coal core from the same sample, is shown in Figure 4. Visually, it is evident that differential swelling has occurred, and that small microfractures and some pores are no longer evident, presumably being closed by swollen coal. Again, the differential is on the order of 1 micron only in the boxed region. The rough surface is clarain and the smooth region is a thin vitrain band.

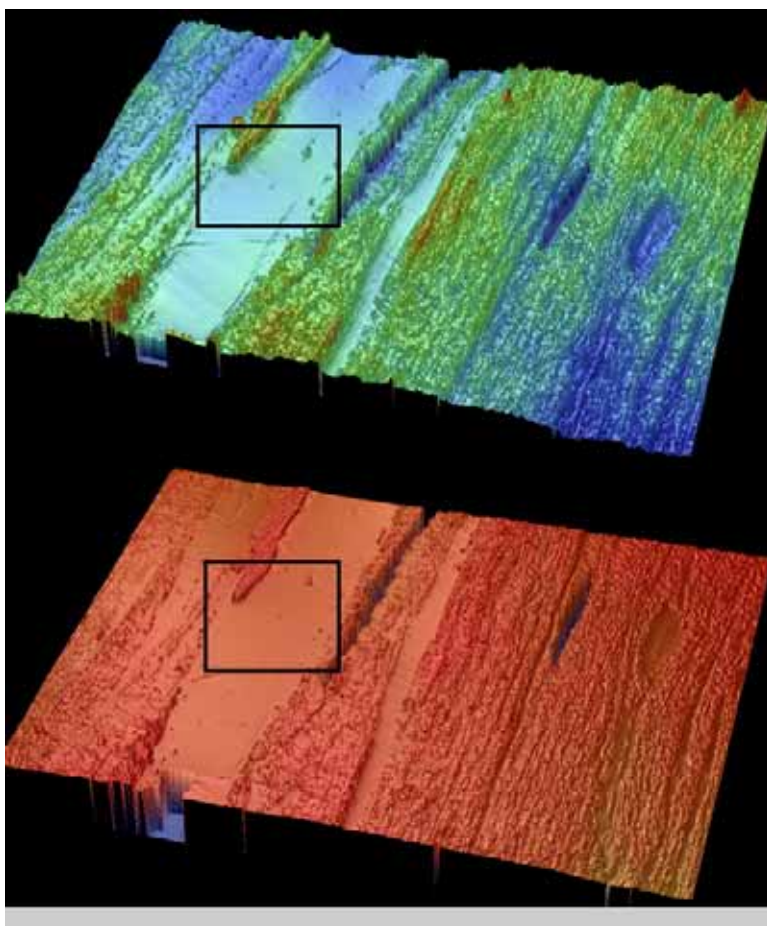


Figure 4. False-colored polished coal surface topography before (upper image) and after CO<sub>2</sub> exposure. Note the reduced vertical morphology in the boxed region (on the order of 1 micron) also note the apparent absence of the micro cleat in the box within the 2<sup>nd</sup> image.

To determine any potential impact of differential swelling on a micro-cleat petrographic observation was performed on a bituminous Kentucky coal. A composite mosaic of microscope images of a micro-cleat observed with transmitting light microscope is shown in Figure 5. The cleat is open and transmits more light than the thin slice of coal. In this petrographic approach, the maceral vitrinite will appear red in color. This cleat is on the order of 500 microns in aperture. Thus, differential swelling is not likely to impact cleat closure unless they are very small micro-cleats. Cleat surface roughness may be impacted. However, it does not appear that CO<sub>2</sub> induced

swelling will close cleats due to the postulated differential swelling caused by lithotype differences in: water storage (Unsworth et al., 1989), hydrophobicity and hence ease of water removal (Arnold et al., 1989), porosity (Clarkson et al., 1996; Clarkson et al., 1997; Lamberson et al., 1993; Smyth et al., 1993) and hence also in methane storage capacity (Beamish et al., 1998; Crosdale et al., 1998), mineral matter content (Lamberson et al., 1993), cleat frequency (Smyth et al., 1993), and thus degree of swelling or contraction. Rather, it appears likely that adjacent lithotypes attenuate the aptitude for differential swelling.

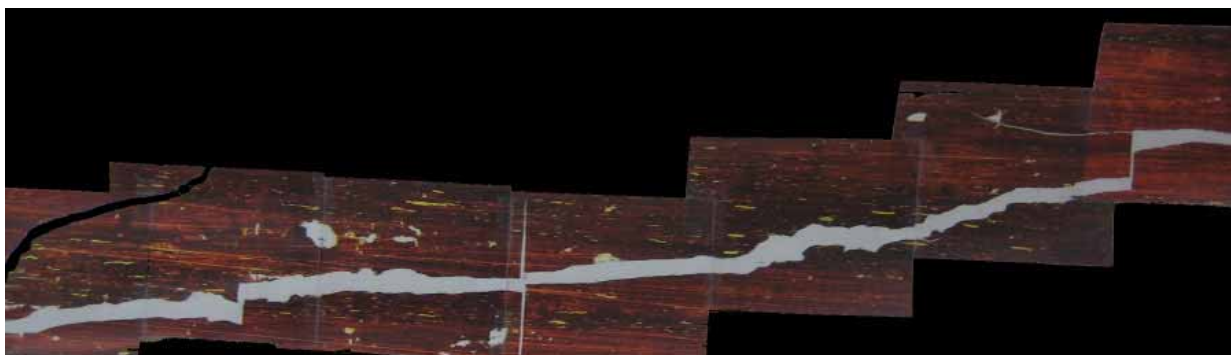


Figure 5. A photographic mosaic of a coal micro-cleat, observed with a transmitted light microscope. The cleat (white jagged thick line) is on the order of 500 microns aperture.

## CONCLUSION

The CO<sub>2</sub>-induced surface deformation of a polished coal surface was quantified with optical interferometry. The coal core was confined on all other sides by a stainless steel jacket. It was postulated that lithotypes would differentially swell resulting in changes to the surface typology. While this did occur, the magnitude of these differentials, for example the differential of the relative heights of vitrain and clarain bands, was only 1 micron. It is thought that the adjacent lithotypes attenuate the aptitude for differential swelling. Thus, differential swelling is unlikely to impact all but the smallest micro-cleats.

**REFERENCES**

- Arnold, B.J. and Aplan, F.F., 1989. The hydrophobicity of coal macerals. *Fuel*, 68: 651-658.
- ASTM, 1995. D 2797-07, Standard practice for preparing coal samples for microscopical analysis by reflected light, ASTM International, pp. 274-77.
- Beamish, B.B. and Crosdale, P.J., 1998. Instantaneous outbursts in underground coal mines: An overview and association with coal type. *International Journal of Coal Geology*, 35: 27-55.
- Clarkson, C.R. and Bustin, R.M., 1996. Variation in micropore capacity and size distribution with composition in bituminous coal of the Western Canadian sedimentary basin. Implications for coalbed methane potential. *Fuel*, 75(13): 1483-1498.
- Clarkson, C.R. and Bustin, R.M., 1997. Variation in permeability with lithotype and maceral composition of Cretaceous coals of the Canadian Cordillera. *International Journal of Coal Geology*, 33(2): 135-151.
- Clarkson, C.R. and Bustin, R.M., 2000. Binary gas adsorption/desorption isotherms: effect of moisture and coal composition upon carbon dioxide selectivity over methane. *International Journal of Coal Geology*, 42: 241-271.
- Close, J.C., 1993. Natural fractures in coal. In: R. Law, D.D. (Editor), *Hydrocarbons from Coal*. AAPG Studies in Geology, pp. 119-132.
- Crosdale, P.J., Beamish, B.B. and Valix, M., 1998. Coalbed methane sorption related to coal composition. *International Journal of Coal Geology*, 35(1-4): 147-158.
- Durucan, S. and Shi, J.-Q., 2009. Improving the CO<sub>2</sub> well injectivity and enhanced coalbed methane production performance in coal seams. *International Journal of Coal Geology*, 77(1-2): 214-221.
- Fokker, P.A. and van der Meer, L.G.H., 2004. The injectivity of coalbed CO<sub>2</sub> injection wells. *Energy*, 29: 1423-1429.
- Gao, H., Artok, L., Kidena, K., Murata, S., Mashahiro, M. and Nomura, M., 1999. A novel orthogonal microscope image analysis method for evaluation solvent-swelling behavior of single coal particles. *Energy & Fuels*, 12: 881-890.
- Gao, H., He, J., Cai, J., Ishigaki, M. and Nomura, M., 2009. An improved three-dimensional microscope image analysis method for studying solvent swelling of single coal particles. *Energy & Fuels*, 23(1): 342-348.
- Goodman, A.L., Busch, A., Duffy, G.J., Fitzgerald, J.E., Gasem, K.A.M., Gensterblum, Y., Krooss, B.M., Levy, J., Ozdemir, E., Pan, Z., Robinson, R.L.J., Schroeder, K., Sudibandriyo, M. and White, C.M., 2004. An inter-laboratory comparison of CO<sub>2</sub>

- isotherms measured on Argonne Premium coal samples. *Energy & Fuels*, 18(4): 1175-1182.
- Gray, I., 1987. Reservoir Engineering in Coal Seams: Part 1—The physical process of gas storage and movement in coal seams. *SPE Reservoir Engineering*, February: 28-34.
- Green, D.J., 1998. *An Introduction to the Mechanical Properties of Ceramics*. Cambridge Solid State Series. Cambridge University Press, UK, 336 pp.
- Jahediesfanjani, H. and Civan, F., 2007. Effect of resident water on enhanced coal gas recovery by simultaneous CO<sub>2</sub>/N<sub>2</sub> injection, SPE Annual Technical Conference and Exhibition, San Antonio, TX, pp. 1-18.
- Karacan, C.O., 2003. Heterogeneous sorption and swelling in a confined and stressed coal during CO<sub>2</sub> injection. *Energy & Fuels*, 17(6): 1595-1608.
- Lamberson, M.N. and Bustin, R.M., 1993. Coalbed Methane Characteristics of Gates Formation Coals, Northeastern British-Columbia - Effect of Maceral Composition. *Aapg Bulletin-American Association of Petroleum Geologists*, 77(12): 2062-2076.
- Mazumder, S., Karnik, A. and Wolf, K.H., 2006. Swelling of coal in response to CO<sub>2</sub> sequestration for ECBM and its effect on fracture permeability. *SPE Journal*, 11(3): 390-398.
- Milligan, J.B., Thomas, K.M. and Crelling, J.C., 1997. Solvent swelling of maceral concentrates. *Energy & Fuels*, 11(2): 364-371.
- Pone, J.D.N., Halleck, P.M. and Mathews, J.P., 2008. Methane and carbon dioxide sorption and transport rates in coal at in-situ conditions, 9th International Conference on Greenhouse Gas Control Technologies, Washington, D.C., 16-20 November.
- Pone, J.D.N., Hile, M., Halleck, P.M. and Mathews, J.P., 2009. Three-dimensional carbon dioxide-induced strain distribution within a confined bituminous coal. *International Journal of Coal Geology*, 77(1-2): 103-108.
- Reeves, S.R., 2003. Enhanced CBM recovery, coalbed CO<sub>2</sub> sequestration assessed. *Oil & Gas Journal*, 101(27): 49.
- Romanov, V., 2008. Poster: Multi-scale modeling of CO<sub>2</sub> sequestration in unmineable coal seams, Seventh Annual Conference on Carbon Capture & Sequestration, Pittsburgh, PA.
- Roy, S. and Pyrak-Nolte, L.J., 1995. The effect of drying and re-saturation on the gas permeability of coal. In: D. Shultz (Editor), *Rock Mechanics*. Balkema, Rotterdam.
- Schroeder, K., Ozdemir, E. and Morsi, B.I., 2001. Sequestration of carbon dioxide in coal seams, First National Conference on Carbon Sequestration, Washington, DC.
- Smyth, M. and Buckley, M.J., 1993. Statistical-analysis of the microlithotype sequences in the Bulli seam, Australia, and relevance to permeability for coal-gas. *International Journal of Coal Geology*, 22(3-4): 167-187.

- Unsworth, J.F., Fowler, C.S. and Jones, L.F., 1989. Moisture in coals. 2. Maceral effects on coal structure. *Fuel*, 68: 18-26.
- Van Bergen, F., Krzystolik, P., van Wageningen, N., Pagnier, H., Jura, B., Skiba, J., Winthagen, P. and Kobiela, Z., 2009. Production of gas from coal seams in the Upper Silesian Coal Basin in Poland in the post-injection period of an ECBM pilot site. *International Journal of Coal Geology*, 77(1-2): 175-187.
- Van Niekerk, D. and Mathews, J.P., 2007. Solvent swelling of similar rank South African vitrinite-rich and inertinite-rich coals: swelling extent and maceral influences, International Conference on Coal Science and Technology, The University of Nottingham, England, 28-31 August.